On The Evolution of Light Signaling: The COP1/SPA complex in *Physcomitrella patens*

Inaugural-Dissertation
zur
Erlangung des Doktorgrades
der Mathematisch-Naturwissenschaftlichen Fakultät
der Universität zu Köln

vorgelegt von

Oliver Artz

aus

Goch

Berichterstatter:	Prof. Dr. Ute Höcker
	Prof. Dr. Martin Hülskamp
Prüfungsvorsitzender:	Prof. Dr. Wolfgang Werr
Tag der mündlichen Prüfung:	25. Februar 2019

Table of Contents

List of Figures iv

List of Tables v

Abbreviations vi

Nomenclature x

Abstract xi

Zusammenfassung xii

1 Introduction 1

1.1 Light signaling in *Arabidopsis thaliana* 1

1.1.1 Light is perceived via photoreceptors 1

1.1.2 The COP1/SPA complex represses photomorphogenesis in darkness 4

1.1.3 HY5 promotes photomorphogenesis in light 10

1.2 Terrestrialization of plants was a crucial event in the history of life 11

1.3 *Physcomitrella patens* is a model organism for early land plant evolution . 13

1.4 Components of the light signaling cascade are highly conserved 14

2 Aims 20

3 Results 21

3.1 *PpspaAB* double knock-out lines generated via homologous recombination harbor multiple insertions 21

3.2 *PpspaAB* double knock-out lines were generated using CRISPR/Cas9 . . 23

3.3 *Ppspa* mutant lines exhibit retarded gametophore development 25

3.4 Physcomitrella *SPA* genes negatively regulate protonemal growth in light and darkness 30

3.5 Dark repression of light-regulated genes is mostly maintained in *PpspaAB* mutants 33

3.6 Light-regulation of PpHY5b protein abundance is not affected by *PpSPAab* 35

3.7 PpCOP1a interacts with PpSPAb and PpHY5b 37

4 Discussion **40**
4.1 The CRISPR/Cas9 technology is highly efficient for generating higher order knock-out mutants in *Physcomitrella patens* 40
4.2 *PpSPAa* and *PpSPAb* regulate gametophore and protonemal development in Physcomitrella 42
4.3 PpHY5b might be a target of the COP1/SPA complex in Physcomitrella, but the *PpSPA* genes might not be involved in PpHY5b regulation 45
4.4 Further investigations of the evolutionary conservation 46

5 Materials & Methods **52**
5.1 Materials 52
5.1.1 Chemicals 52
5.1.2 Buffers and solutions 52
5.1.3 Antibiotics 57
5.1.4 Growth media 57
5.1.5 Antibodies 58
5.1.6 Enzymes 58
5.1.7 Kits for molecular biology 59
5.1.8 Oligonucleotides 59
5.1.9 Molecular markers 64
5.1.10 Plasmids 64
5.1.11 Bacterial and yeast strains 67
5.1.12 Plant material 68
5.1.13 Physcomitrella genes 69
5.2 Methods 70
5.3 General cultivation of Physcomitrella 70
5.3.1 Phenotypic analysis of gametophores in light 70
5.3.2 Phenotypic analysis of gametophores in darkness 71
5.3.3 Phenotypic analysis of colony growth 71
5.3.4 Phenotypic analysis of gravitropic response 72
5.4 Molecular biology methods 72
5.4.1 Agarose gel electrophoresis 72
5.4.2 Polymerase chain reaction (PCR) 72
5.4.3 DNA sequencing and sequence analysis 73

5.4.4 Cloning 73
5.4.5 Cloning strategy for *PpHY5b-3HA*knock-in construct 73
5.4.6 Cloning strategy for the *PpHY5b* CDS 75
5.4.7 Preparation and transformation of chemically competent *E. coli* . 75
5.4.8 Transformation of Physcomitrella - knock-in 76
5.4.9 Transformation of Physcomitrella - CRISPR/Cas9 77
5.4.10 Isolation of genomic DNA from Physcomitrella 78
5.4.11 Genotyping 79
5.4.12 Isolation of total RNA from Physcomitrella 80
5.4.13 DNase treatment of RNA 80
5.4.14 Reverse transcription of RNA to cDNA 81
5.4.15 Quantitative real-time PCR 81
5.4.16 Southern blotting 81
5.5 Biochemical methods 82
5.5.1 Isolation of total protein from Physcomitrella 82
5.5.2 Bradford assay 83
5.5.3 Immunoprecipitation 83
5.5.4 SDS polyacrylamide gel electrophoresis (SDS-PAGE) 83
5.5.5 Western blotting 84
5.5.6 Immunodetection 84
5.6 Protein-protein interaction assays 84
5.6.1 Colocalization studies in leek epidermal cells 84
5.6.2 FRET-FLIM studies in leek epidermal cells 85
5.6.3 Yeast-Two-Hybrid 86

6 References **87**

7 Supplement **113**

8 Acknowledgements **118**

9 Declaration **119**

10 Erklärung **120**

11 Lebenslauf **121**

List of Figures

1 Light is perceived through different classes of photoreceptors 2

2 The COP1/SPA complex is a central repressor of photomorphogenesis in darkness 6

3 Mosses are among the first diverged land plants 11

4 Life cycle of Physcomitrella 13

5 *PpspaB* and *PpspaAB* mutant lines harbor multiple insertions of the knock-out construct 22

6 *PpspaAB* double knock-out lines were generated using CRISPR/Cas9 . . 24

7 *PpSPAa* and *PpSPAb* regulate gametophore growth in long-day conditions 27

8 *PpSPAa* and *PpSPAb* regulate gametophore growth in R light 28

9 *PpSPAa* and *PpSPAb* do not regulate gametophore growth in darkness . . 29

10 *PpSPAa* and *PpSPAb* regulate plant size in long-day conditions 31

11 *PpSPAa* and *PpSPAb* regulate protonemal growth in darkness 32

12 *PpspaAB* mutant lines do not show constitutive photomorphogenesis on the molecular level 34

13 Mutation of PpSPAab does not stabilize PpHY5b in darkness 36

14 PpCOP1a interacts with PpSPAb and PpHY5b in leek cells 39

15 Plasmid map of the PpHY5b-3HA knock-in construct 74

S1 No interaction of PpCOP1a, PpSPAb and PpHY5b was detected in yeast-two-hybrid assay (LexA system) 117

List of Tables

1 Abbreviations used in this study vi

2 Buffers and solutions used in this study 52

3 Antibiotics used in this study 57

4 Growth media used in this study 57

5 Antibodies used in this study 58

6 Enzymes used in this study 58

7 Kits for molecular biology used in this study 59

8 Oligonucleotides used in this study 60

9 Molecular markers used in this study 64

10 Plasmids used in this study 64

11 Physcomitrella mutant lines used in this study 68

12 Physcomitrella genes mentioned in this study 69

13 Primer combinations used for genotyping of putative *PpspaAB* mutant lines 79

S1 CRISPR/Cas9 sgRNA sequences used to generate *PpSPAab* double knock-out mutants 113

S2 Tested off-target sequences in *PpspaAB* double knock-out lines 114

S3 Summary of sequencing results for the *PpSPAb* locus after transformation 115

Abbreviations

Abbreviations used in this study are listed in Table 1. Units being part of the International System of Units (SI units) are not listed.

Table 1: Abbreviations used in this study

Abbreviation	**Definition**
35S	35S promoter of the cauliflower mosaic virus
AD	activation domain
APS	ammonium persulfate
Ath	*Arabidopsis thaliana*
B	blue
BD	binding domain
bHLH	basic helix loop helix
bp	basepair(s)
BSA	bovine serum albumin
bZIP	basic leucine zipper
cDNA	complementary DNA
CDS	coding sequence
CFP	cyan fluorescent protein
CoIP	coimmunoprecipitation
CSPD	Disodium 3-(4-methoxyspiro (1,2-dioxetane-3,2'-(5'-chloro)tricyclo (3.3.1.13,7)decan)-4-yl)phenyl phosphate
CTAB	cetyltrimethylammonium bromide
C-terminal	carboxy-terminal
D	darkness
dai	day(s) after inoculation
DIG-dUTP	digoxigenin-deoxyuridone triphosphate
DNA	deoxyribonucleic acid

Table 1: (continued)

Abbreviation	Definition
DNase	deoxyribonuclease
dNTP	deoxynucleoside triphosphate
DTT	1,4-dithiothreitol
EDTA	ethylenediaminetetraacetic acid
et al.	at alii (and others)
FAD	flavin adenine dinucleotide
FLIM	fluorescence lifetime imaging
FMN	flavin mononucleotide
FR	far-red
FRET	Foerster resonance energy transfer
gDNA	genomic deoxyribonucleic acid
GFP	green fluorescent protein
H	histidine
HA	human influenza hemagglutinin
HIR	high irradiance response
HRP	horseradish peroxidase
i.e.	id est (that is)
KO	knock-out
L	leucine
LB	Luria-Bertani
LFR	low fluence response
LOV	light oxygen voltage
LRE	light responsive element
MES	2-(N-morpholino)ethanesulfonic acid
mRNA	messenger-ribonucleic acid
n	number of elements per sample

Table 1: (continued)

Abbreviation	**Definition**
neoR	resistance to neomycin
NLS	nuclear localization signal
N-terminal	amino-terminal
OD	optical density
Os	*Oryza sativa*
P	p-value
Pp	*Physcomitrella patens*
PAGE	polyacrylamide gel electrophoresis
PCR	polymerase chain reaction
PEG	polyethylene glycol
Pfr	red light absorbing form of Phytochromes
PHR	photolyase-homologous region
PI	propidium iodide
Pr	far-red light absorbing form of Phytochromes
PVDF	polyvinyledene difluoride
qRT-PCR	quantitative real-time polymerase chain reaction
R	red
RING	really interesting new gene
RNase	ribonuclease
RT	room temperature
SD	synthetic dropout
SDS	sodium dodecyl sulfate
SEM	standard error of the mean
sgRNA	short-guiding ribonucleic acid
Taq	*Thermus aquaticus*
TBE	Tris/borate/EDTA

Table 1: (continued)

Abbreviation	Definition
TBS	Tris-buffered saline
TE	Tris/EDTA
TEMED	tetramethylethylendiamine
TF	transcription factor
Tris	tris(hydroxymethyl)aminomethane
U	uracil
UV	ultraviolet light
UV-A	ultraviolet A
UV-B	ultraviolet B
v/v	volume per volume
VLFR	very low fluence response
W	white
w/v	weight per volume
WD	aspartic acid, tryptophan
YFP	yellow fluorescent protein

Nomenclature

If not further specified, genes and proteins without a prefix do not relate to a specific organism. Prefixes such as 'At' (*Arabidopsis thaliana*) or 'Pp' (*Physcomitrella patens*) are used when necessary to avoid ambiguities.

Nomenclature of genes and proteins

SPAb	Gene, locus, wild-type allele
spaB	Mutant allele
SPAb	Protein

Exception: Nomenclature of photoreceptors

PHYB	Gene, locus, wild-type allele
phyB	Mutant allele
PHYB	Apoprotein
phyB	Holoprotein (with chromophore)

Abstract

Plants rely on light as an environmental signal and primary source of energy. In the course of evolution plants have developed a sophisticated signaling network enabling them to fine-tune their growth and development according to the ambient light conditions and ensure sustained reproductive success. A major regulator of light signaling is the COP1/SPA complex which targets positively acting light-signaling intermediates such as HY5 for proteolytic degradation. So far, only very few studies have investigated the evolutionary conservation of light signal transduction and our understanding of the COP1/SPA complex beyond *Arabidopsis thaliana* is very limited.

Here, I genetically and biochemically characterized the COP1/SPA complex in the early diverged land plant *Physcomitrella patens*. *PpspaAB* double knock-out plants were generated using the CRISPR/Cas9 technology. Other than full *spa* knock-out lines in Arabidopsis, *PpspaAB* double knock-out lines exhibited rather mild phenotypic aberrations from wild-type plants in that they developed shorter gametophores but a larger colony diameter when grown in white light. Mutating the *spa* genes did not lead to strong constitutive photomorphogenesis in darkness. Light-regulation of endogenous protein levels of PpHY5b, a putative target of the COP1/SPA complex in Physcomitrella, was not mediated by PpSPA proteins. These results suggest that either PpCOP1 activity might be more independent of PpSPA proteins than in Arabidopsis or that the light signaling cascade plays a smaller role in Physcomitrella development. *In vivo* PpCOP1a interacted with PpSPAb and PpHY5b, indicating an evolutionary conservation of a functional PpCOP1/PpSPA complex. More studies investigating the role of not only *PpSPA* but also *PpCOP1* genes are necessary to further elucidate the function of the complex in Physcomitrella.

Zusammenfassung

Pflanzen sind auf Licht als Umweltsignal und primäre Energiequelle angewiesen. Im Lauf der Evolution haben sie ein kompliziertes Signalnetzwerk entwickelt, welches ihnen erlaubt ihr Wachstum und ihre Entwicklung an das Umgebungslicht anzupassen und so langfristig Fortpflanzungserfolg zu sichern. Ein Hauptregulator der Lichtsignaltranduktion ist der COP1/SPA Komplex. Dieser induziert die proteolytische Degradierung von positiv agierenden Intermediaten der Lichtsignaltransduktion wie z.B. HY5. Bisher haben nur sehr wenige Studien die evolutionäre Konservierung der Lichtsignaltansduktion untersucht und unser Verständnis des COP1/SPA Komplexes jenseits von *Arabidopsis thaliana* ist äußerst limitiert.

In dieser Arbeit habe ich den COP1/SPA Komplex in der früh divergierten Landpflanze *Physcomitrella patens* genetisch und biochemisch charakterisiert. *PpspaAB* Doppel-Knockout Mutanten wurden mit Hilfe der CRISPR/Cas9 Technologie generiert. Anders als *spa* Knockout Mutanten in Arabidopsis zeigten die *PpspaAB* Knockout Linien eher milde phänotypische Abweichungen vom Wildtyp. Die Physcomitrella Mutanten entwickelten kürzere Gametophore, zeigten aber einen größeren Koloniedurchmesser unter Weisslichtbedingungen. Die Mutation der *spa* Gene ging nicht mit starker konstitutiver Photomorphogenese einher. Die Lichtregulation der Proteinmengen von endogenem PpHY5b, welches ein putatives Zielprotein des COP1/SPA Komplexes in Physcomitrella darstellt, war nicht über PpSPA Proteine reguliert. Die Ergebnisse deuten darauf hin, dass entweder die PpCOP1 Aktivität unabhängiger von den PpSPA Proteinen ist als in Arabidopsis oder die Lichtsignaltranduktionskaskade eine kleinere Rolle in der Entwicklung von Physcomitrella spielt. *In vivo* interagierte PpCOP1a mit PpSPAb und PpHY5b, was eine evolutionäre Konservierung eines funktionellen COP1/SPA Komplexes suggeriert. Weitere Studien der *PpSPA* und *PpCOP1* Gene sind für die Funktionsaufklärung des Komplexes in Physcomitrella notwendig.

1 Introduction

1.1 Light signaling in *Arabidopsis thaliana*

A plant's evolutionary success is highly dependent on its capacity to adapt to surrounding conditions. Plant growth and development are shaped by a multitude of biotic and abiotic factors. For photoautotrophs light is inarguably the most crucial factor. Hence, plants evolved a sophisticated signaling network to translate the outer light signal into an appropriate developmental response. Quality, quantity, direction and periodicity of light are perceived and utilized to control phenotypic outputs such as seed germination, seedling deetiolation, phototropic growth, shade avoidance and floral transition (Kami et al., 2010).

1.1.1 Light is perceived via photoreceptors

Higher plants as represented by the model Brassicaceae *Arabidopsis thaliana* have evolved five different classes of photoreceptors (Figure 1): Phytochromes (phyA-E) mainly act as the red (R) and far-red (FR) light receptors. Ultraviolet-A (UV-A) and blue (B) light are mainly perceived via cryptochromes (cry1 and cry2), phototropins (phot1 and phot2) and members of the ZEITLUPE (ZTL) protein family. UV-B RESISTANCE LOCUS 8 (UVR8) was identified as the receptor for ultraviolet-B (UV-B) light (Galvão and Fankhauser, 2015).

A very well characterized class of photoreceptors are the phytochromes. In Arabidopsis phytochromes comprise a gene family with five members encoding phyA-E (Sharrock and Quail, 1989). They absorb R and FR light as a dimer through a covalently bound phytochromobilin, a linear tetrapyrrole. Biosynthesis of phytochromes takes place in the cytosol, where the biologically inactive Pr form is produced. Upon R light exposure, phytochromes undergo a conformational change into the active Pfr form. Absorption of FR light leads to a rapid reconversion of Pfr to Pr. Moreover, a slower form of inactivation can occur in a light-independent way as a process of thermal relaxation, called dark reversion (Rockwell et al., 2006). In plants, Pr and Pfr are in a dynamic

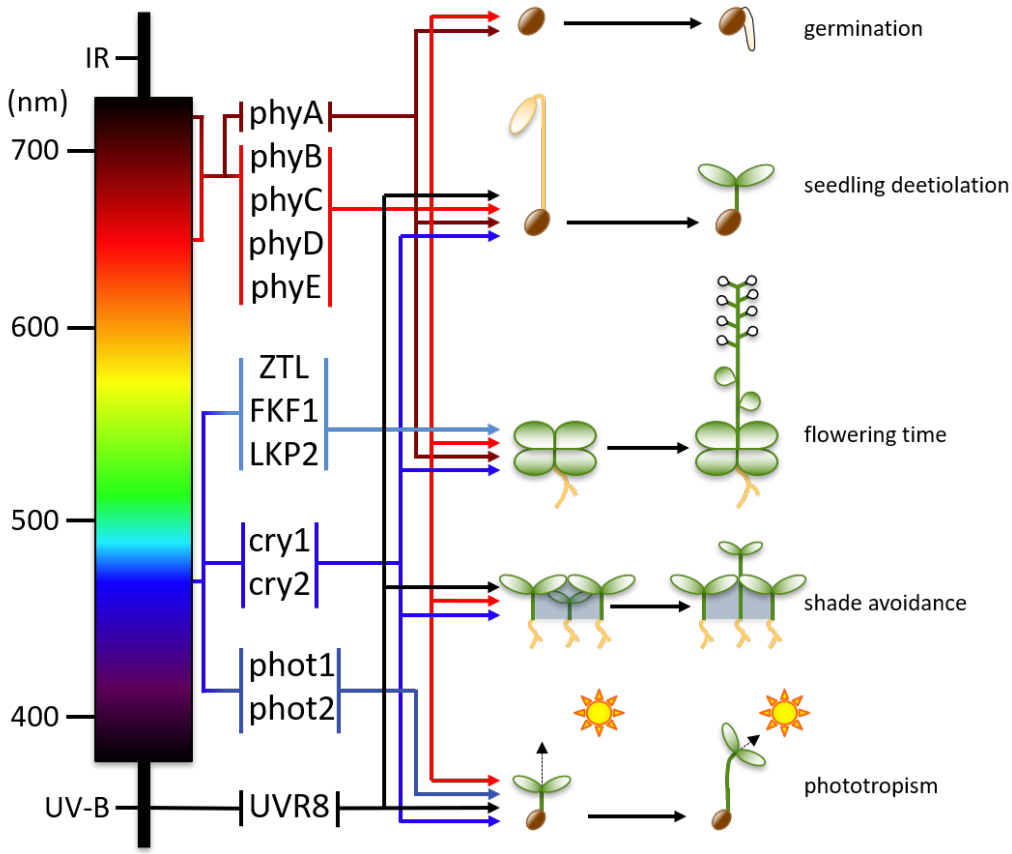

Figure 1: **Light is perceived through different classes of photoreceptors.**
Five classes of photoreceptors have evolved to perceive light of specific wavelengths: Phytochromes mainly control responses to R and FR light. B light receptors comprise cryptochromes, phototropins and members if the ZTL family. UVR8 mediates the UV-B response. Figure adapted from Artz (2014).

photoequilibrium which makes it possible to monitor not only the intensity of R and FR light but also the R/FR light ratio (Franklin and Quail, 2010).

The five family members are further classified into type I, i.e. light-labile, and type II, i.e. light-stable phytochromes. phyA is the only light-labile isoform, whereas phyB-E are light-stable (Sharrock and Clack, 2002). phyA responses comprise the very low fluence response (VLFR) under extremely low irradiances and the FR light high irradiance response (FR-HIR) necessary for successful seedling deetiolation under dense canopies (Casal et al., 1998; Li et al., 2011). The Pr form of the phytochromes is mainly located in

the cytosol. Upon light exposure and conformational change, phytochromes are rapidly translocated into the nucleus (Kircher et al., 1999, 2002). Nuclear import of phyA is dependent on FAR-RED ELONGATED HYPOCOTYL 1 (FHY1) and FHY1-LIKE (FHL) which form an import complex after light activation (Genoud et al., 2008; Hiltbrunner et al., 2006; Pfeiffer et al., 2009; Rosler et al., 2007). Low fluence responses (LFR) and the R light high irradiance response (R-HIR) are predominantly mediated via type II phytochromes. Other than phyA, the other phytochromes do not rely on an import complex for light-dependent nucleocytoplasmic shuttling to the same extent as phyA. The conformational change after light-activation leads to the unmasking of an NLS which in turn results in nuclear import (Chen et al., 2005). Additionally, PHYTOCHROME INTERACTING FACTORs (PIFs) can facilitate shuttling of phyB into the nucleus (Pfeiffer et al., 2012).

Two cryptochrome-encodig genes were identified in Arabidopsis that mediate responses to blue (B) and UV-A light (*CRY1, CRY2)* (Ahmad and Cashmore, 1993; Lin et al., 1996). The function of a third cryptochrome gene, called *CRY3* is not well understood (Yu et al., 2010). cry1 and cry2 perceive light signals through photoreduction of a non-covalently bound flavin adenin dinucleotide (FAD) chromophore (Chaves et al., 2011). CRY1 and CRY2 are mostly localized in the nucleus, where they exert their main function (Guo et al., 1999; Wu and Spalding, 2007). However, cytosolic CRY1 mediates responses such as primary root growth and cotyledon expansion in B light (Wu and Spalding, 2007). Similar to the phytochromes, the cryptochromes have a light-stable and a light-labile form: The light-independent proteins levels of cry1 enable plants to perceive high and low B light intensities. cry2 is rapidly degraded after B light exposure, hence functioning predominantly in low B light detection and photoperiod sensing (Ahmad and Cashmore, 1993; Lin et al., 1998; Mockler et al., 1999; Shalitin et al., 2002, 2003; Yu et al., 2007).

Another class of B light receptors are the phototropins, phot1 and phot2. The chromophore of these receptors is a flavin mononucleotide (FMN) which binds to the love

oxygen voltage (LOV) domain of the respective apoprotein (Christie, 2007). Phototropins are localized at the plasma membrane (Kong et al., 2006; Sakamoto and Briggs, 2002). Together both receptors are responsible for mediating phototropism towards unilateral B light, stomatal opening, chloroplast accumulation, cotyledon/leaf expansion and leaf hyponasty (Inoue et al., 2005; Kinoshita et al., 2001; Ohgishi et al., 2004; Sakamoto and Briggs, 2002; Wada et al., 2003).

Similar to phototropins, the ZTL family of photoreceptors perceives B light via a light-sensitive LOV domain (Banerjee and Batschauer, 2005). The ZTL family consists of three members: ZTL, FLAVIN-BINDING KELCH F-BOX 1 (FKF1) and LOV KELCH PROTEIN 2 (LKP2). All three members are localized in the cytosol and the nucleus (Takase et al., 2011). They play a role in circadian clock function and photoperiod-dependent flowering (Jarillo et al., 2001; Kiyosue and Wada, 2000; Nelson et al., 2000; Schultz et al., 2001; Somers et al., 2000).

Plants have also evolved a photoreceptor to specifically adapt to UV-B radiation called UVR8 (Yin and Ulm, 2017). Interestingly, UVR8 does not rely on a chromophore to perceive light but specific tryptophans within the protein (Christie et al., 2012; Rizzini et al., 2011). Presumably inactive UVR8 forms homodimers in the cytosol. Upon UV-B irradiation, the homodimers dissociate into active monomers that accumulate in the nucleus (Kaiserli and Jenkins, 2007; Rizzini et al., 2011). The most important functions of UVR8 are the mediation of UV-B-induced photomorphogenesis and stress acclimation (Brown et al., 2005).

1.1.2 The COP1/SPA complex represses photomorphogenesis in darkness

Sessile plants are not able to relocate when faced with unfavorable conditions. They respond by substantially altering their gene expression, thus achieving a remarkable plasticity. In Arabidopsis, approximately 20% of the genome is differentially regulated when seedlings are either grown in W light or darkness (Jiao, 2005). This genetic reprogramming is achieved through different transcription factors, that can bind to

light responsive elements (LREs) of their respective target genes, thus regulating gene expression (Jiao et al., 2007). Some of these transcription factors, such as the PIFs can be regulated by direct interaction with the photoreceptors (Leivar and Monte, 2014). PIFs belong to a basic-helix-loop-helix (bHLH) family of transcription factors with seven members. They mainly promote skotomorphogenesis and shade avoidance (Leivar and Monte, 2014). Upon light exposure photo-activated phytochrome (Pfr) is shuttled into the nucleus and interacts with the PIFs which in turn leads to a rapid degradation of PIF proteins (Al-Sady et al., 2006; Shen et al., 2005, 2007, 2008).

Many positive regulators of the light response are regulated post-translationally by the CONSTITUTIVE PHOTOMORPHOGENIC 1/SUPPRESSOR OF PHYTOCHROME A-105 (COP1/SPA) complex (Figure 2). The COP1/SPA complex predominantly acts in darkness to polyubiquitinate these positive regulators, thus marking them for degradation via the 26S proteasome (Hoecker, 2017; Lau and Deng, 2012; Menon et al., 2016). Well-studied targets of the complex are ELONGATED HYPOCOTYL 5 (HY5), a promoter of photomorphogenesis (Osterlund et al., 2000), LONG HYPOCOTYL IN FAR-RED 1 (HFR1), an inhibitor of shade avoidance (Jang et al., 2005; Yang et al., 2005), PRODUCTION OF ANTHOCYANIN PIGMENT 1 (PAP1), a promoter of anthocyanin accumulation (Maier et al., 2013), and CONSTANS (CO), a promoter of photoperiodic flowering (Jang et al., 2008; Laubinger et al., 2006; Liu et al., 2008).

COP1 was discovered in a mutant screen by the striking constitutively photomorphogenic phenotype of dark-grown seedlings exhibited by *cop1* mutants (Deng et al., 1991, 1992). A full knock-out of *COP1*, however, leads to an arrested development at the seedling stage (McNellis et al., 1994). Since its discovery *COP1* has been implicated in numerous other developmental processes beyond seedling photomorphogenesis stressing its importance for plant growth (Huang et al., 2014).

In Arabidopsis *COP1* is a single-copy gene which encodes a protein with three distinct domains: An N-terminal RING-finger domain, a central coiled-coil domain and a C-terminal WD40 repeat domain. A RING domain is typical for many E3 ubiquitin ligases

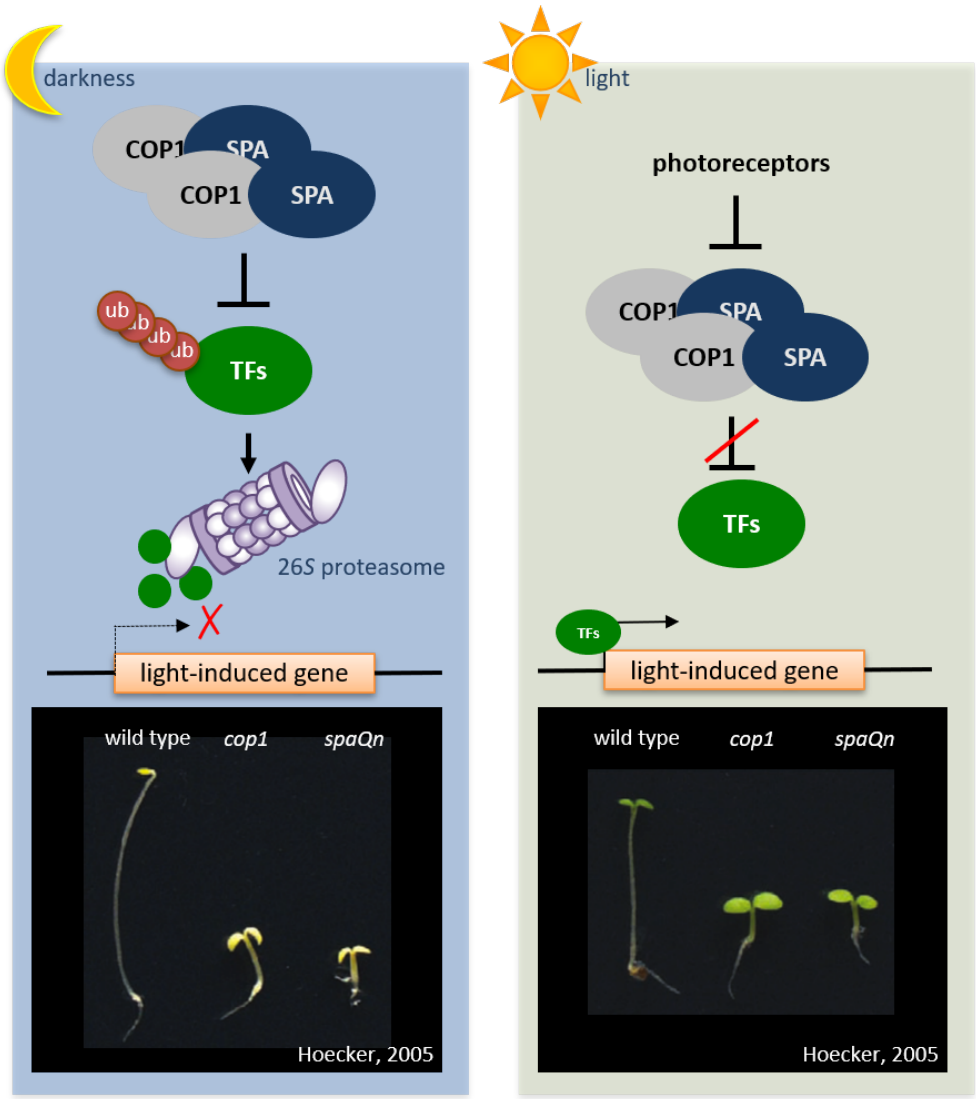

Figure 2: **The COP1/SPA complex is a central repressor of photomorphogenesis in darkness.**
The COP1/SPA complex polyubiquitinates photomorphogenesis-promoting transcription factors (TFs) in darkness. Subsequently polyubiquitinated transcription factors are degraded via the 26S proteasome. Light-activated photoreceptors can inhibit the E3 ubiquitin ligase activity of the COP1/SPA complex which leads to a stabilization of the substrates which can in turn exert their function as promoters of photomorphogenesis. In Arabidopsis *COP1* and *SPA* are necessary for an efficient repression of photomorphogenesis in darkness. *cop1* and *spaQn* mutants exhibit constitutive photomorphogenesis. Figure adapted from Artz (2014).

and often responsible for binding E2 ubiquitin conjugating enzymes (Freemont, 2000; Seol et al., 1999). *In vitro* COP1 possesses E3 ubiquitin ligase activity, polyubiquitinating targets such as LONG AFTER FAR-RED 1 (LAF1) (Osterlund et al., 2000; Seo et al., 2003; Yang et al., 2005). The coiled-coil domain is important for homodimerization and mediates interaction with the SPA proteins leading to a functional tetrameric complex of two COP1 and two SPA proteins (Hoecker and Quail, 2001; Saijo et al., 2003; Zhu et al., 2008). Substrate recognition is mediated via the WD40 repeat domain. This domain forms a seven-bladed β-propeller which binds to highly conserved Valin-Prolin (VP) motifs in substrate proteins (Holm et al., 2001; Uljon et al., 2016). Additionally, direct interactions with phytochromes and cryptochromes are established through the WD40 repeat domain (Seo et al., 2004; Wang et al., 2001).

To successfully suppress photomorphogenesis in darkness, COP1 acts in concert with SPA proteins. In Arabidopsis, four paralogs have been identified: *SPA1-4* (Laubinger and Hoecker, 2003). Analyses of higher order *spa* mutants suggest overlapping but distinct functions (Menon et al., 2016). While *SPA1* and *SPA2* act primarily in early plant development, *SPA3* and *SPA4* have their main functions in later developmental stages: *SPA1* and *SPA2* both suppress photomorphogenesis in darkness (Laubinger et al., 2004). In light, *SPA1* controls hypocotyl growth, leaf development and photoperiodic flowering (Fittinghoff et al., 2006; Laubinger et al., 2004, 2006). *SPA3* and *SPA4* mainly control vegetative plant growth (Laubinger and Hoecker, 2003; Laubinger et al., 2004). The shade avoidance response as well as photoperiodic flowering are mainly mediated by *SPA1* and *SPA4* (Rolauffs et al., 2012; Ordoñez-Herrera et al., 2015). Additionally, *spa1*, *spa3* and *spa4* single mutants exhibit an excessive light response at the seedling stage (Balcerowicz et al., 2011; Laubinger et al., 2004; Fittinghoff et al., 2006). *spa* quadruple knock-out plants (*spaQ*) exhibit strong constitutive photomorphogenesis, severe dwarfism and are day length-insensitive with regard to photoperiodic flowering (Laubinger et al., 2004; Ordoñez-Herrera et al., 2015). Notably, in contrast to *cop1* full knock-out mutants *spaQ* mutants do not arrest development at the seedling stage and can complete their entire life cycle (Ordoñez-Herrera et al., 2015).

SPA1 was originally identified through a screen for suppressors of the weak *phyA-105* allele (Hoecker et al., 1998). *SPA2-4* were subsequently found based on sequence homology. The four family members can be further classified into two groups: SPA1 and SPA2 derived from a gene duplication event and comprise the first group (Simillion et al., 2002). They both contain an N-terminal extension and NLSs, which are not found in SPA3 and SPA4, that comprise the second group (Laubinger and Hoecker, 2003; Laubinger et al., 2004). All SPA proteins contain an N-terminal kinase-like domain with sequence similarity to *bona fide* Serine/Threonine protein kinases, but have not been shown to exhibit any kinase activity. Moreover, similar to COP1, SPA proteins harbor a central coiled-coil and a C-terminal WD40 repeat domain. All domains are necessary for full SPA protein function mediating different protein-protein interactions. As described above, COP1/SPA complex formation is established by the coiled-coil domain (Hoecker and Quail, 2001; Saijo et al., 2003; Zhu et al., 2008). However, the kinase-like domain of SPA1 also contributes to this process (Holtkotte et al., 2016). phyA interacts with the kinase-like domain of SPA1 (Sheerin et al., 2015), while phyB interacts with the coiled-coil domain (Lu et al., 2015; Zheng et al., 2013). CRY1 mainly binds to the WD40 repeat domain (Lian et al., 2011; Liu et al., 2011) and CRY2 binds to the kinase-like domain (Zuo et al., 2011). Furthermore, there is evidence that the kinase-like domain modulates light-responsiveness among the SPA proteins as shown by domain swaps of SPA1 and SPA2 (Chen et al., 2016).

While COP1 alone has E3 ubiquitin ligase activity that can be modulated by SPA proteins *in vitro* (Saijo et al., 2003; Seo et al., 2003), current evidence suggests that the COP1/SPA complex acts as part of a higher order E3 ubiquitin ligase *in vivo*. It is likely that it forms a complex with CULLIN4 (CUL4), RING BOX 1 (RBX1) and DAMAGED DNA BINDING PROTEIN 1 (DDB1) (Chen et al., 2010). Here, CUL4 acts as a scaffold to bind DDB1 and RBX1. RBX1 is responsible for recruiting an E2 ubiquitin conjugating enzyme (Biedermann and Hellmann, 2011) and DDB1 is an adapter protein interacting with so-called DDB1-CUL4 ASSOCIATED FACTOR (DCAF) proteins, which contain WD40 repeats, in this case COP1/SPA (Chen et al., 2010).

The activity of the COP1/SPA complex is regulated via different mechanisms: Direct interaction with light-activated photoreceptors such as phyA, phyB or cry1 leads to a dissociation of the COP1/SPA complex (Lian et al., 2011; Liu et al., 2011; Lu et al., 2015; Sheerin et al., 2015). A second mechanism is the light-dependent nucleoplasmic partitioning of COP1. Light exposure leads to a rapid shuttling of COP1 from the nucleus into the cytoplasm (von Arnim and Deng, 1994; Pacin et al., 2014). This process leads to a physical separation of COP1 from its target proteins. Additionally, COP1 activity can be modulated by sumoylation via the SUMO E3 ligase SIZ1. Sumoylation of COP1 increases COP1 activity *in vitro*. *siz1* mutants are mildly hypersensitive to light and show features of constitutively photomorphogenic seedlings in darkness (Lin et al., 2016). The protein abundance of at least SPA1 and SPA2 is reduced by light. Particularly SPA2 protein is rapidly degraded below detectable levels in light (Balcerowicz et al., 2011). This rapid degradation is dependent on the interaction with COP1, suggesting that COP1 is responsible for ubiquitinating SPA2, thus marking it for degradation (Chen et al., 2015). Interestingly in darkness but not in light, COP1 and SPA1 protein levels are reduced by COP1 SUPPRESSOR 1 (CSU1) (Xu et al., 2014a). Finally PIF1, which is known for its skotomorphogenesis-promoting function on the transcriptional level, has been proposed to act as a molecular clamp strengthening the interaction of COP1 and SPA proteins in darkness, thus promoting the degradation of substrates such as HY5 (Xu et al., 2014b).

Although the majority of regulatory mechanisms aims to deactivate the COP1/SPA complex in the light, residual activity can be observed in light-grown Arabidopsis seedlings (Figure 2). Both *cop1* and *spaQn* mutant seedlings exhibit an enhanced light response when grown in the light. Interestingly, the photoreceptors phyA, phyB and cry2 are targets of the COP1/SPA complex, which could be a means to prevent this enhanced light response of the wild type (Jang et al., 2010; Shalitin et al., 2002; Seo et al., 2004).

1.1.3 HY5 promotes photomorphogenesis in light

One of the most well-studied targets of the COP1/SPA complex in Arabidopsis is HY5, a basic leucine zipper (bZIP) transcription factor (Jakoby et al., 2002). *HY5* was identified in a mutant screen as *hy5* light-grown mutant seedling exhibit a long hypocotyl (Koornneef et al., 1980). Chromatin-immunoprecipitation on a DNA microarray (ChIP-chip) coupled with RNA-sequencing (RNA-seq) revealed that HY5 can bind more than 9000 genomic loci and affects the expression of over 1100 genes (Zhang et al., 2011). Many of these genes are components of the light signaling cascade such as *FAR-RED ELONGATED HYPOCOTYL 1* (*FHY1*) or *HFR1* and are induced by HY5 (Lee et al., 2007; Li et al., 2010). Important genes for cell elongation such as *EXPANSIN 2* (*EXP2*) are being repressed (Jing et al., 2013). Additionally, HY5 induces genes of anthocyanin and chlorophyll biosynthesis (Gangappa and Botto, 2016). Interestingly, HY5 also induces its own expression in the light (Abbas et al., 2014; Binkert et al., 2014).

HY5 mainly exerts its function through the interaction with other proteins. Regarding light signaling, HY5 directly interacts with HFR1 and LAF1. This interaction has been proposed to stabilize all interaction partners, thus promoting photomorphogenesis (Jang et al., 2013). HY5 can indirectly influence nuclear phyA level by repressing FAR-RED ELONGATED HYPOCOTYL 3 (FHY3) and FAR-RED IMPAIRED RESPONSE 1 (FAR1), which are important for the expression of the phyA nuclear import complex (Lin et al., 2007). HY5 represses cell elongation by inhibiting the activity of PICKLE (PKL) after direct interaction (Jing et al., 2013). COP1 and SPA1 also directly interact with HY5 (Saijo et al., 2003). The interaction leads to polyubiquitination and subsequent degradation of HY5 (Ang et al., 1998; Osterlund et al., 2000). The COP1-mediated degradation of HY5 is promoted by all four SPA proteins (Zhu et al., 2008).

HY5 mRNA and protein levels are strongly positively correlated with light exposure in Arabidopsis seedlings (Osterlund et al., 2000). Phosphorylation of HY5 leads to a higher affinity to target promoter regions and COP1 (Hardtke et al., 2000).

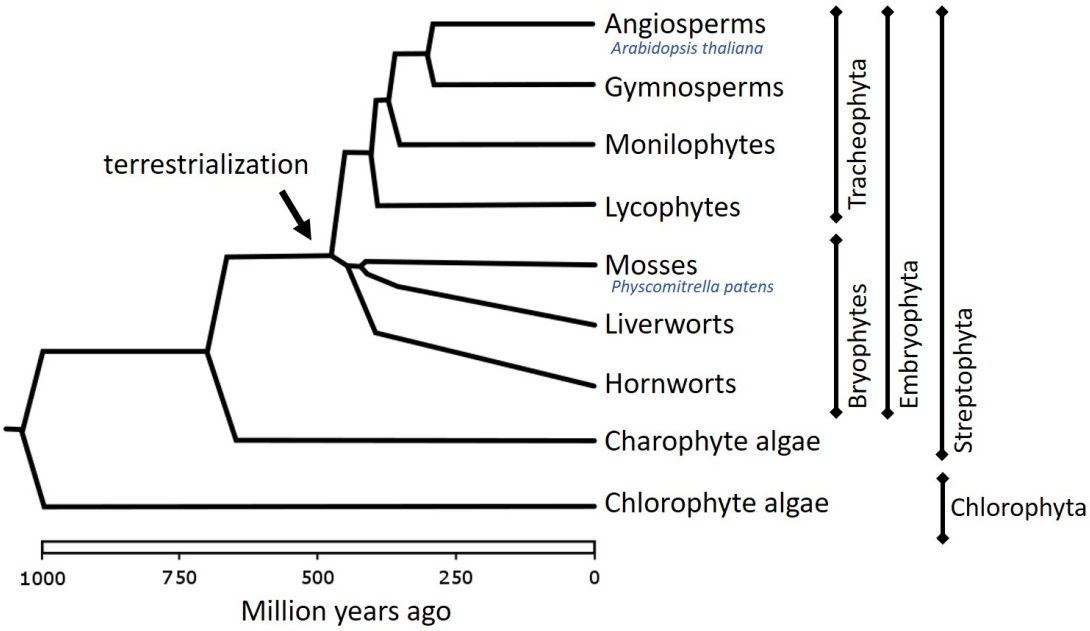

Figure 3: **Mosses are among the first diverged land plants.**
Viridiplantae can be divided into Streptophyta and Chlorophyta. Embryophyta comprise all land plants. Bryophytes are a monophyletic group that first diverged from the rest of the Embryophyta after terrestrialization. Figure adapted from Prigge and Bezanilla (2010).

1.2 Terrestrialization of plants was a crucial event in the history of life

Plants making the transition from living in water to living on land dramatically shaped the world as we know it. So far, there is no unison about the exact course of events: It is possible that green algae (Chlorophyta) first developed in freshwater and subsequently conquered the sea as well as the land (Dittami et al., 2017). The more likely scenario is that the first green algae evolved in a marine environment, transitioned to freshwater and then made the step onto land (Becker and Marin, 2009). What both scenarios have in common is that the last common ancestor of all land plants came from freshwater, not seawater.

Green plants or Viridiplantae, comprising both green plants and green algae, can be subdivided into two phyla: Chlorophyta and Streptophyta (Figure 3). The latter is

further subdivided into Charophyta (algae) and Embryophyta (land plants). Our current understanding is that Charophyta gave rise to the monophyletic group of Embryophyta (Bateman et al., 1998; Delwiche and Cooper, 2015; Wickett et al., 2014).

Bryophytes diverged from Tracheophyta (vascular plants) approximately 450 million years ago, temporally close to the the first terrestrialization of plants. Hence, groups directly related to bryophytes are thought to be the first plants to successfully colonize land (Kenrick and Crane, 1997). Bryophytes are subdivided into hornworts such as *Anthoceros agrestis*, liverworts such as *Marchantia polymorpha* and mosses such as *Physcomitrella patens*. The exact phylogenetic relationship within the bryophytes is not well-understood and various models have been proposed. The most likely scenario based on current evidence is that mosses and liverworts represent a monophyletic group identifying hornworts as the sister group to all other Embryophyta (Wickett et al., 2014).

In the process of evolving from a freshwater- to a land-adapted plant, early organisms had to solve a plethora of different issues: For example water limitations, strong temperature fluctuations, new pathogen attacks and mineral scarcity had to be dealt with. Another challenge were novel light conditions: Water has the capacity to reduce the intensity of photosynthetically active and UV-B light much more than air. Additionally, suspended particles of organic or inorganic matter can further decrease light intensity (Maberly, 2014). The consequence of a higher fluence rate on land can be beneficial due to a higher photosynthetic rate but also harmful due to more photodamage. Competition for light might have been the driving force for innovations such as lignin production and lateral meristems as these are the basis for growing tall and complex growth programs such as the shade avoidance syndrome. Notably, plants also compete for light in an aquatic habitat, where for example planktonic algae might significantly reduce the amount of light penetrating deeper layers of water (Talling et al., 1973).

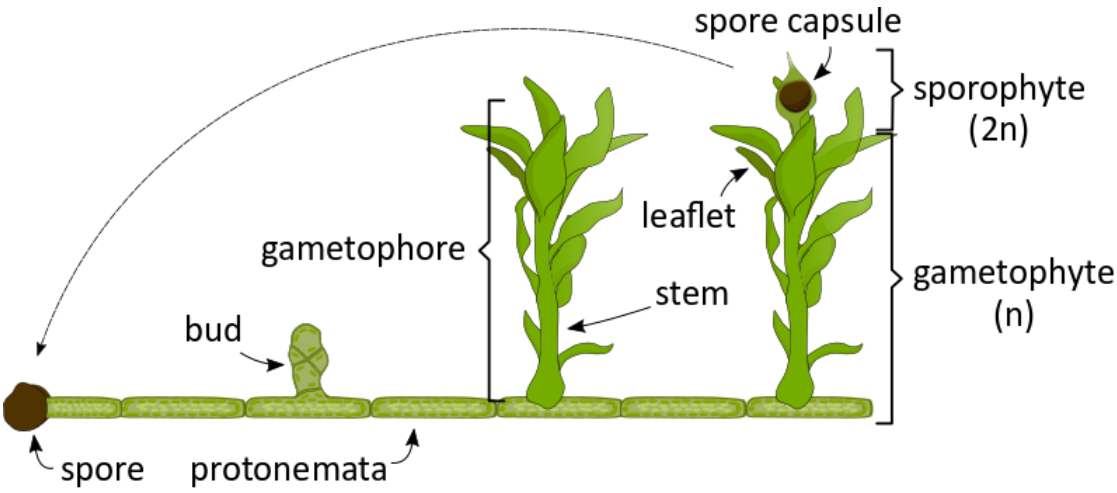

Figure 4: **Life cycle of Physcomitrella**
The lifecycle of Physcomitrella starts with the germination of protonemata from a spore. When protonemal filaments age, they produce buds that develop into leafy gametophores. On top of the gametophores sexual organs will form that, after fertilization, give rise to the sporophytic spore capsule containing new spores.

1.3 *Physcomitrella patens* is a model organism for early land plant evolution

Early diverged land plants such as the moss *Physcomitrella patens* are valuable models to understand plant terrestrialization and infer evolutionary events or processes. Very few fossil records have helped with the basic categorization but molecular and genetic analyses are necessary to comprehend the evolutionary conservation of molecular pathways such as light signal transduction. Physcomitrella makes it possible to investigate how early plants were already preadapted to the new environment and which innovations had to evolve to ensure reproductive success.

Physcomitrella is an established model organism to study land plant evolution (Frank et al., 2005; Prigge and Bezanilla, 2010). Like many other plants Physcomitrella exhibits an alternation of generations: A haploid gametophyte and a diploid sporophyte (Figure 4). In Physcomitrella, the haploid gametophyte is the dominant phase. Protonemal filaments germinate from spores representing the juvenile stage of the gametophyte. The first filament to germinate is always a chloronemal filament harboring many chloroplasts and

having perpendicular cell walls between adjacent cells. This filament grows by apical growth and can develop into caulonemal filaments with fewer chloroplasts and oblique cell walls between adjacent cells. Based on their morphology it is thought that chloronemata have more of an assimilatory function, while caulonemata are more important to extend the plant area and colonize more substrate. The transition from the juvenile to the adult stage of the gametophyte is represented by the development of buds that grow into leafy shoots, called gametophores. Physcomitrella is monoecious and develops both antheridia and archegonia on the same gametophore. Motile spermatozoids move from the male to the female gametes under moist conditions, very often leading to self-fertilization. After fertilization the diploid sporophyte comprises a short seta with a spore capsule on top. A single spore capsule contains approximately 4000 spores (Engel, 1968).

Several different traits make Physcomitrella a particularly useful model organism: The plant can go through its entire life cycle in the laboratory. It can easily be propagated clonally by tissue disruption and subsequent cultivation. Most cells can regenerate to whole plants without external application of hormones. Moreover, the Physcomitrella genome has been sequenced and annotated (Rensing et al., 2008). Since the first draft genome, assemblies and annotations have been incrementally improved so that a chromosome-scale assembly is now publicly available (Lang et al., 2016, 2018). Physcomitrella protoplasts can efficiently be transformed via polyethylene glycol (PEG) (Schaefer and Zrÿd, 1997). In addition to gene targeting via homologous recombination, the CLUSTERED REGULARLY INTERSPACED SHORT PALINDROMIC REPEATS/CRISPR-associated protein 9 (CRISPR/Cas9) technology was established for Physcomitrella to generate single and higher order mutants (Collonnier et al., 2017; Lopez-Obando et al., 2016).

1.4 Components of the light signaling cascade are highly conserved

The vast majority of Viridiplantae rely on light as their primary energy source. An endosymbiosis established between an early eukaryote and a Cyanobacterium around 1 to 1.5 billion years ago enabled early plants to perform photosynthesis (McFadden, 2001). Since then using light most efficiently was utterly advantageous for these organisms to

harvest the most energy and thus gain a competitive advantage. Therefore, components of the light signaling pathway as it is described for higher plants can also be found in green algae. *Chlamydomonas reinhardtii*, the most prominent model organism to study Chlorophyta, posseses a whole host of photoreceptors: Similar to higher plants, Chlamydomonas harbors genes encoding cryptochromes, phototropins and UVR8. However, unlike plants it also expresses rhodopsin-like photoreceptors, that are more closely related to photoreceptors found in animals. Notably, no phytochrome-encoding genes were found in Chlamydomonas (Kianianmomeni and Hallmann, 2014). Knowledge about the signaling mechanisms beyond the photoreceptors is very sparse. Based on sequence homology Chlamydomonas harbors one gene encoding COP1, but no gene encoding SPA (Merchant et al., 2007). The most well-studied Charophyte with respect to light signaling is *Mougeotia scalaris* but also here molecular processes are not well understood (Kianianmomeni and Hallmann, 2014). Notably, the genome of the closely related Charophyte *Klebsormidium nitens* encodes for one putative homolog of COP1 and one of SPA (Hori et al., 2014).

Light responses and the underlying molecular mechanisms were also investigated in early diverged land plants, especially in *Physcomitrella patens*. Similar to higher plants, the growth and development of Physcomitrella is influenced by light throughout the entire life cycle. Spores mainly germinate if they have been exposed to W or R light, although spores also germinate in B and FR light at very low rates (Cove et al., 1978). Light-grown protonemata and gametophores show phototropic growth towards unilateral W or R light, unlike in higher plants where phototropism is mainly mediated by B light (Cove et al., 1978). Moreover, chloroplast relocation, side branching and gametophore development are controlled by R and B light in Physcomitrella (Imaizumi et al., 2002; Kadota et al., 2000; Uenaka et al., 2005; Uenaka and Kadota, 2007).

In darkness, Physcomitrella plants produce more caulonemal filaments, whereas the production of chloronemal filaments is substantially reduced. Additionally, caulonemata exhibit a negatively gravitropic growth response in darkness, which is abolished when

grown in the light (Cove et al., 1978; Jenkins et al., 1986). Although no new gametophores are initiated in darkness, already established gametophores continue to grow. They exhibit an etiolation-like response in that the stem elongates much more than in light. Leaflets are initiated on the stem, but stop developing quickly and remain relatively small (Cove et al., 1978). Interestingly, protonemata as well as gametophores show a light-grown phenotype if the darkness treatment is broken by a daily 1 h R light pulse. If the R light pulse is followed by a 15 min FR light pulse, the dark-grown phenotype is maintained, suggesting the involvement of phytochromes in this process (Cove et al., 1978).

Indeed, the Physcomitrella genome contains seven genes encoding phytochromes (*PpPHY1-PpPHY4* and *PpPHY5A-C*) (Li et al., 2015). The paralogs probably emerged from whole genome duplication events after Physcomitrella diverged from the first vascular plants. Hence, *PpPHY* genes cannot be assigned to the type I or type II clades of phytochromes in higher plants but are more similar to *AtPHYB* based on sequence homology (Mathews, 2006). Reports on the subcellular localization of the Physcomitrella phytochromes are partly contradicting: Uenaka and Kadota (2007) report that YFP-fusion proteins of PpPHY1-PpPHY4 are localized in the cytoplasm of protoplasts after 12 h in darkness and that localization does not change after R light irradiation. In contrast, Possart and Hiltbrunner (2013) describe a light-induced nuclear accumulation of endogenous PpPHY1-PpPHY4. Single knock-out mutant analysis of *PpPHY1-4* revealed that *PpPHY4* is most important for the phototropic response of protonemal filaments and the chloroplast accumulation response (Mittmann et al., 2004). The chloroplast avoidance response is mostly regulated by *PpPHY1-3* (Uenaka and Kadota, 2007). To generate phytochrome-signaling deficient mutants, that mimic complete phytochrome knock-out mutants, enzymes necessary for phytochromobilin biosynthesis were targeted (Chen et al., 2012). Knocking out *LONG HYPOCOTYL 2* (*HY2*) and *PHYCOUROBILIN SYNTHASE* (*PpPUBS*) was sufficient to effectively inhibit phytochromobilin biosynthesis. *Pphy2 Pppubs* double mutant plants have a smaller colony diameter than wildtype plants in W and R light. Gametophores of the double mutant plants show an elongation response in W light and a growth arrest in R light. Due to the underdeveloped leaflets in

R light, these gametophores look very similar to etiolated dark-adapted gametophores (Cove et al., 1978).

Interestingly, phytochromes in Physcomitrella can mediate a far-red high-irradiance response (FR-HIR), which was thought to be unique to seed plants and mediated exclusively via phyA (Possart and Hiltbrunner, 2013). However, PpPHY1 and PpPHY3 are rapidly degraded after light-activation thus mediating FR light responses. Moreover, the homolog of *AtFHY1* in Physcomitrella (*PpFHY1*) is essential for these responses. Analogous to Arabidopsis, PpFHY1 most likely facilitates the nuclear import of PpPHY proteins. On the molecular level, light-induced alternative splicing events are mainly regulated via PpPHY2 and PpPHY4 (Wu et al., 2014).

The fact that phytochromes in Physcomitrella can elicit responses that are vectorial such as phototropism and are too quick to be explained by an altered gene expression such as chloroplast movement suggests a function of these photoreceptors at the plasma membrane or the in the cytosol. Indeed, a subpopulation of PpPHY4 interacts with phototropins at the plasma membrane after illumination with R light (Jaedicke et al., 2012).

Physcomitrella possesses four phototropin-encoding genes: *PpPHOTA1, PpPHOTA2, PpPHOTB1, PpPHOTB2*, that expanded from a single *PHOT* after the divergence from seed plants (Kasahara, 2004). Similar to higher plants, phototropins in Physcomitrella are localized at the plasma membrane (Jaedicke et al., 2012). All four phototropins control the B and R light-mediated chloroplast avoidance response (Kasahara, 2004). Moreover, phototropins and phytochromes are involved in the light induction of protonemal side branching (Uenaka et al., 2005).

B light is not only perceived via phototropins, but also cryptochromes in Physcomitrella. The two paralogs *PpCRY1a* and *PpCRY1b* are almost identical, hence the encoded proteins differ in only one amino acid (Imaizumi et al., 2002). PpCRY1a and PpCRY1b constitutively localize in the nucleus. Mutant analysis revealed that both cryptochromes mediate B light-induced branching of protonemal filaments and are important for the tran-

sition from chloronemal to caulonemal filaments. Additionally, both cryptochromes play a role in gametophore development. In B light *Ppcry1ab* double mutant lines produce fewer gametophores than wild-type plants, possibly due to the general reduction in side branch initials. Gametophores grown in B light exhibit increased stem elongation and reduced leaf development, a phenotype reminiscent of dark-adapted wild-type gametophores as described in Cove et al. (1978) (Imaizumi et al., 2002).

Outside the visible spectrum, Physcomitrella can also perceive UV-B light, most likely via two encoded AtUVR8 homologs (Rensing et al., 2008; Richardt et al., 2007). Until now, molecular and physiological responses have only been investigated in wild-type Physcomitrella plants (Wolf et al., 2010). When irradiated with UV-B light, colonies have a smaller diameter but produce more gametophores. Interestingly, gametophores can tolerate more UV-B light than Arabidopsis seedlings and can regenerate after being substantially bleached. Microarray data show a highly specific molecular response to UV-B irradiation with the induction of 12 putatively orthologous genes to the Arabidopsis UV-B response.

Signaling mechanisms downstream of the photoreceptors have been investigated, but our current understanding of the light signaling cascade in Physcomitrella is very limited. One conserved component are the *PIF* genes. Four *AtPIF* orthologs were identified in Physcomitrella (Possart et al., 2017). They are localized in the nucleus and interact with phytochromes in a light-dependent manner. Moreover, PpPIF proteins can complement an Arabidopsis *pif* quadruple mutant phenotype (Xu and Hiltbrunner, 2017).

Both *COP1* and *SPA* genes are conserved in Physcomitrella as well. Based on sequence homology nine paralogs of *PpCOP1* (*COP1a-i*) were found (Ranjan et al., 2014; Rensing et al., 2008; Richardt et al., 2007). Given that *COP1* in *Arabidopsis thaliana* is a single copy gene, it is likely that the expansion of the *PpCOP1* gene family has happened after the divergence of Physcomitrella and Arabidopsis. All PpCOP1 proteins contain all three functional domains identified in AtCOP1: A RING-finger, coiled-coil and WD40 repeat domain. Functionally *PpCOP1a* is highly conserved as it can almost fully

reconstitute the wild-type phenotype of *cop1* mutant plants in Arabidopsis (Ranjan et al., 2014). In contrast to the quartet of four *SPA* genes in Arabidopsis, the genome of Physcomitrella harbors two SPA-encoding genes (*PpSPAa* and *PpSPAb*) that are most similar to *AtSPA1* and *AtSPA2*. The N-terminal kinase-like domain, the coiled-coil domain and the WD40 repeat domain found in AtSPA proteins are conserved in both Physcomitrella homologs. Expression of PpSPAb in Arabidopsis higher order *spa* mutant plants does not complement the mutant phenotype, suggesting a higher degree of evolutionary divergence than observed for *PpCOP1a* (Ranjan et al., 2014).

In addition to *PpCOP1* and *PpSPA* putative targets of a PpCOP1/PpSPA complex were identified: Besides three AtCO-like orthologs (Shimizu et al., 2004; Zobell et al., 2005), two orthologs of AtHY5 (*PpHY5a* and *PpHY5b*) exist in Physcomitrella (Yamawaki et al., 2011b). Both paralogs redundantly regulate the protrusion of caulonemata from the main colony in that *Pphy5ab* double mutant plants develop very few protruding filaments in light and darkness. Gametophore development is not reported to be affected in these mutants. The expression of *PpHY5a* is induced by light, whereas expression of *PpHY5b* is relatively stable. Transgenic Arabidopsis seedlings overexpressing the bZIP domain of PpHY5a exhibit a phenotype similar to *AtHY5* overexpressing lines, which suggests a conserved function in the light signaling pathway (Yamawaki et al., 2011b). Interestingly, *PpHY5b* transcripts are alternatively spliced in light leading to up to nine PpHY5b isoforms of various lengths (Wu et al., 2014).

2 Aims

During the course of evolution plants have evolved a sophisticated regulatory network to optimally react to constantly changing ambient light conditions, thus ensuring reproductive success. Higher plants have evolved the COP1/SPA complex as a major regulator for light-dependent growth and development. Research of the molecular mechanisms underlying the function of the complex have greatly expanded our knowledge about the light signaling cascade. However, while the COP1/SPA complex has been investigated in angiosperms to a great extent, the knowledge about its evolutionary conservation is still very limited. Especially the exact role of the *SPA* genes in the complex are not well understood. Hence, this thesis aimed to elucidate the evolutionary conservation of the COP1/SPA complex by investigating its role in the early diverged land plant *Physcomitrella patens*:

(1) Generating *PpspaAB* double knock-out lines via CRISPR/Cas9

While one set *PpspaAB* double knock-out mutants was generated via homologous recombination prior to this project, I generated another set via CRISPR/Cas9 to establish CRISPR/Cas9 as a method for targeting multiple genes at the same time and to have a genetically independent set of mutant plants.

(2) Elucidating the role of *SPA* genes in Physcomitrella growth and development

So far, there have been almost no studies about the evolutionary conservation of the COP1/SPA complex. To better understand the role of *PpSPAa* and *PpSPAb* in Physcomitrella growth and development, double knock-out lines were extensively phenotyped on the visual and molecular level.

(3) Analysing the putative COP1/SPA target PpHY5b in Physcomitrella

If COP1 and SPA in Physcomitrella regulate protein levels of light signaling intermediates has not been investigated. Hence, I investigated whether PpHY5b might be regulated by PpCOP1/PpSPA in Physcomitrella.

3 Results

3.1 *PpspaAB* double knock-out lines generated via homologous recombination harbor multiple insertions

One of the most important steps to elucidate gene function is the generation of knock-down or knock-out mutants as an important tool for reverse genetics. Gene targeting has been used in Physcomitrella since the 1990s to specifically mutate genes *in planta*. The long-standing method of choice was using Physcomitrella's capacity to perform homologous recombination at extraordinarily high rates (Schaefer and Zrÿd, 1997). However, whereas targeting can be very efficient, concatenation and multiple integration of the knock-out constructs frequently occur (Kamisugi et al., 2006). Especially off-site integrations diminish the scientific value of generated mutant plants because phenotypic observations might not be attributed to the disruption of the respective gene-of-interest alone.

To investigate the function of *PpSPAa* and *PpSPAb*, double knock-out lines (*PpspaAB)* had been generated previously via homologous recombination (Dickopf, 2015). Here, *PpSPAb* was targeted first. Subsequently, *PpSPAa* was knocked out in *PpspaB* line 7-3-A1 resulting in *PpspaAB* double knock-out lines, that are independent for the *PpspaA* but not the *PpspaB* locus. Transgenic lines were genotyped for the presence or absence of the knock-out cassette and its insertion site. However, the occurrence of unintended integration events was not tested previously.

Being independent for the *PpspaA* locus, transgenic plants were only tested for the *PpspaB* locus via Southern blotting (Figure 5). The probe was designed to hybridize with a specific region in the second intron of the *PpSPAb* genomic locus (Figure 5 A). This region was used as a flanking region for the adjacent knock-out cassette to replace exon 3 and should remain intact after successful targeting. The restriction enzyme HindIII has a predicted restriction site right before this region and another restriction site in intron 3. Hence, the probe was predicted to hybridize with a 1550 bp gDNA fragment after HindIII

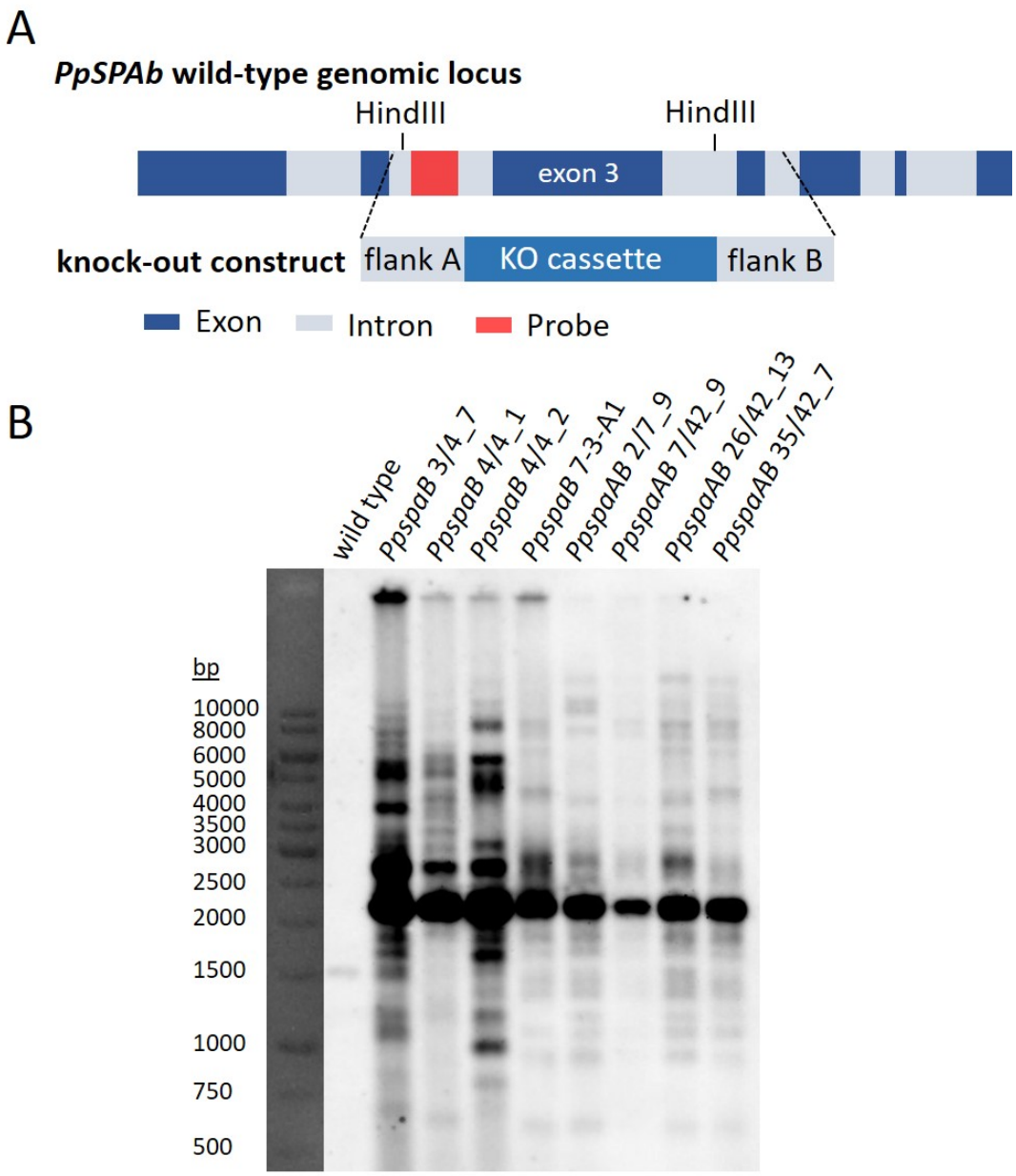

Figure 5: ***PpspaB* and *PpspaAB* mutant lines harbor multiple insertions of the knock-out construct.**
A. Schematic representation of the *PpSPAb* genomic locus and the construct used to generate *PpspaB* knock-out lines. **B.** Southern Blot of *PpspaB* and *PpspaAB* lines. The probe was designed against a region in flank A. After digestion of genomic DNA with HindIII the probe was predicted to hybridize with DNA fragments of 1550 bp (wild-type allele) or 2182 bp (knock-out allele).

digestion in the wild type. After successful replacement of exon 3 with the knock-out cassette, the gDNA fragment for hybridization was predicted to be 2182 bp in size. For the wild type, one distinct band at 1550 bp was detected. All tested single or double mutants exhibited a complex band pattern after Southern blotting. A prominent band at 2182 bp indicated the correct insertion of the knock-out cassette. Additional bands represented a range of fragments of more than 10.000 bp to less than 750 bp in size. Larger fragments than the predicted 2182 bp could be a sign for concatenated integration or an incomplete digestion. A very high molecular weight band in the pockets of most lanes indicates, that not all gDNA samples were fully digested. Bands representing fragments less than 2182 bp in size are likely a sign of ectopic integration. Notably, the signal derived from the probe hybridized to wild-type gDNA was substantially weaker than when hybridized to mutant gDNA. The signal representing the predicted fragment size of 2182 bp was particularly strong. Since the same amount of gDNA was loaded for all samples, it is possible that an increased signal strength indicated concatenated integration of the knock-out construct. In conclusion, Southern blotting revealed that all tested *PpspaB* single and *PpspaAB* double mutants generated via homologous recombination probably harbor ectopic integrations of the knock-out cassette at unknown sites in the genome. Concatenated integrations cannot be excluded. Therefore, these lines alone are not sufficient to derive hypotheses about *PpSPA* function.

3.2 *PpspaAB* double knock-out lines were generated using CRISPR/Cas9

To circumvent the described shortcomings of the *PpspaAB* double knock-out lines generated via homologous recombination, a new set of knock-out mutants was generated. To this end, the CRISPR/Cas9 technology for Physcomitrella as described in Collonnier et al. (2017) and Lopez-Obando et al. (2016) was established. In this method a plasmid encoding a codon-optimized version of the *Streptococcus pyogenes* Cas9 driven by the rice Actin 1 promoter was transformed into Physcomitrella protoplasts. At the same time resistance to G418 was introduced by cotransforming the pBNRF plasmid encoding a 35S-driven neoR cassette (Schaefer et al., 2010). Two sgRNAs per locus

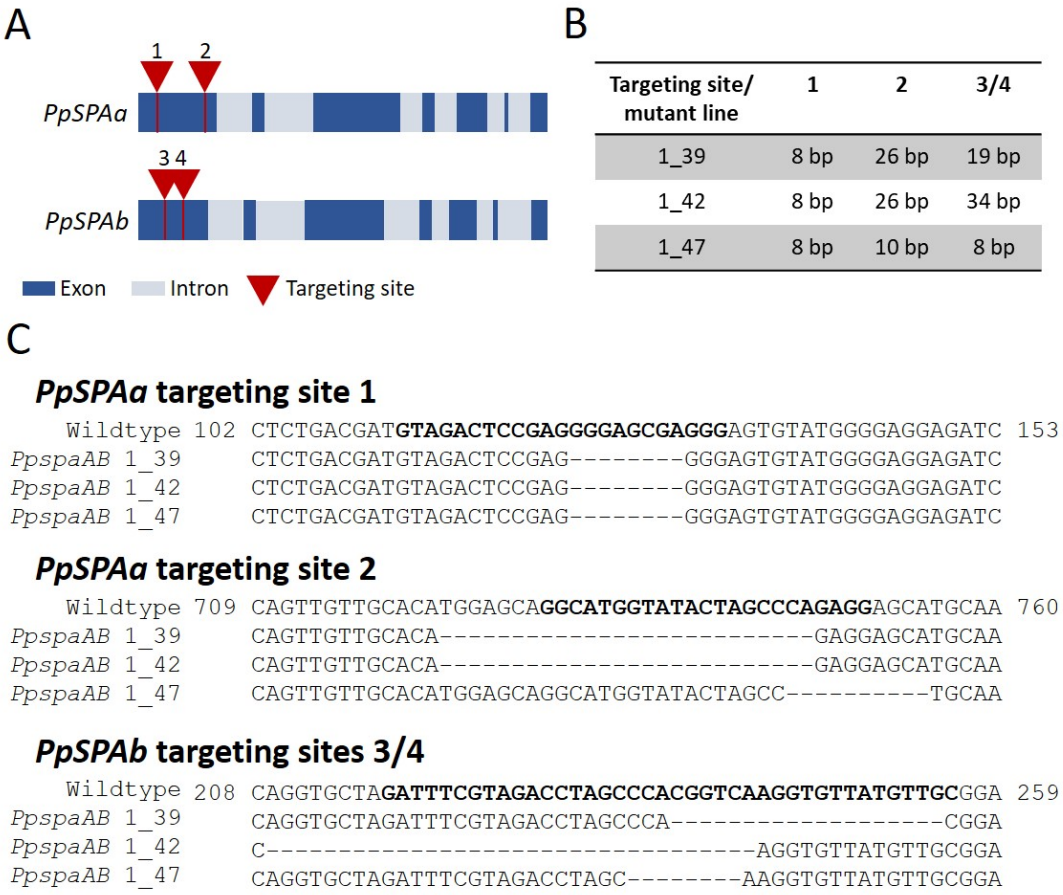

Targeting site/ mutant line	1	2	3/4
1_39	8 bp	26 bp	19 bp
1_42	8 bp	26 bp	34 bp
1_47	8 bp	10 bp	8 bp

Figure 6: ***PpspaAB* double knock-out lines were generated using CRISPR/Cas9.** **A.** Schematic representation of the *PpSPAa* and *PpSPAb* genomic loci and the positions targeted via CRISPR/Cas9 through four different sgRNAs. **B.** Summary of deleted basepairs in respective mutant lines on all loci. **C.** Multiple sequence alignments of targeted loci in wild-type and three independent PpspaAB double knock-out lines. Numbers flanking the sequence indicate the position at the genomic locus with the START-codon as position 1. Regions for sgRNA hybridization are highlighted in bold.

were designed to hybridize to the first exon of *PpSPAa* or *PpSPAb*, respectively, using the web-based CRISPOR program (Haeussler et al., 2016) (Figure 6 A, Supplemental Table S1). Different combinations of sgRNA-encoding plasmids were transformed into protoplasts targeting either one or two sites per gene (Supplemental Table S3). After transformation, regenerating plants were genotyped by Sanger sequencing of the *PpSPAb* targeting site first. Individuals harboring a mutation that leads to a premature stop

codon in the first exon were further analyzed with respect to a premature stop codon in the first exon of *PpSPAa*. Three different lines (1_39, 1_42 and 1_47) were isolated as novel *PpspaAB* double knock-out lines and used for further analyses (Figure 6 B, C). All three lines harbor an 8 bp deletion as well as a 26 bp or 10 bp deletion in *PpSPAa*. In *PpSPAb* mutations vary among the lines, ranging from 8 bp to 34 bp deletions. For each sgRNA three to five off-targets were predicted and Sanger-sequenced (Supplemental Table S2). None of these off-targets were modified in any of the analyzed lines. Interestingly, 41 of 43 lines, that regenerated after G418 selection and were sequenced, showed a modification at the *PpSPAb* locus. All lines that were then tested at the *PpSPAa* locus were modified on both targeting sites, indicating a very high efficiency of CRISPR/Cas9 in *Physcomitrella patens*. Notably, 34 of 43 lines exhibited 6, 9 or 12 bp deletions at the *PpSPAb* locus not leading to a premature stop codon (Supplemental Table S3).

3.3 *Ppspa* mutant lines exhibit retarded gametophore development

In *Arabidopsis thaliana* both components of the COP1/SPA complex are essential to effectively repress photomorphogenesis in darkness (Hoecker, 2017). *AtSPA* quadruple knock-out mutants (*spaQ*) show features of light-grown seedlings when grown in complete darkness (Laubinger et al., 2004). Additionally, these plants exhibit severe dwarfism in the adult stage and produce very few seeds, indicating that the *AtSPA* genes play an important role not only in seedling skotomorphogenesis but also in later developmental stages of the plant (Laubinger et al., 2004).

When Physcomitrella *Ppspa* single or double mutant lines were grown in long-day conditions (16 h light, 8 h darkness) retarded development of gametophores, the adult structures of the plant, was observed (Figure 7). Single gametophores were inoculated and incubated in long-day W light conditions at 100 μmol $m^{-2}s^{-1}$ W light for 35 d. All tested single mutant lines as well the double mutant lines 26/42_13 and 35/42_7 were generated using homologous recombination (Dickopf, 2015). The double mutant lines 1_39, 1_42 and 1_47 were generated using CRISPR/Cas9. Gametophores of *PpspaA* mutants exhibited a length reduction of about 50-70 % when compared to wild-type

gametophores. Depending on the respective line, gametophore length in *PpspaB* mutant lines was not significantly reduced (lines 3/4_7 and 4/4_1) or reduced to about 65 % of the wild-type length in *PpspaB* mutant line 7-3-A1. Notably, this line was used to knock-out *PpSPAa* via homologous recombination to generate the double mutant lines described above. All of the tested *PpspaAB* double knock-out lines showed a highly significant reduction in gametophore size ranging from approximately 15-40 % of the wild-type gametophore length. Apart from the reduced size no striking aberration from the wild-type gametophore phenotype was observed (Figure 7 A).

To further characterize the growth of Physcomitrella gametophores, plants were grown in monochromatic R light (46 μmol m^{-2}s^{-1}) for 21 d (Figure 8). Gametophore length and leaflet number were significantly reduced in both investigated mutants when compared to the wild type. Size reduction in R light was slightly less pronounced (25-45 % reduction compared to wild type) than in W light. Gametophores of the *PpspaAB* double mutants were shorter and had fewer leaflets than the wild type (Figure 8 D), indicating that the observed growth defect is not due to true dwarfism but rather caused by a retarded development of the adult plant. Cell sizes in the stem of gametophores were measured to determine whether the observed effect was due to a change in cell size or cell number (Figure 8 E). Since the differences in cell area were not significant between the tested genotypes, it is very likely that smaller gametophores in the *PpspaAB* double mutant lines are due to a lower cell number.

One of the most striking phenotypes of the Arabidopsis *spaQ* mutants is constitutive photomorphogenesis. These plants are unable to maintain skotomorphogenesis emphasizing the importance of *AtSPA* genes in darkness. Although true photomorphogenesis vs. skotomorphogenesis is not well-defined for Physcomitrella, gametophores grown in darkness show an etiolation response similar to Arabidopsis seedlings: While no new gametophores are initiated in the absence of light, existing gametophores continue to grow. Stem elongation is increased when compared to growth in light and leaflets are initiated but remain small (Cove et al., 1978). This response is not altered in Physcomitrella

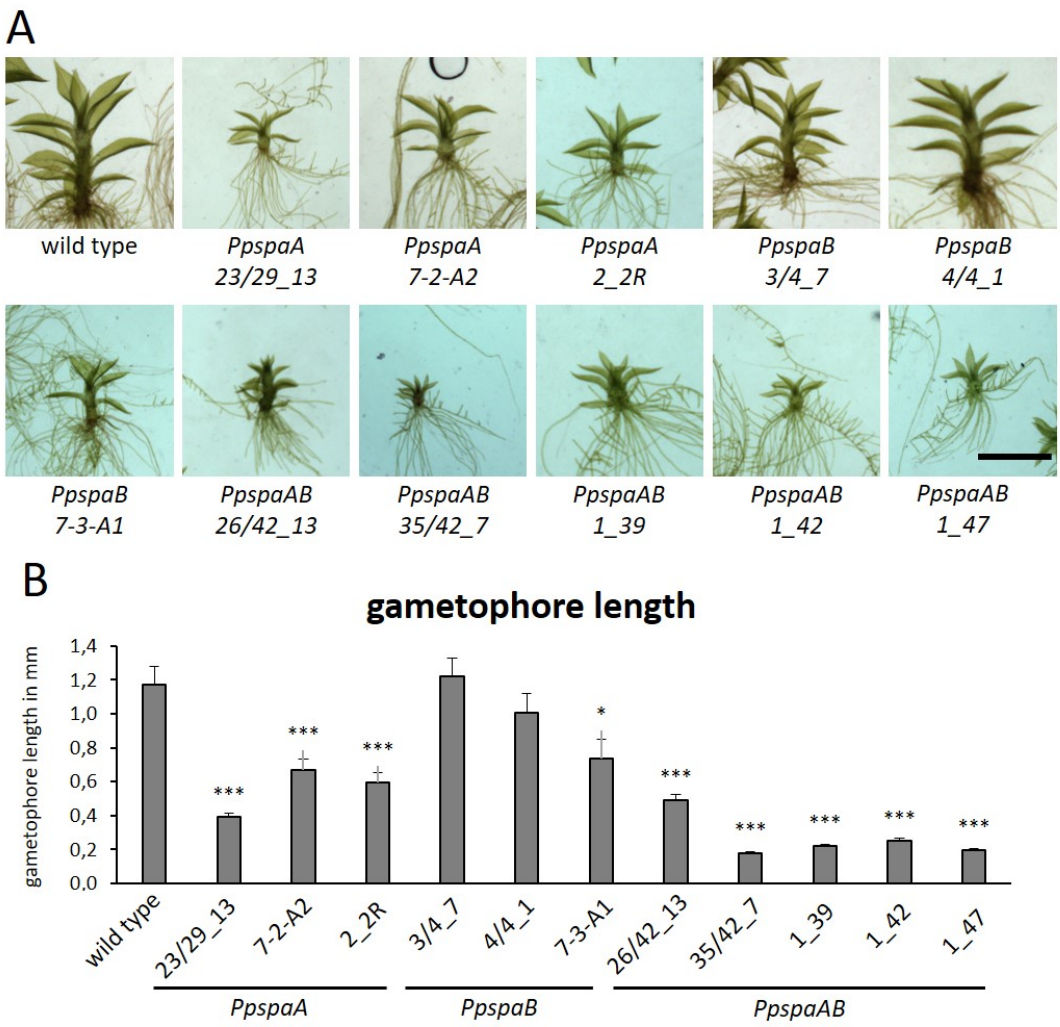

Figure 7: ***PpSPAa* and *PpSPAb* regulate gametophore growth in long-day conditions.** **A.** Representative pictures of isolated gametophores of wildtype, *PpspaA*, *PpspaB* and *PpspaAB* mutant lines grown in long-day conditions (80 μmol m^{-2}s^{-1} W light) for 35 d. Scale bar represents 1 mm. **B.** Quantification of gametophore lengths. Error bars represent SEM (n $\geq$ 29). Asterisks indicate significant differences between wildtype and the respective mutant line (t-test, *P $<$ 0.05, **P $<$ 0.005, ***P $<$ 0.0005).

SPA double knock-out lines (Figure 9): Gametophores of plants grown in long-day conditions were transferred to fresh growth medium and incubated for another week in long-day conditions. Afterwards gametophores were transferred to darkness on medium supplemented with 0.5% glucose for two weeks. Gametophore tissue that had newly

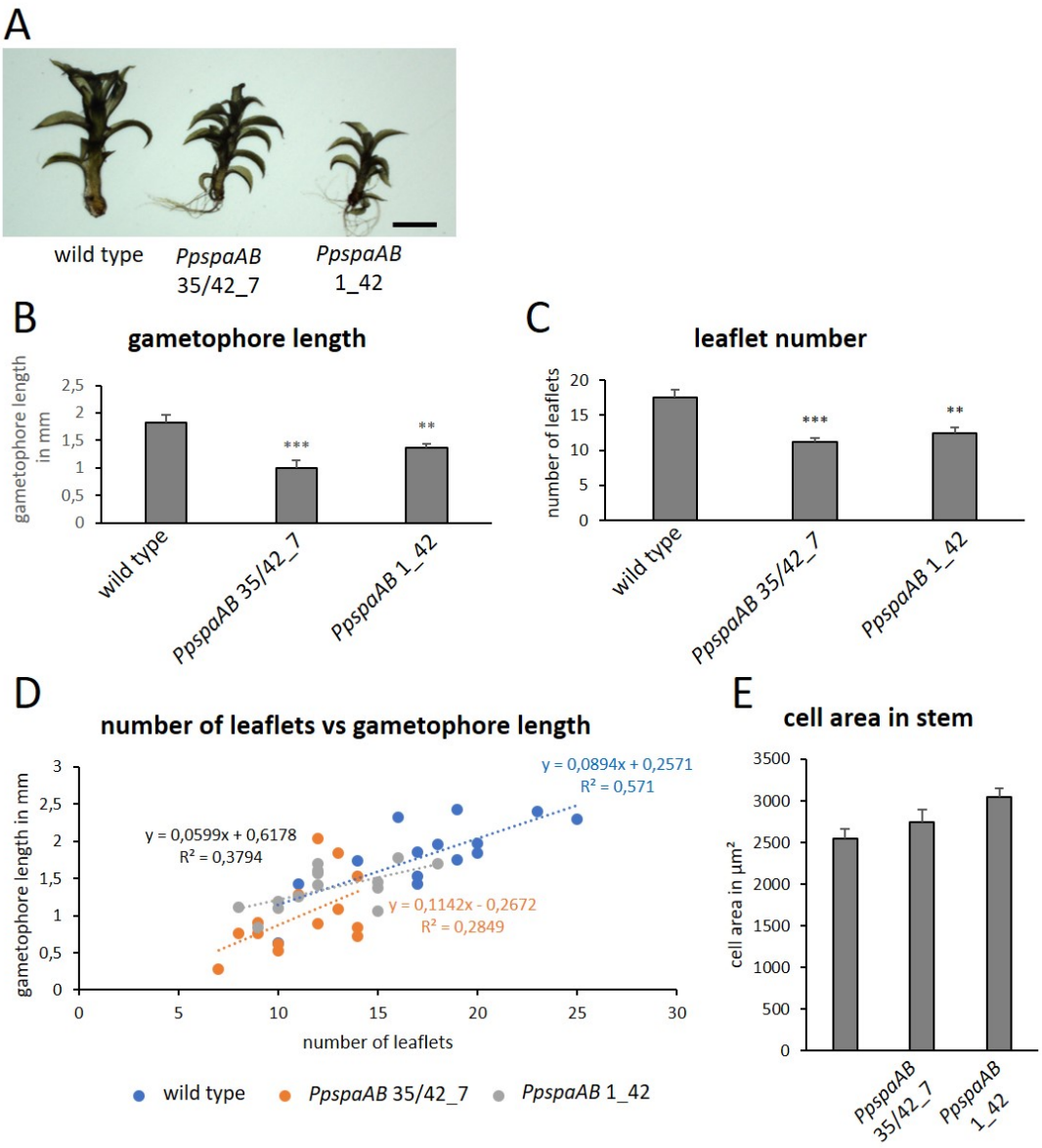

Figure 8: ***PpSPAa* and *PpSPAb* regulate gametophore growth in R light.**
A. Representative pictures of isolated gametophores of wildtype and PpspaAB mutant lines grown in continuous R light (46 μmol m^{-2}s^{-1}) for 21 d. Scale bar represents 1 mm. **B.** Quantification of gametophore lengths. Error bars represent SEM (n = 14). Asterisks indicate significant differences between wildtype and the respective mutant line. **C.** Quantification of number of leaflets per gametophore. Error bars represent SEM (n = 14). Asterisks indicate significant differences between wildtype and the respective mutant line. **D.** Number of leaflets are plotted against the length of each gametophore. A regression line was calculated for each genotype. **E.** Quantification of cell area in stem of gametophores. Error bars represent SEM (n $\geq$ 44) (t-test, *P $<$ 0.05, **P $<$ 0.005, ***P $<$ 0.0005).

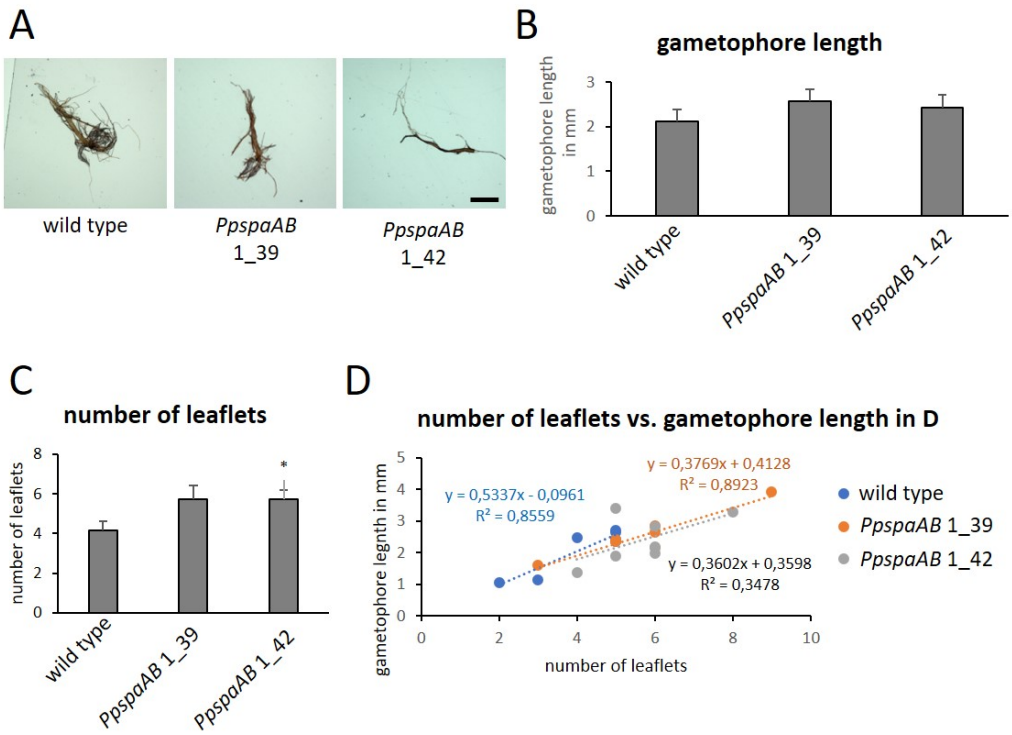

Figure 9: ***PpSPAa* and *PpSPAb* do not regulate gametophore growth in darkness.** **A.** Representative pictures of isolated gametophores of wildtype and two PpspaAB lines. Gametophores were grown in darkness for 2 weeks. Scale bar represents 1 mm. **B.** Quantification of gametophore lengths. Error bars represent SEM (n = 7). **C.** Quantification of number of leaflets per gametophore. Error bars represent SEM (n = 7). Asterisks indicate significant differences between wildtype and the respective mutant line (t-test, *P $\geq$ 0.05). **D.** Number of leaflets are plotted against the length of each gametophore. A regression line was calculated for each genotype.

developed in darkness was measured. Wild-type and *PpspaAB* knock-out plants did not exhibit significantly different gametophore lengths and a comparable number of leaflets. Thus, *SPA* genes in Physcomitrella do not play a major role in regulating the etiolation response of gametophores.

3.4 Physcomitrella *SPA* genes negatively regulate protonemal growth in light and darkness

Gametophores represent the adult stage of Physcomitrella development and protonemal filaments make up the juvenile stage of the gametophyte. Protonemal filaments can be further divided into chloronemal and caulonemal filaments. Both types differ in morphology and function (Reski, 1998). In short, chloronemata have more chloroplasts and play an assimilatory role, whereas caulonemata contain fewer chloroplasts and expand the plant area. The first structures germinating from a spore or regenerating after tissue disruption are protonemata, which then start to colonize the substrate. To investigate this process in *PpspaAB* mutant lines, protonemal tissue from a freshly disrupted liquid culture was spotted on growth medium and incubated in long-day conditions (80 μmol $m^{-2}s^{-1}$ W light) for 21 d (Figure 10). Wild-type plants quadrupled the area they occupied within the 21 d time period. The investigated *PpspaAB* mutant lines grew by factor 6 to 6.5. This increase in plant diameter is exclusively achieved by protonemal growth. Hence, *SPA* genes in Physcomitrella seem to limit colony expansion by inhibiting proliferation of protonemal filaments under the tested long-day conditions.

In darkness, chloronemata stop growing whereas caulonemata keep growing away from the gravitropic vector (Jenkins et al., 1986). This negatively gravitropic response is easily overwritten by small quantities of light such as 200 nmol $m^{-2}s^{-1}$ at 665 nm. Interestingly, this response was abolished in *PpspaAB* double knock-out lines (Figure 11). Freshly disrupted liquid culture was spotted on growth medium and incubated in long-day conditions for a week. Colonies were transferred to glucose-supplemented growth medium and incubated for two weeks in darkness. During the darkness period, plates were oriented vertically. In the wild type filaments protruding from the main colony almost exclusively grew away from the gravitropic vector. In contrast to that, both tested *PpspaAB* mutant lines exhibited uniform protonemal growth radiating from the main colony (Figure 11 A). Similarly to the observed colony growth in long-day conditions the *PpspaAB* mutant lines produced more protonemata. Close-up pictures revealed different morphologies of

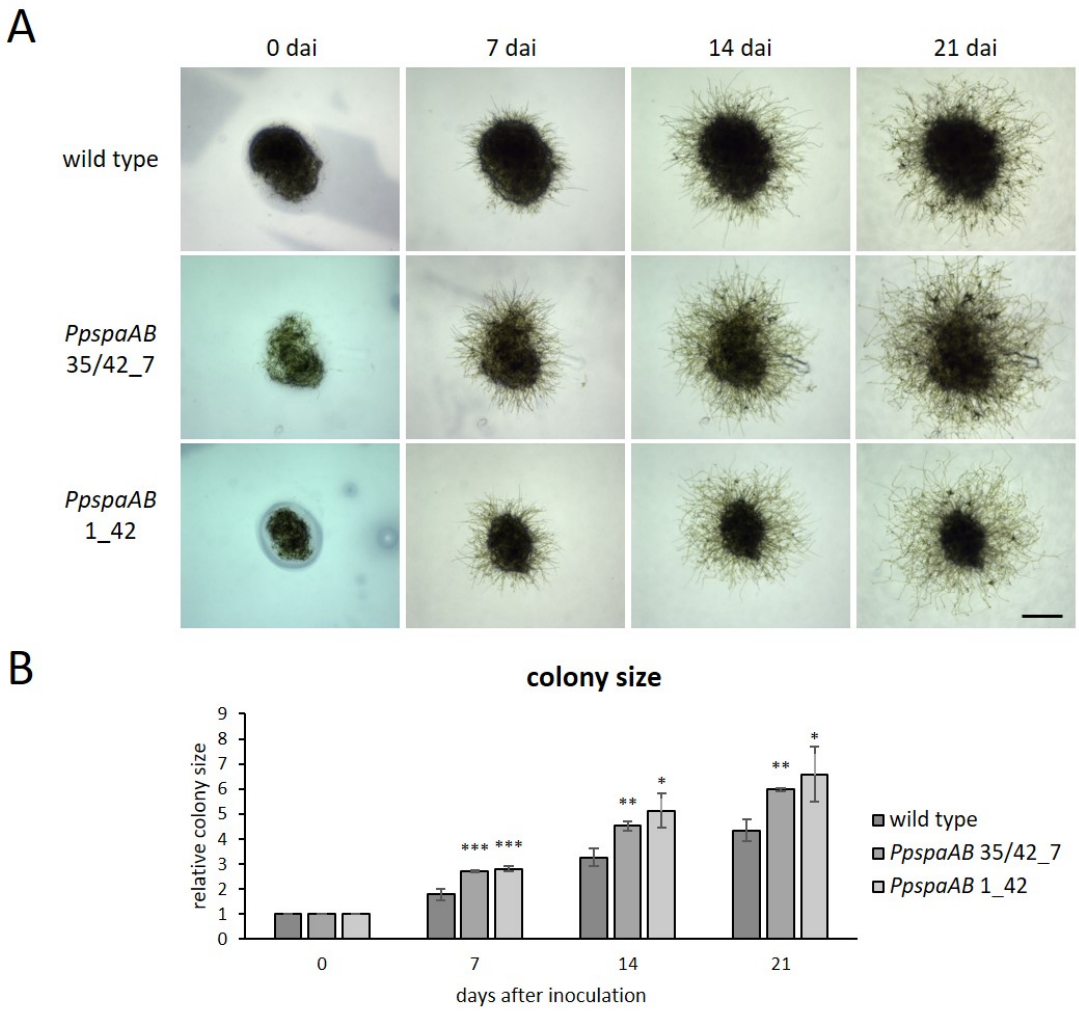

Figure 10: ***PpSPAa* and *PpSPAb* regulate plant size in long-day conditions.**
A. Representative pictures of colonies of wildtype and *PpspaAB* mutant lines grown in long-day (80 μmol m^{-2}s^{-1}) for 21 d. Scale bar represents 2 mm. **B.** Quantification of relative colony size normalized to day 0. Error bars represent SEM (n = 6). Asterisks indicate significant differences between wildtype and the respective mutant line (t-test, *P < 0.05, **P < 0.005, ***P < 0.0005).

the filaments (Figure 11 B): The wild type produced mainly unbranched filaments with very few chloroplasts, which resembled caulonemata. The mutants grew filaments with numerous buds and branches as well as more chloroplasts, which resembled chloronemata. These results indicate that the *SPA* genes in Physcomitrella negatively control protonemal growth in darkness and might be involved in the transitions of chloronemal to caulonemal

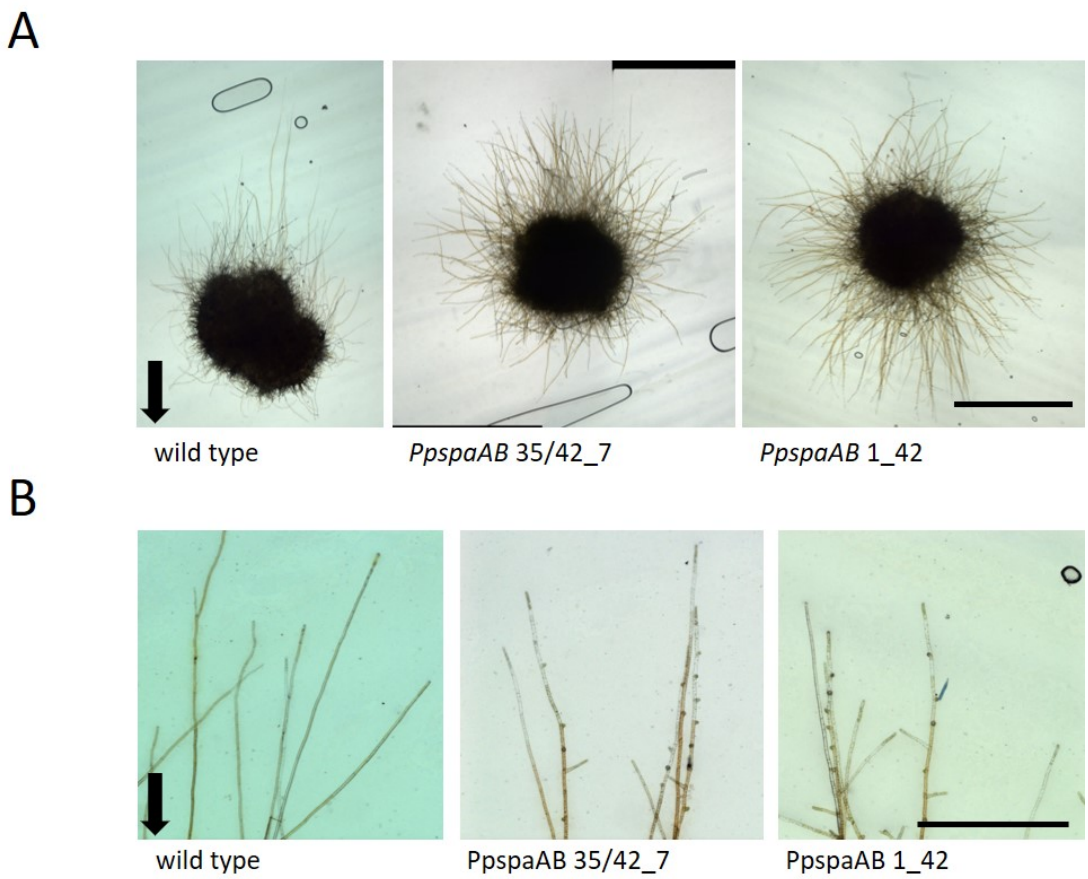

Figure 11: ***PpSPAa* and *PpSPAb* regulate protonemal growth in darkness.**
A. Representative pictures of colonies of wildtype and *PpspaAB* mutant lines grown in darkness for 14 d. Scale bar represents 5 mm. Black arrow indicates direction of gravity. **B.**Representative pictures of protonemal filaments of wildtype and *PpspaAB* mutant lines grown in darkness for 14 d. Scale bar represents 1 mm. Arrowheads indicate oblique cell walls. Black arrow indicates direction of gravity.

filaments. Whether the observed effects are due to a disturbed gravitropic or light response cannot be discerned based on this experiment. Since gravitropic growth is not affected in light-grown plants, it is more likely that the light signaling and not the gravitropism signaling cascade is affected in the *PpspaAB* double knock-out lines.

3.5 Dark repression of light-regulated genes is mostly maintained in *PpspaAB* mutants

In contrast to Arabidopsis *spaQ* mutants, the Physcomitrella *PpspaAB* mutant phenotype is very mild when compared to the wild-type phenotype. Moreover, extensive visual phenotyping of the Physcomitrella mutants did not indicate strong constitutive photomorphogenesis. To further study the involvement of the *PpSPA* genes in light signaling I investigated the molecular phenotype of the *PpspaAB* knock-out lines. Expression levels of *PpPOR* and *PpFNR* are elevated in light (Koduri et al., 2010; Possart, 2013). Moreover, the *PpFEDa* homolog in Arabidopsis is misregulated in higher-order *Atspa* mutants showing constitutively elevated levels in darkness (Laubinger et al., 2004). Here, Physcomitrella plants were dark-adapted for 3 d and irradiated with 40 μmol $m^{-2}s^{-1}$ W light for 24 h. Expression levels of *PpPOR*, *PpFNR* and *PpFEDa* were analyzed by qRT-PCR (Figure 12 A-C). All three transcripts were strongly light-induced in wild-type and the three tested *PpspaAB* mutant lines. Levels of *PpPOR* in light were strongly reduced in the mutants when compared to wild type. However, a clear repression in darkness was still visible in the mutants. In the case of *PpFEDa* and *PpFNR* expression levels in darkness were elevated when compared to wild type. A higher expression level of genes repressed in darkness in the *PpspaAB* mutants when compared to wild-type levels might be evidence for a very mild form of constitutive photomorphogenesis on the molecular level. Notably, the weak repression of *PpFEDa* in darkness could not be consistently reproduced in other experiments.

To obtain more insight into the temporal resolution of the molecular light response, plants were irradiated with W light for 1, 3 and 24 h after dark-adaption (Figure 12 D, E). Transcript levels of *PpHY5a* and *PpPOR* were measured. Expression of *PpHY5a* was light-induced until 3 h and substantially dropped at 24 h in the wild type and *PpspaAB* 1_42. However, the light induction of gene expression was less pronounced in the *PpspaAB* double mutant. Expression levels of *PpPOR* were also comparable between both genotypes exhibiting lowest levels in darkness and an increasing abundance with increased

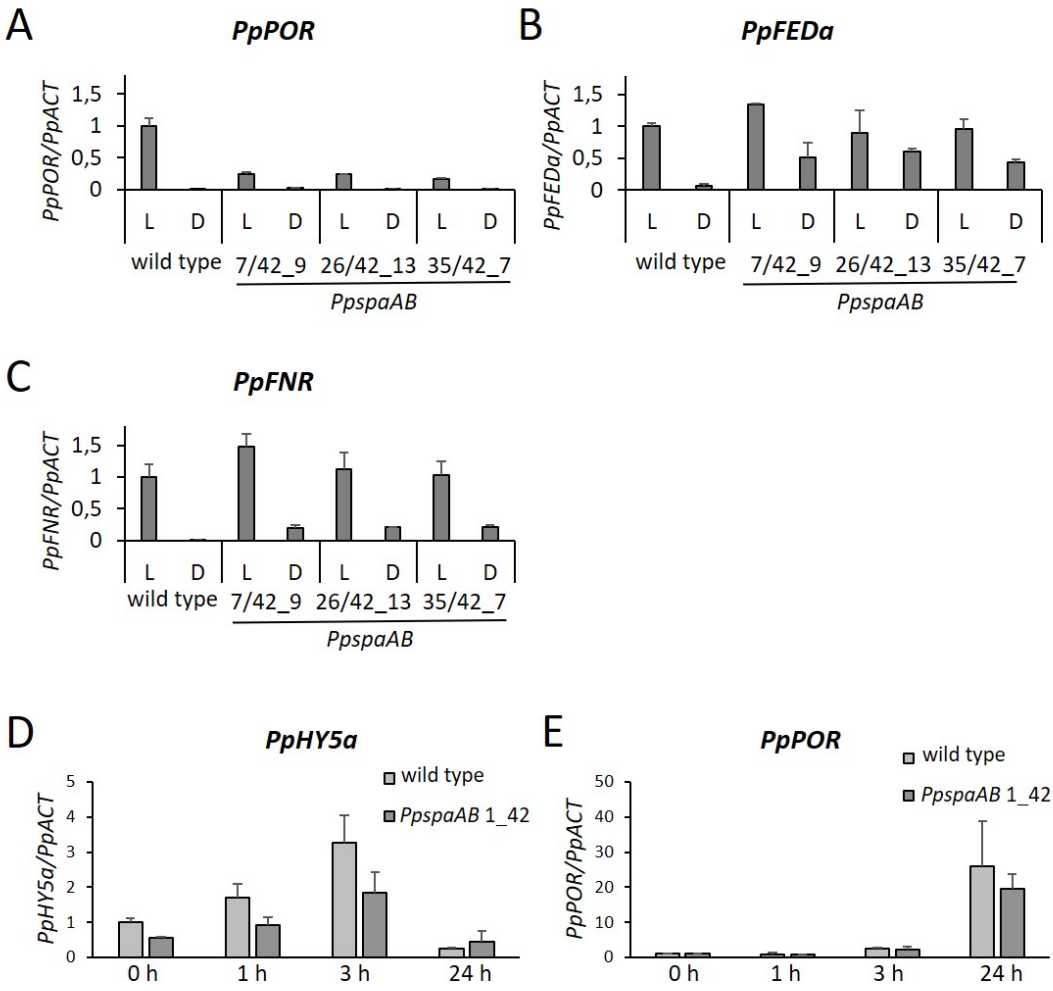

Figure 12: ***PpspaAB* mutant lines do not show constitutive photomorphogenesis on the molecular level.**
A-C. Wild-type and *PpspaAB* mutant plants were dark-adapted for 3 d and treated with 40 μmol m^{-2}s^{-1} W light for 24 h. Expression of *PpPOR* **(A)**, *PpFEDa* **(B)** and *PpFNR* **(C)** was normalized to *PpACT* expression. D indicates that samples were harvested after darkness treatment, L indicates samples were harvested after light treatment. **D, E.** Wild-type and *PpspaAB* 1_42 mutant plants were dark-adapted for 3 d and treated with 80 μmol m^{-2}s^{-1} W light for the indicated period of time. Expression of *PpHY5a* **(D)** and *PpPOR* **(E)** was normalized to *PpACT* expression. Error bars represent SEM (3 technical replicates, 2 biological replicates).

duration of light exposure. In both cases no obvious constitutive photomorphogenesis was observed.

3.6 Light-regulation of PpHY5b protein abundance is not affected by *PpSPAab*

One of the most prominent targets of the COP1/SPA complex in Arabidopsis is HY5 (Osterlund et al., 2000). HY5 protein accumulates in light and its degradation in darkness is mediated by the COP1/SPA complex (Nixdorf and Hoecker, 2010; Saijo et al., 2003). Physcomitrella harbors two homologs of *AtHY5* called *PpHY5a* and *PpHY5b* (Yamawaki et al., 2011a). Complementation analyses in Arabidopsis indicate that the *HY5* function is evolutionarily conserved (Yamawaki et al., 2011a). Moreover, PpCOP1a seems to possess a conserved E3-ubiquitin ligase activity, as overexpression of PpCOP1a can complement the *cop1-5* null mutant phenotype in Arabidopsis (Ranjan et al., 2014). To investigate whether the COP1/SPA complex is functionally conserved with regard to the post-translational regulation of PpHY5b, protein abundance of PpHY5b was analyzed under different conditions. Endogenous PpHY5b was tagged with triple HA (3HA) via homologous recombination (Figure 13 A). In initial experiments no PpHY5b-3HA could be detected by Western blotting. Therefore, for following experiments α-HA immunoprecipitations were conducted to enrich samples for PpHY5b-3HA to detectable levels (Figure 13 B). Immunodetection of PpHY5b-3HA in both independent knock-in lines 27 and 42 showed mutliple bands between an apparent molecular weight of approximately 20-50 kDa. PpHY5b-3HA has a predicted apparent molecular weight of 33.6 kDa. No bands were detected for the wild type, indicating that the detected signal in the knock-in lines is specific for PpHY5b-3HA. Alternative splicing of *PpHY5b* transcript leads to nine putative isoforms with varying sizes (Wu et al., 2014) which might explain the high number of detected bands. Since the knock-in was generated via homologous recombination, which is based on sequence similarity, I also tested if the close homolog *PpHY5a* was targeted. Sanger sequencing revealed that the PpHY5a locus was not altered after the knock-in. Both independent *PpHY5b-3HA* knock-in lines 27

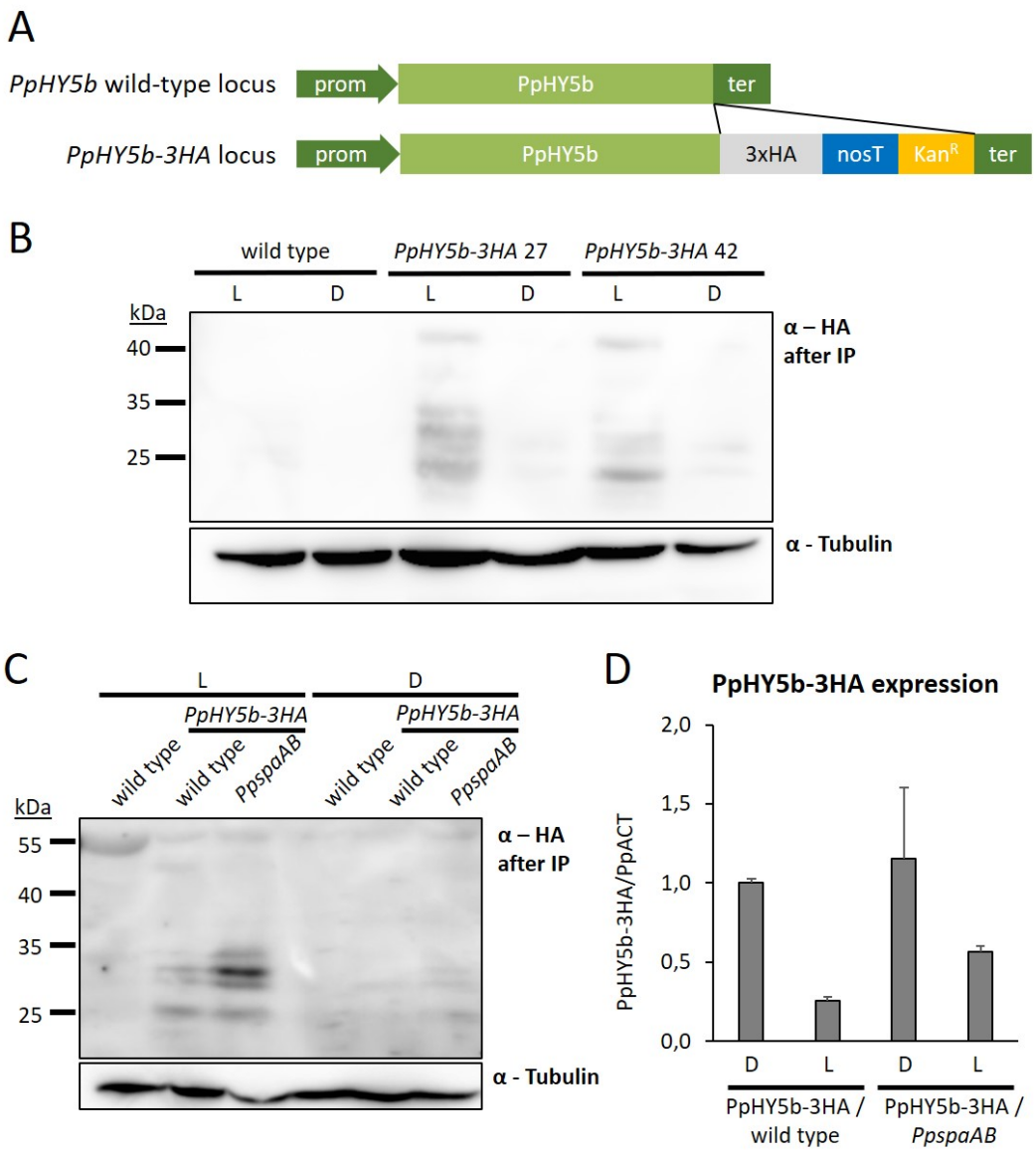

Figure 13: **Mutation of PpSPAab does not stabilize PpHY5b in darkness.**
A. Schematic representation of the *PpHY5b* genomic locus prior to and after knock-in of the 3xHA construct. **B, C.** Immunodetection of endogenous PpHY5b in two independent *PpHY5b-3HA* knock-in lines (27, 42) **(B)** and *PpHY5b-3HA* knock-in lines with wildtype (27) or *PpspaAB* knock-out (2_18) background **(C)**. Plants were dark-adapted for 3 d and exposed to 80 μmol m^{-2}s^{-1} W light for 24 h. Protein samples were immunoprecipitated using HA-magnetic beads prior to Western blotting. Tubulin was detected to compare input protein abundance. **D.** Transcript abundance of *PpHY5b-3HA* in tissue samples used for immunodetection **(C)**. Transcript abundance was normalized using *PpACT*. Error bars represent SEM (3 technical replicates, 2 biological replicates). D indicates that samples were harvested after darkness treatment, L indicates samples were harvested after light treatment.

and 42 showed light regulated protein abundance of PpHY5b-3HA. After dark-adaption for 3 d, PpHY5b-3HA protein levels were below the detection limit. Irradiation with 80 μmol $m^{-2}s^{-1}$ W light for 24 h lead to an accumulation of PpHY5b-3HA in both tested lines. To investigate the influence of the *PpSPA* genes on PpHY5b abundance, *PpHY5b-3HA* knock-in *PpspaAB* knock-out lines were generated via CRISPR/Cas9. To this end, *PpHY5b-3HA* line 27 was transformed with the same plasmids used for generating the *PpspaAB* knock-out lines described above. *PpHY5b-3HA PpspaAB* line 2_18 was used for further experiments. Other than in Arabidopsis, the mutation of SPA proteins did not lead to a higher abundance of HY5 in darkness (Figure 13 C). Higher PpHY5b-3HA levels in plants with *PpspaAB* mutant background in light, which can were observed here, were not consistent among experiments. To test whether different protein levels were due to higher protein stability or gene expression, PpHY5b-3HA expression was tested in the same tissue used for protein isolation and subsequent immunodetection (Figure 13 D). Interestingly, the *PpHY5b-3HA* transcript level was approximately 2-fold increased in darkness when compared to light. This effect was independent of the genetic background. Taken together these results indicate that elevated PpHY5b levels in light are due to increased PpHY5b protein stability and that the degradation of PpHY5b in darkness is mainly SPA-independent.

3.7 PpCOP1a interacts with PpSPAb and PpHY5b

The COP1/SPA complex of higher plants acts as a tetrameric complex consisting of two COP1 and two SPA proteins (Zhu et al., 2008). The homo- and heterodimerization of AtCOP1 and AtSPA proteins is mediated via their respective coiled-coil domains (Hoecker and Quail, 2001; Saijo et al., 2003; Zhu et al., 2008). This direct interaction is essential for COP1/SPA functionality: Expression of SPA1 without a coiled-coil domain, in transgenic Arabidopsis plants fails to rescue the *spa1* mutant phenotype (Fittinghoff et al., 2006; Yang and Wang, 2006). Moreover, direct interaction with target proteins, such as HY5 is a prerequisite for their destabilization in darkness (Saijo et al., 2003). Consistent with previously reported results (Dickopf, 2015; Ranjan, 2010) PpCOP1a recruited PpSPAb

into nuclear speckles when transiently expressed in leek cells, suggesting an interaction of both proteins (Figure 14 A). Moreover, PpCOP1a and PpHY5b colocalized in nuclear speckles (Figure 14 B). Coexpression of PpSPAb and PpHY5b indicated that both fusion proteins were localized in the nucleus (Figure 14 B). In contrast to PpCOP1a, neither PpSPAb nor PpHY5b formed speckles on their own. Notably, subnuclear cloud-like structures were observed when PpSPAb and PpHY5b were coexpressed. These structures mostly overlapped and differed in appearance from structures observed when the fluorophores alone were coexpressed, indicating that there might be an interaction of both fusion proteins. FRET-FLIM analyses showed a significantly reduced donor lifetime for YFP-PpCOP1a when coexpressed with mCherry-PpHY5b compared to the expression of YFP-PpCOP1a alone (Figure 14 C), suggesting a direct interaction of both fusion proteins. In contrast to that, coexpression of YFP-PpHY5b and mCherry-PpSPAb did not lead to a reduced donor lifetime. These results suggest that PpCOP1a and PpSPAb form a complex in Physcomitrella, that can also interact with PpHY5b through PpCOP1a. The interaction of PpSPAb and PpHY5b needs to be further characterized. Notably, none of the described interactions could be reproduced in yeast-two-hybrid experiments (Supplemental Figure S1, Boll (2017)).

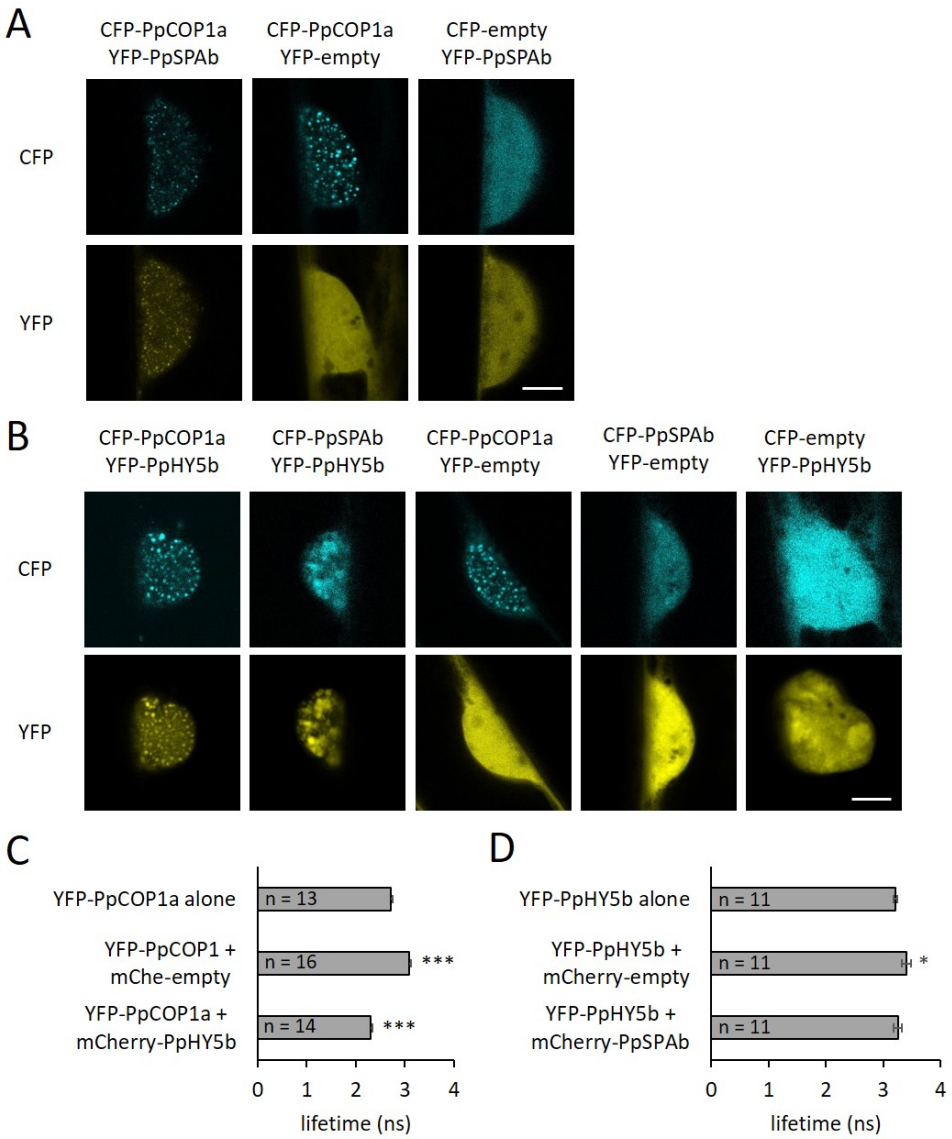

Figure 14: **PpCOP1a interacts with PpSPAb and PpHY5b in leek cells.**
CFP-, YFP- and mCherry-fusion proteins of PpCOP1a, PpSPAb and PpHY5b were transiently coexpressed in leek epidermal cells after particle bombardment. **A, B.** Microscopy pictures of leek nuclei. Scale bars represent 10 μm. **C, D.** FRET-FLIM analysis of transformed cells. Asterisks indicate significant differences between measured lifetime of the donor alone and the respective combination (t-test, *P $<$ 0.05, **P $<$ 0.005, ***P $<$ 0.0005). Error bars represent SEM (n depicted in graphs).

4 Discussion

4.1 The CRISPR/Cas9 technology is highly efficient for generating higher order knock-out mutants in *Physcomitrella patens*

To uncover the evolutionary conservation of genes, often genes with known functions are knocked out in evolutionarily distantly related species. Hence, it is of utter importance to establish tools that can effectively target one gene or a set of genes in the respective model organism. In this project I wanted to investigate the role of the COP1/SPA complex, a major repressor of photomorphogenesis in higher plants, in the early diverged land plant *Physcomitrella patens*, thus enabling us to better understand the evolutionary trajectory of the complex. To this end *PpspaA* and *PpspaB* single as well as *PpspaAB* double mutant lines had previously been generated via homologous recombination (Dickopf, 2015). Until recently homologous recombination was the preferred method to target genes in Physcomitrella (Schaefer and Zrÿd, 1997). Although homologous recombination is very efficient in Physcomitrella, multiple concatenated insertions or insertions in unintended loci of the genome frequently occur (Kamisugi et al., 2006). Moreover, only one locus is targeted per transformation. If higher order knock-out mutants are desired, either multiple rounds of transformation or crossings are necessary. As a consequence the generation of higher order knock-out lines via homologous recombination is very labor- and time-intensive. Notably, Physcomitrella has undergone several recent whole genome duplication events leading to the expansion of many gene families (Lang et al., 2016). Since genes within a family often act redundantly, generating higher order mutant plants might be necessary for understanding gene functions. As an alternative to homologous recombination, RNA interference was established in Physcomitrella targeting up to eight different genes (Vidali et al., 2009). One major drawback of this method is that RNA interference usually leads to a knock-down and not a knock-out. Very recently the CRISPR/Cas9 technology was adapted for Physcomitrella and has helped to generate quintuple knock-out lines in a single transformation experiment without any observed off-target effects (Collonnier et al., 2017; Lopez-Obando et al., 2016).

Previously generated *PpspaAB* double knock-out lines derive from independent transformation events of the *PpSPAa* but not the *PpSPAb* locus. The *PpspaB* 7-3-A1 single knock-out line was used to generate all *PpspaAB* double knock-out lines. Analysis of the genomic DNA of of these double knock-out lines suggested multiple ectopic insertions of the knock-out constructs for all lines (Figure 5). Hence, it cannot be excluded that observed phenotypic effects in these plants are due to the possibly shared ectopic insertions. To validate the observed effects a new set of double mutants was generated. I decided to establish the CRISPR/Cas9 technology in our laboratory as an alternative approach to homologous recombination for gene targeting. In the future, this tool could be useful to knock out substantially larger gene families such as the *PpCOP1* family.

Using the same CRISPR/Cas9-based approach as described in Collonnier et al. (2017) and Lopez-Obando et al. (2016), I generated three new *PpspaAB* double knock-out lines (Figure 6). All three lines harbor deletions in the coding sequences of *PpSPAa* and *PpSPAb* with varying sizes of 8 to 34 bp leading to premature stop codons. Interestingly, only 5% of the 43 initially sequenced plants showed a wild-type genotype for the *PpSPAb* locus. However, 70% of the plants harbored a 12 bp deletion. It is very likely this issue is a consequence of poor sgRNA design. sgRNAs were chosen based on results from the web-based CRISPOR program (Haeussler et al., 2016). Main characteristics for choosing suitable sgRNAs were predicted specificity and efficiency. The most recent version of CRISPOR (V4.5) includes an out-of-frame score based on the evaluation of microhomology in the neighbouring regions of the targeting site (Bae et al., 2014). Both targeting sites for the *PpSPAb* locus (234 and 237) are predicted to produce mainly 6, 12 or 15 bp deletions, which is in line with the Sanger sequencing results obtained for our transformants.

CRISPR/Cas9 was established as a highly efficient tool to generate multiplexed mutants in Physcomitrella. However, the quality of the generated mutants strongly correlates with the quality of the targeting sequences. In future experiments, not only specificity and efficiency but also the out-of-frame score need to be carefully considered when

choosing sgRNAs. A first outlook on the potency of this method is the generation of *Ppcop1* quintuple and hexuple knock-out mutants (Kreiss (2018), Melanie Kreiss, personal communication). In conclusion, this newly established method makes it possible to quickly generate higher order full knock-out mutants of virtually any gene of interest or entire gene families.

4.2 *PpSPAa* and *PpSPAb* regulate gametophore and protonemal development in Physcomitrella

Terrestrialization brought about some very specific challenges as growth conditions differ greatly if an organism is submerged in water or air. One factor that substantially changes during the transition from an aquatic to a terrestrial lifestyle is the surrounding light (Maberly, 2014). When the highly absorbent layer of water vanishes, light intensities of photosynthetically active and UV-B light increase significantly.

Flowering plants today as represented by *Arabidopsis thaliana* evolved the ability to fine-tune their development to ambient light conditions. One of the most important molecular switches mediating a light response is the COP1/SPA complex (Hoecker, 2017). *COP1* is evolutionarily very conserved and can be found in plants and mammals, such as humans, where it acts as an E3 ubiquitin ligase (Lau and Deng, 2012). In contrast to that, *SPA* genes are a relatively new innovation being exclusive to the green lineage. Based on sequence homology no *SPA* homolog was found in the chlorophyte alga *Chlamydomonas reinhardtii*. The most distant relative to Arabidopsis in which a *SPA* gene was identified so far is *Klebsormidium nitens* (Hori et al., 2014).

Here, I investigated the evolutionary conservation of the COP1/SPA complex in early diverged land plants, specifically its role in light signaling. New insights could help to not only understand the evolutionary trajectory of the complex but also aid in pinpointing the exact role of the SPA proteins within the complex. To this end, I genetically and biochemically characterized *COP1* and *SPA* homologs in the model moss *Physcomitrella patens*. Physcomitrella harbors two paralogs of *SPA* namely *PpSPAa* and *PpSPAb* (Ranjan

et al., 2014). Both genes encode proteins, that contain all three important domains for SPA function: An N-terminal kinase-like, a central coiled-coil and a C-terminal WD40-repeat domain. Interestingly, expressing *PpSPAb* in higher order *spa* knock-out Arabidopsis mutants fails to rescue their constitutively photomorphogenic phenotype in darkness (Ranjan et al., 2014). This is first evidence for a possibly high degree of functional divergence of the *SPA* genes.

To further investigate the function of *PpSPAa* and *PpSPAb* previously generated single and double knock-out lines were analyzed alongside newly generated CRISPR/Cas9 double knock-out lines. The most striking phenotype observed was a growth retardation in gametophores (Figures 7, 8). Gametophores in mutant plants were significantly shorter and had fewer leaflets than the wild type when grown in long-day W light and continuous R light. The gametophore size difference was not due to cell size but rather cell number. Therefore, the *PpSPA* genes seem to play a role in promoting cell differentiation in developing gametophores under W and R light conditions.

Physcomitrella wild-type gametophores exhibit an etiolation response in darkness. Gametophores elongate and leaflet growth ceases early to produce only very stunted leaflets (Cove et al., 1978). A remarkably similar phenotype can also be observed in the *Ppcry12* double mutant in B light and the phytochrome-deficient *Pphy2 Pppubs* double mutant in R light. The data suggest that this deetiolation is an immediate light response reminiscent of skotomorphogenic growth of wild-type Arabidopsis seedlings in darkness. In Arabidopsis, *AtSPA* genes are essential to effectively suppress photomorphogenesis in darkness. Full *Atspa* knock-out plants (*spaQn*) exhibit constitutive photomorphogenesis (Laubinger et al., 2006; Ordoñez-Herrera et al., 2015). In contrast to that, full *Ppspa* knock-out plants did not exhibit an altered gametophore etiolation response (Figure 9). Neither the wildtype nor any of tested double mutant lines showed constitutively photomorphogenic growth of gametophores in darkness. As no growth defects in the gametophores were seen under these conditions, it is feasible that the *PpSPA* genes only regulate gametophore growth in the light and do not promote skotomorphogenesis in darkness.

PpspaAB double mutant lines also showed deviations from the wild type in protonemal growth: In the light, colonies of mutant plants had a significantly larger diameter than wild-type colonies (Figure 10). Hence, *PpSPA* genes might control the protrusion of protonemal filaments from the main colony. Interestingly, *PpHY5ab* double mutant plants exhibit particularly small colonies and show significantly fewer protonemal protrusions from the main colony (Yamawaki et al., 2011b). AtHY5 is a well-characterized target of the AtCOP1/AtSPA complex. If the function of the complex in regulating HY5 is conserved in Physcomitrella, PpHY5 protein would accumulate in *PpspaAB* knock-out lines. Hence, *PpspaAB* knock-out lines could have a phenotype opposite to the *PpHY5ab* knock-out lines. When protonemal colonies were grown in darkness, caulonemal filaments grew away from the gravitropic vector in the wild type (Figure 11). In contrast to that, *PpspaAB* mutant lines developed protonemal filaments radiating in all directions. Moreover, filaments in the double mutants were more branched and generally looked more similar to light-grown filaments. The agravitropic response of caulonemal filaments can be overwritten by small amounts of light (Jenkins et al., 1986). If, analogous to Arabidopsis, the *PpSPA* genes act to suppress light signals in darkness, an over-active light signaling cascade could explain this phenotype. The *PpspaAB* double mutant plants might not be able to correctly suppress a light response and initiate an agravitropic response of protonemata. Hence, these plants fail to develop unbranched caulonemal filaments at the same rate as the wild type in darkness. However, experiments conducted so far have not excluded the possibility that the gravitropic response of protonemata itself is disturbed in the *PpspaAB* mutants. In conclusion, it is possible that *PpSPA* genes suppress photomorphogenesis in the juvenile protonemal stage but not the adult gametophore stage of the plant.

Orthologs of genes that are expressed in a constitutively photomorphogenic manner in higher order *spa* mutants in Arabidopsis were tested in *PpspaAB* knock-out lines via qRT-PCR (Figure 12). Here, Physcomitrella *PpspaAB* mutants did not exhibit a strong misregulation of light-regulated genes. However, there was a trend towards a more similar expression in light and darkness in the double mutants when compared to the wild type,

suggesting a minor involvement of the *SPA* genes in light-dependent gene regulation. The overall influence of the *PpSPA* genes on the expression of the tested genes is much smaller than the influence of the *AtSPA* genes in Arabidopsis.

Notably, all investigated phenotypes of *PpspaAB* double knock-out lines generated via homologous recombination or CRISPR/Cas9 were very similar. Hence, putative unintended integrations of the knock-out construct after homologous recombination are probably not causal for the observed phenotypic responses.

In conclusion, *PpSPA* genes in Physcomitrella do not affect plant growth as strongly as *AtSPA* genes in Arabidopsis. Our data suggest that knocking out *PpSPAa* and *PpSPAb* does not lead to strong constitutive photomorphogenesis but rather influences the long-term development of gametophores and protonemata under long-day W and continuous R light conditions.

4.3 PpHY5b might be a target of the COP1/SPA complex in Physcomitrella, but the *PpSPA* genes might not be involved in PpHY5b regulation

AtHY5 is one of the most prominent targets of the COP1/SPA complex in Arabidopsis (Osterlund et al., 2000). The Physcomitrella genome encodes two orthologs of AtHY5 (PpHY5a and PpHY5b). Overexpression of a truncated version of PpHY5a in Arabidopsis leads to a reduced hypocotyl length, hence a function of *PpHY5* genes in photomorphogenic growth regulation might be conserved. Physcomitrella *Pphy5ab* double mutants exhibit reduced protonemal branching (Yamawaki et al., 2011b). To see whether the function of COP1/SPA in regulating this photomorphogenesis-promoting transcription factor is conserved, I examined endogenous PpHY5b levels (Figure 13). After immunodetection PpHY5b-3HA did not appear as a single distinct band but several different bands with predicted sized of approximately 20-50 kDa. Nine different splice variants of PpHY5b are predicted that have different apparent molecular weights ranging from 22 to 33.6 kDa which could explain the additional bands (Wu et al., 2014). More variety might come from

post-translational modifications. AtHY5 is post-translationally phosphorylated which results in the detection of two closely migrating isoforms after immunodetection (Hardtke et al., 2000). PpHY5b protein accumulated in the light and PpHY5b levels were highly reduced in darkness. This held true independent of the genetic background. Notably, on the gene expression level, *PpHY5b* expression was increased approximately 2-fold in darkness both in wild-type and *PpspaAB* double knock-out background. This upregulation of *PpHY5b* expression but lower protein levels in darkness suggest a strong post-translational light-dependent regulation. Our data indicate that PpSPA proteins do not play a major role in this regulatory process. Interestingly, protein-protein interaction studies showed an interaction of PpCOP1a and PpSPAb as well as PpCOP1a and PpHY5b, but possibly no interaction of PpSPAb and PpHY5b (Figure 14). Since direct interactions of AtCOP1 and AtSPA proteins with their targets are essential for mediating the destabilization of target such as AtHY5 (Saijo et al., 2003), a lack of interaction of of PpSPAb and PpHY5b might be the underlying reason for the lack of PpHY5b stabilization in the *PpspaAB* mutant background in darkness. At the same time the interaction of PpCOP1a and PpSPAb suggests the formation of a PpCOP1a/PpSPAb complex in Physcomitrella. Although PpHY5a and PpHY5b are very similar, it cannot be excluded that PpHY5a protein abundance is affected by the *PpSPA* genes. Considering that *PpspaAB* double knock-out mutants exhibit the opposite phenotype of *Pphy5ab* double knock-out mutants, the mutation of PpSPAa and PpSPAb might lead to an accumulation of PpHY5a but not PpHY5b. As PpHY5a and PpHY5b have highly redundant functions (Yamawaki et al., 2011b), higher levels of PpHY5a in darkness might be sufficient to cause the observed phenotype. Hence, it might be worth investigating PpHY5a levels in *PpspaAB* double knock-out lines.

4.4 Further investigations of the evolutionary conservation

Since the discovery of the *SPA* genes in Arabidopsis efforts have been made to pinpoint their exact function within the COP1/SPA complex. The structure of COP1 with its RING-finger domain suggests that it might have evolved from a single subunit RING E3

ubiquitin ligase (Freemont, 2000). Moreover, there is good evidence that AtCOP1 has E3 ubiquitin ligase activity by itself (Osterlund et al., 2000; Seo et al., 2003; Yang et al., 2005). In humans, COP1 does indeed act as an E3 ubiquitin ligase on its own. The human genome does not contain any *SPA* genes (Lau and Deng, 2012). Hence, in plants COP1 might be able to act without any involvement of SPA proteins. However, strong defects in plant growth and development in *Atspa* full knock-out plants especially with regard to light-dependent processes can be observed (Menon et al., 2016). A possible mechanism to explain the necessity of SPA proteins for the full function of the COP1/SPA complex in plants is that the SPA proteins have evolved to modulate the E3 ubiquitin ligase activity of COP1 specifically to fine-tune light responses. Indeed, AtSPA proteins can modulate the ability of AtCOP1 to ubiquitinate targets such as AtHY5 and AtLAF1 *in vitro* (Saijo et al., 2003; Seo et al., 2003). It is conceivable that in Physcomitrella the PpSPA proteins have much less influence on PpCOP1 activity. Here, we might be presented with a more ancestral state of the complex where the SPA proteins did not evolve to mediate a light-signaling response but play a different role in plant development. Notably, PpCOP1a recruits PpSPAb into speckles, hence PpCOP1a and PpSPAb probably interact and might form a PpCOP1/PpSPA complex *in planta*. Maybe the function of AtSPA to modulate AtCOP1 function has evolved after complex formation and Physcomitrella today harbors an evolutionary intermediate. It is conceiveable that if there is a functional PpCOP1/PpSPA complex in Physcomitrella, the role of PpSPA proteins or their action mechanism is different from Arabidopsis SPA proteins. This idea is supported by the first functional studies of PpSPAb in Arabidopsis higher order *spa* mutants. Here, expression of PpSPAb cannot reconstitute the wild-type phenotype (Ranjan et al., 2014). In addition, the fact that PpSPAb does not form speckles when overexpressed in leek cells is in line with the notion of a functional diversification. In Arabidopsis, speckles have been described as nuclear bodies containing proteins for light-signaling (Van Buskirk et al., 2012) and AtSPA proteins are localized in these speckles (Maier et al., 2013; Laubinger et al., 2006). PpSPAb not being localized in nuclear speckles could be evidence for functional diversification and a role of PpSPA protein outside the light signaling cascade.

Alternatively, it cannot be fully excluded that earlier in evolutionary history PpSPA proteins did indeed modulate PpCOP1 activity and extant moss plants have lost this ability secondarily. Analyses of the COP1/SPA complex in plants earlier diverged from the green lineage as Physcomitrella such as Klebsormidium might help clarifying the order of events.

To further investigate the role of the *PpSPA* genes in Physcomitrella it would be very interesting to look into more putative targets of a PpCOP1/PpSPA complex. Coevolution of the complex and its targets in Arabidopsis might have been a stepwise process and different interaction partners were likely recruited sequentially in temporal accordance with the respective selective pressure. Hence, while PpHY5b might not interact with PpSPAb, other putative targets might very well interact with and be regulated by PpSPAb or PpSPAa. In this regard, the three identified *CONSTANS-like* (*COL*) genes *PpCOL1*, *PpCOL2* and *PpCOL3* are of particular interest. *CONSTANS* (*CO*) and *COL* genes are substrates of the COP1/SPA complex in Arabidopsis (Laubinger et al., 2006; Liu et al., 2008; Jang et al., 2008; Ordoñez-Herrera et al., 2017). While the protein levels and gene function of *PpCOL* genes have not been studied, gene expression is regulated by light and photoperiod (Shimizu et al., 2004; Zobell et al., 2005). Seeing an involvement of the *PpSPA* genes in regulating the *PpCOL* genes or their products but not PpHY5b could be an indication for the stepwise coevolution of the complex and its targets. Moreover, it could aid to better understand the *PpCOL* genes *per se*. It would be very interesting to see the role of these genes in a non-flowering plant, since in Arabidopsis their major role is to regulate flowering. In addition to that, other orthologs of AtCOP1/AtSPA substrates could be identified via sequence comparison and could subsequently be tested regarding their interaction, regulation and function. Screening a yeast-two-hybrid transcription factor library, such as the REGIA library (Paz-Ares et al., 2002), might help to find new targets of the complex. Although no library for Physcomitrella transcription factors is available to date, commonly used libraries containing transcription factors from Arabidopsis might help to find highly conserved motifs, targets or possibly pathways of the PpCOP1/PpSPA complex. To complement

this approach, a broad overview of the differential gene expression of the wild type and the *PpspaAB* double knock out mutant under different conditions, especially in light and darkness, might be helpful. RNAseq analysis might provide novel evidence about the exact function of the *PpSPA* genes.

Although the function of *PpSPAa* and *PpSPAb* seems to differ from the Arabidopsis *SPA* genes, the function of *PpCOP1* seems to be rather conserved. Overexpression of PpCOP1a in Arabidopsis *cop1* mutants almost fully reconstitutes the wild-type phenotype (Ranjan et al., 2014). Moreover, PpCOP1a interacted with PpSPAb and PpHY5b (Figure 14). The observation that PpHY5b abundance in darkness was not regulated by PpSPA proteins (Figure 13), does not exclude the possibility that PpHY5b abundance might be regulated by PpCOP1. It would be very interesting to see, whether PpHY5b protein levels in darkness are higher in multiplexed *Ppcop1* mutants. Additionally, a detailed analysis of higher order *Ppcop1* mutants will be instrumental for understanding the evolutionary conservation of the complex and light signaling as such in Physcomitrella. Phenotypic responses of these mutants might help to better understand constitutive photomorphogenesis in this early diverged land plant. As the *PpSPA* genes might not play an important role in light signaling, phenotypic responses could be substantially different between *Ppspa* and *Ppcop1* multiple knock-out mutant plants.

If more evidence points towards the fact that PpCOP1 activity is mainly independent of the PpSPA proteins it will be worth investigating whether the COP1/SPA complex is part of a higher order CUL4-based E3 ubiquitin ligase in Physcomitrella like it has been described for the complex in Arabidopsis (Lau and Deng, 2012). Since COP1 harbors a RING domain it is possible that COP1 evolved from a protein that was able to recruit E2 enzymes by itself. Typical RING/U-box E3 ubiquitin ligases are independent of a higher order protein complex to provide a RING domain for E2-recruitment (Moon et al., 2004). PpCOP1 might be an evolutionary intermediate between the two states. Thus, advancements might help to not only understand the evolutionary conservation of COP1/SPA but also the evolution of higher order multi-subunit E3 ubiquitin ligases.

An additional approach to investigate the evolutionary conservation of the COP1/SPA complex apart from looking at the complex itself and its downstream targets could be to look into the interaction of the complex with photoreceptors. In Arabidopsis photoreceptors regulate the activity of COP1/SPA through direct protein-protein interaction (Hoecker, 2017). Hence, an interaction of the photoreceptors with either PpCOP1 or PpSPA would be very good evidence that the respective protein is indeed part of the light signaling cascade in Physcomitrella. Both higher order phytochrome and cryptochrome Physcomitrella mutants are defective in their light response (Chen et al., 2012; Imaizumi et al., 2002). Therefore, phytochromes and cryptochromes are interesting putative interaction partners of PpCOP1 and PpSPA. Additionally, interactions with UVR8 could be analyzed. In higher plants, UVR8 interacts with COP1, but not SPA in a UV-B-dependent manner leading to a reduced affinity of COP1 to its targets, such as HY5, and DDB1 (Podolec and Ulm, 2018). Interestingly, UV-B-induced photomorphogenesis and stress acclimation in Arabidopsis are both dependent on COP1 (Favory et al., 2009). Physcomitrella grows in sun-exposed open fields and is more UV-B-tolerant than Arabidopsis (Wolf et al., 2010). Moreover, the moss possesses a greatly expanded *COP1* gene family (Rensing et al., 2008; Richardt et al., 2007). It would be very interesting to investigate whether *PpCOP1* genes are also important for UV signaling and particularly if the expansion of the *COP1* gene family in Physcomitrella was an adaption to better cope with high amounts of UV-B irradiation. Since early land masses were presumably very bleak and UV-B levels were probably higher than today (Rozema et al., 2009) early land plants might have been exposed to higher levels of UV irradiation. Hence, a high tolerance to UV light might have been an evolutionary advantage.

Possibly, the relatively mild phenotypes of *PpspaAB* double knock-out mutant plants could indicate that the *PpSPA* genes or even the entire light signaling cascade plays a less important role in Physcomitrella than in higher plants. However, photoreceptor or *Pphy5ab* mutants do show substantial growth defects (Chen et al., 2012; Imaizumi et al., 2002; Yamawaki et al., 2011b), indicating that light-adaptive mechanisms exist. It is conceivable that due to their relatively simple morphology and the small nature of

the plant, phenotypic aberrations in Physcomitrella are generally more subtle than in Arabidopsis. Being a more simple organism might make Physcomitrella less frail.

Finally, one aspect of the evolutionary conservation of *SPA* genes goes beyond early diverged land plants but is truly worth investigating: The SPA N-terminus in Arabidopsis harbors a kinase-like domain that resembles Serine/Threonine protein kinases but lacks kinase activity (Dieterle, 2013; Hoecker et al., 1999). Physcomitrella SPA proteins also harbor a predicted N-terminal kinase-like domain. The sequence of this N-terminal domain suggests that the *SPA* genes originate from a kinase-encoding gene but so far no direct relationship to such a gene could be determined. Elucidating how a gene encoding for a protein-kinase was recruited for light signaling and how the kinase domain was neofunctionalized would be very interesting. With efforts such as the 1kP initiative (Matasci et al., 2014) more plant genome sequences are made available that might provide the missing links between the Physcomitrella *SPA* genes and their kinase-encoding ancestor. However, the N-terminus of *SPA* might be the result of exon shuffling or gene translocation and subsequent neofunctionalization (Long, 2001). If the latter were true, identifying the exon donor might be very difficult. However, finding a *SPA* homolog encoding a functional kinase would be a great advancement in our understanding of the evolution of light signaling.

In conclusion, this work provides novel evidence on the evolutionary conservation of the COP1/SPA complex in early diverged land plants. The molecular mechanisms underlying the light-dependent control of plant growth and development differ substantially between between Physcomitrella and Arabidopsis. The data presented here suggests (1) that COP1 in Physcomitrella might act more independently of the SPA proteins and (2) that *SPA* genes in Physcomitrella might play a different role in plant development than in higher plants. However, further analyses particularly in higher order *Ppcop1* mutants are necessary to elucidate the evolutionary conservation of the complex and its importance for reproductive success.

5 Materials & Methods

5.1 Materials

5.1.1 Chemicals

Chemicals in research were purchased from AppliChem GmbH (Darmstadt, Germany), BD Biosciences (Heidelberg, Germany), Bio-Rad Laboratories GmbH (Munich, Germany), Calbiochem (Darmstadt, Germany), Carl Roth GmbH (Karlsruhe, Germany), Duchefa Biochemie B.V. (Haarlem, Netherlands), Life Technologies GmbH (Karlsruhe, Germany), Merck KGaA (Darmstadt, Germany), Miltenyi Biotec (Bergisch Gladbach, Germany), p.j.k GmbH (Kleinblittersdorf, Germany), Promega (Mannheim, Germany), Roche Diagnostics GmbH (Mannheim, Germany), SERVA Electrophoresis GmbH (Heidelberg, Germany), Sigma Aldrich Chemie GmbH (Munich, Germany), Thermo Fisher Scientific (Schwerte, Germany) and VWR International GmbH (Darmstadt, Germany).

5.1.2 Buffers and solutions

All buffers and solutions were prepared with double-distilled water (ddH_2O) if not otherwise stated. Buffers and solutions that do not represent a simple solution or dilution of a single stock chemical are listed in Table 2. Unless otherwise stated, buffers were stored at room temperature.

Table 2: Buffers and solutions used in this study

Buffer/Solution	Components
Phenotypic analysis of gametophores	
Fixing solution	75% (v/v) ethanol
	25 (v/v) acetic acid
Standard molecular biology methods	
CTAB buffer	Tris/HCl pH 8
	2% (w/v) CTAB
	1.4 M NaCl

Table 2: (continued)

Buffer/Solution	**Components**
	0.2% (v/v) β-mercaptoethanol
	20 mM EDTA
	0.5% (w/v) polyvinylpyrrolidone
10 x DNA loading dye	30% (v/v) glycerol
	0.25% (w/v) Bromphenol Blue
EB buffer (Thompson buffer)	200 mM Tris/HCl pH 7.5
	250 mM NaCl
	25 mM EDTA
	0.5% SDS
10 x PCR reaction buffer[1]	100 mM Tris/HCl pH 9.0
	500 mM KCl
	15 mM $MgCl_2$
TB buffer[2]	10 mM PIPES/KOH pH 6.7
	10 mM $CaCl_2$
	250 mM KCl
	55 mM $MnCl_2$ (added after pH adjustment)
10 x TBE	890 mM Tris
	890 mM Boric acid
	20 mM EDTA
Washing buffer (CTAB gDNA isolation)	76% (v/v) ethanol
	10 mM ammonium acetate
Southern blotting	
B1	0.1 M maleic acid
	0.15 M NaCl
	pH 7.5

Table 2: (continued)

Buffer/Solution	**Components**
B2[3]	1 x blocking solution diluted with B1
Antibody solution[3]	α-DIG-AP in B2 (1: 5000)
B3	0.1 M Tris/HCl pH 9.5
	0.1 M NaCl
Washing buffer	0.1 M maleic acid
	0.15 M NaCl
	0.3% (v/v) Tween®20
	pH 7.5
10 x blocking solution[4]	10% (w/v) Blocking reagent (Boehringer Ingelheim, Ingelheim, Germany, Cat. 1096 176) diluted in B1 at 65°C under constant stirring
Hybridizing buffer[3]	100 ml Roti®Hybri-Quick (Roth, Karlsruhe, Germany, Cat. A981.1)
	1 g Blocking reagent
Denaturing buffer	0.5 M NaOH
	1,5 M NaCl
Neutralizing buffer	1 M Tris/HCl pH 7.5
	1.5 M NaCl
20 x SSC buffer[4]	3 M NaCl
	0.3 M sodium citrate
	pH 7.0
Transformation of Physcomitrella	
3 M medium[2,3]	15 mM $MgCl_2$
	5.123 mM MES
	479.77 mM mannitol
	pH 5.6 with KOH

Table 2: (continued)

Buffer/Solution	Components
0.5 M mannitol[2,3]	0.5 M mannitol
	pH 5.6-5.8 with HCl or KOH
Regeneration medium[2,3]	164.68 mM mannitol
	277.55 mM glucose
	in KNOP medium
	pH 5.8 with KOH
Standard biochemical methods	
5 x Lämmli buffer[1]	310 mM Tris/HCl pH 6.8
	10% (w/v) SDS
	50% (v/v) glycerol
	0.25% (w/v) Bromphenol Blue
	500 mM DTT
YODA buffer	50 mM Tris/HCl pH 7.5
	150 mM NaCl
	1 mM EDTA
	10% (v/v) glycerol
	1% (v/v) protease inhibitor cocktail (added freshly)
	5 mM DTT (added freshly)
Immunoblotting	
10 x Carbonate blotting buffer[3]	0.31% (w/v) $NaCO_3$
	0.84% (w/v) $NaHCO_3$
	0.08% (w/v) SDS
SDS-PA separating gel[3]	15% (w/v) acrylamide
	375 mM Tris/HCl pH 8.8
	0.1% (w/v) SDS

Table 2: (continued)

Buffer/Solution	Components
	0.08% (w/v) APS
	0.08% (w/v) TEMED
SDS-PA stacking gel[3]	5% (w/v) acrylamide
	125 mM Tris/HCl pH 6.5
	0.1% (w/v) SDS
	0.05% (w/v) APS
	0.1% (w/v) TEMED
10 x SDS running buffer	1.9 M glycine
	240 mM Tris
	1% (w/v) SDS
10 x TBS buffer	200 mM Tris/HCl pH 7.5
	1.5 M NaCl
TBS-T	1 x TBS
	0.1% (v/v) Tween® 20
Yeast-two-hybrid assays	
10 x TE buffer[4]	0.1 M Tris/HCl pH 7.5
	10 mM EDTA
1 x TE/LiAc[2,3]	1 x TE buffer
	0.1 M lithium acetate
PEG/LiAc[2,3]	1 x TE buffer
	0.1 M lithium acetate
	40% (w/v) PEG 4000

[1] Solution was stored at -20°C.

[2] Solution was filter-sterilized.

[3] Solution was prepared freshly before use.

[4] Solution was autoclaved.

5.1.3 Antibiotics

Antibiotics used in this study are listen in Table 3. Stock solution were filter-sterilized and stored at -20°C unless otherwise stated.

Table 3: Antibiotics used in this study

Chemical	Solvent	Working conc.	Manufacturer
Ampicillin	ddH_2O	100 μg/ml	Duchefa (Haarlem, Netherlands)
G418[1]	ddH_2O	50 μg/ml	Thermo Fisher Scientific (Schwerte, Germany)
Kanamycin	ddH_2O	50 μg/ml	Duchefa (Haarlem, Netherlands)

[1] Stock solution was stored at 4°C.

5.1.4 Growth media

Media used for bacterial, yeast and plant growth used in this study are listed in Table 4. Solid media were prepared by adding 1.5% (w/v) (bacteria), 1.8% (w/v) (yeasts) or 1.2% (w/v) (plants) agar. All media were autoclaved prior to use.

Table 4: Growth media used in this study

Medium	Components
KNOP medium	1.8 mM (0.25 g/l) KH_2PO_4
	3.35 mM (0.25 g/l) KCl
	2.07 mM (0.25 g/l) $MgSO_4$ x 7 H_2O
	4.24 mM (1 g/l) $Ca(NO_3)_2$ x 4 H_2O
	44.96 μM (12.5 mg/l) $FeSO_4$ x 7 H_2O
	if applicable: 27.76 mM (5 g/l) glucose
Synthetic drop-out (SD) medium	6.7 g/l nitrogen base without amino acids
	40 mg/l adenine hemisulfate
	X g/l drop-out supplement[1]
	20 g/l glucose

Table 4: (continued)

Medium	Components
	pH 5.8 with KOH
Luria-Bertani (LB) broth	10 g/l tryptone
	5 g/l yeast extract
	10 g/l NaCl

[1] According to manufacturer's instructions.

5.1.5 Antibodies

Antibodies used in this study are listed in Table 5. Primary antibodies were diluted in TBS containing 3% (w/v) milk powder, horseradish peroxidase (HRP)-coupled (secondary) antibodies were diluted in TBS containing 5% (w/v) milk powder.

Table 5: Antibodies used in this study

Antibody	Host	Dilution	Manufacturer
α-HA-HRP	rat	1:1 000	Roche Diagnostics (Mannheim, Germany)
α-mouse IgG-HRP	goat	1:50 000	Sigma-Aldrich (Munich, Germany)
α-Tubulin[1]	mouse	1:10 000	Sigma-Aldrich (Munich, Germany)

[1] This antibody was originally raised against Tubulin from Arabidopsis.

5.1.6 Enzymes

Enzymes used in this study are listed in Table 6. Unless otherwise stated all enzymes were stored at -20°C.

Table 6: Enzymes used in this study

Enzyme	Manufacturer
DreamTaq™Hot Start DNA polymerase	Thermo Fisher Scientific (Schwerte, Germany)

Table 6: (continued)

Enzyme	**Manufacturer**
Gateway® BP Clonase® Mix[1]	Life Technologies (Karlsruhe, Germany)
Gateway® LR Clonase® Mix[1]	Life Technologies (Karlsruhe, Germany)
GoTaq® G2 Hot Start Green Master Mix	Promega (Mannheim, Germany)
KAPA™SYBR® FAST qPCR Mastermix	PEQLAB Biotechnologie (Erlangen, Germany)
Pfu DNA polymerase	Thermo Fisher Scientific (Schwerte, Germany)
Restriction endonucleases	Thermo Fisher Scientific (Schwerte, Germany)
RevertAid™H Minus Rev Transcriptase	Thermo Fisher Scientific (Schwerte, Germany)
Taq DNA polymerase	purified from *E. coli*
TURBO™DNase	Life Technologies (Karlsruhe, Germany)

[1] Enzyme was stored at -80°C.

5.1.7 Kits for molecular biology

Kits for molecular biology used in this study are listed in Table 7.

Table 7: Kits for molecular biology used in this study

Kit	**Manufacturer**
CloneJet PCR Cloning Kit	Thermo Fisher Scientific (Schwerte, Germany)
NucleoSpin® Gel and PCR Clean-up Kit	Macherey Nagel (Düren, Germany)
NucleoSpin® Plasmid Purification Kit	Macherey Nagel (Düren, Germany)
Plasmid Plus Midi Kit	Qiagen, Hilden, Germany)
RNeasy® Plant Mini Kit	Qiagen (Hilden, Germany)

5.1.8 Oligonucleotides

Oligonucleotides used in this study are listed in Table 8.

Table 8: Oligonucleotides used in this study

Name	ID[1]	Sequence (5' to 3')	Reference
Cloning			
AscI-FlankB fwd	-	TTGGCGCGCCAATGGAATATTCGAGAGATGTGT	this study
EcoRI AscI nptII rev	-	CCGGAATTCGGCGCGCCAAGTGTACAATGGTGGAGCACGA	this study
EcoRI-3HA fwd2	-	CCGGAATTCTACCCATATGACGTTCCAGACT	Lyska et al. (2013)
HindIII-NheI-FlankB rev	-	CCCAAGCTTGCTAGCCATACTCATAAGGTTTATTAC	this study
HY5b_CDS_1_ F	322	ATGAACGACTTTGATGAGC	this study
HY5b_CDS_339_F	338	CTCTACTGTGGGTCCCGCTTC	this study
HY5b_CDS_465_R	337	TGGAACCCTCCTAACATCAGAG	this study
HY5b_CDS_834_R	325	TCATTGCGCACCATCCTCAGCGTTA	this study
HY5b_CDSatt_2_ F	327	GGGGACAAGTTTGTACAAAAAAGCAGGCTTAATGAACGACTTTGATGAGCCCCAAGGTGAC	this study
HY5b_CDSatt_834_R	329	GGGGACCACTTTGTACAAGAAAGCTGGGTATCATTGCGCACCATCCTCAGCGTTA	this study
NosT rev2	-	AATTCGATCTAGTAACATAGATGA	Lyska et al. (2013)
nptII fwd	-	GTGTACAATGGTGGAGCACGAC	this study

Table 8: (continued)

Name	ID[1]	Sequence (5' to 3')	Reference
nptII rev2	-	CGGTGTCATCTATGTTACTAGATCGAATTGCGGTGTACAGTCACTGGAT	this study
PstI-FlankA rev	-	AAAACTGCAGTTGCGCACCATCCTCAGCGTT	this study
SacI-NheI-FlankA fwd	-	CGAGCTCGCTAGCATATGTTTGGAAATTGTGGTA	this study
Genotyping			
guideRna237forwLeft	1305	TTGCAACTCGGGAAACAGGT	this study
guideRna237forwRight	1306	CGATTCACGGCTGCTTGATG	this study
guideRna749forwLeft	1303	GACAACCGAAGACCAGAGCA	this study
guideRna749forwRight	1304	GGGAGCAAACGGAATCCAGA	this study
PpHY5b 1,833 F	1307	ATGAACGACTTTGATGAGCCCC	this study
PpHY5b 3,812 F	1308	CCTCTTCGAAGCAGCAGACG	this study
PpHY5b 4,063 R	1309	CCCAGAAACCCCTCCACTAGTC	this study
PpHY5b 4,951 R	1310	AGCGTAGTCAGGTACGTCGTAAGGG	this study
SPAa_132_1,954 F	180	TGGTAGTGGGGTCGGTAGAG	this study
SPAa_132_1F	152	GGTTGAGAGACCGCAGAACA	this study
SPAa_132_1R	153	CCAACACACCCTACGACGAA	this study
SPAa_132_2 F	154	AGCCAGATACCTCCCCTTGT	this study
SPAa_132_2,508 R	181	TGCTCTGGTCTTCGGTTGTC	this study
SPAa_132_2R	155	TCCAAGGTAGTCCAGCGGTA	this study
SPAa_132_3F	156	CTCGTCGATCCTCGGTGAAG	this study

Table 8: (continued)

Name	ID[1]	Sequence (5' to 3')	Reference
SPAa_132_3R	157	ACGGACGAAAAAGCAACTGC	this study
SPAa_132_4F	158	CACTGTCAGAACGAGGGACC	this study
SPAa_132_4R	159	GTCAAGAGCCACGACCTCAA	this study
SPAa_132_5F	160	CATGTTGTCACCGGGAGACA	this study
SPAa_132_5R	161	CTTTCGGACTTGCGCATACG	this study
SPAa_749_1F	162	CATCAAGCAGCCGTGAATCG	this study
SPAa_749_1R	163	ACAAACGACCACACCAAGGT	this study
SPAa_749_2F	164	GGACAGGTTCTCCTCCAAGC	this study
SPAa_749_2R	165	ATTCGGCTTTCCCTTGCTCA	this study
SPAa_749_3_2F	195	GTTTTTCTGTGAAAGTCGATGG	this study
SPAa_749_3_2R	196	GTATGGCTTGGTGTGTTG	this study
SPAb_234_1_2F	193	TTACGTCTGGTTATTAAACAG	this study
SPAb_234_1_2R	194	AATTCTTGACACCTTGCATG	this study
SPAb_234_3F	171	CGTTTGCCGCTGATGGTATG	this study
SPAb_234_3R	170	TTGGTCTGAGCTGCTTCGAG	this study
SPAb_234_4F	169	CCGGGAAGGAGGAAGAGAGA	this study
SPAb_234_4R	168	CTGCACATTGCTCTCCTCCA	this study
SPAb_234_OFF_2_1049 R	208	GACATCTATTGCCACAAAAAAATAATAATGCTCC	this study
SPAb_234_OFF_2_524 F	207	CACTTAATATGACACCAATCAATATCCAATTACA	this study
SPAb_237_1F	149	CGTTTGCCGCTGATGGTATG	this study
SPAb_237_1R	148	TTGGTCTGAGCTGCTTCGAG	this study
SPAb_237_2F	147	CACGGTCTCGAACTTCCACA	this study
SPAb_237_2R	146	CTGACGCTGTGTGCATTTCC	this study

Table 8: (continued)

Name	ID[1]	Sequence (5' to 3')	Reference
SPAb_237_4F	143	CCACAGCAGTTCTACGAGCA	this study
SPAb_237_4R	142	ATCGAGGCTTGTGGACCTTG	this study
SPAb_237_OFF3_1,160R	183	AGAGACATGCAAGTTACTAA AAACA	this study
SPAb_237_OFF3_621F	182	ATTTTTGGTGCTCATGGAGT TTTCA	this study
qRT-PCR			
PpHY5a_L164	1198	CTTTATCGGCAGAAGCGCCG	Lopez-Obando et al. (2018)
PpHY5a_U63	1197	GTTAGGAGAGTGCCCGAGTTG	Lopez-Obando et al. (2018)
PpHY5b RT 726 F	1079	AGAGTGTCCACCCTACAAAGG	this study
PpHY5b RT 845 R	1080	GTAGAATTCCTGCAGTTGCGC	this study
qRT PpACT5 fwd	205	ACCGAGTCCAACATTCTACC	Le Bail et al. (2013)
qRT PpACT5 rev	206	GTCCACATTAGATTCTCGCA	Le Bail et al. (2013)
qRT PpFedA fwd	1002	CGCTTTCTGATTGCTACAAGTG	Dickopf (2015)
qRT PpFedA rev	1003	CTTCGGTTGAGTAAGCACACTG	Dickopf (2015)
qRT PpFNR fwd	998	GCGCGCACATCTACTTCTG	Possart and Hiltbrunner (2013)
qRT PpFNR rev	999	TTGACAGCCTCACACACCTG	Possart and Hiltbrunner (2013)

Table 8: (continued)

Name	ID[1]	Sequence (5' to 3')	Reference
qRT PpPOR fwd	1000	GTTCAATCATTTCGATTCCA GAG	Koduri et al. (2010)
qRT PpPOR rev	1001	GATTTTCATGTCATCGCACA CTA	Koduri et al. (2010)
Southern blotting			
Probe PpSPAb flanka fwd	209	GCTGCCAGTTCTAAGCCATATT	this study
Probe PpSPAb flanka rev	210	TCACAAGGAGGTGAAGGAATTT	this study

[1] ID in oligonucleotide database

5.1.9 Molecular markers

Molecular markers used in this study are liste in Table 9.

Table 9: Molecular markers used in this study

Molecular marker	Manufacturer
GeneRuler™1kb DNA Ladder	Thermo Fisher Scientific (Schwerte, Germany)
GeneRuler™Low Range DNA ladder	Thermo Fisher Scientific (Schwerte, Germany)
PageRuler™Prestained Protein Ladder	Thermo Fisher Scientific (Schwerte, Germany)

5.1.10 Plasmids

Plasmids used in this study are liste in Table 10.

Table 10: Plasmids used in this study

Plasmid	Description	Res.[1]	Reference
pACT-Cas9	hCas9 driven by OsAct promoter	Amp	Lopez-Obando et al. (2016)

Table 10: (continued)

Plasmid	Description	Res.[1]	Reference
pAMARENA	Gateway destination vector for 35S-driven expression of mCherry-fusion proteins	Amp	M. Jakoby, GenBank ID: FR695418
pAMARENA-PpCOP1a	Gateway expression clone for 35S-driven expression of mCherry-PpCOP1a	Amp	this study
pAMARENA-PpHY5b	Gateway expression clone for 35S-driven expression of mCherry-PpHY5b	Amp	this study
pAMARENA-PpSPAb	Gateway expression clone for 35S-driven expression of mCherry-PpSPAb	Amp	this study
pBNRF	35S-driven neoR cassette, confers resistance to G418	Amp	Schaefer et al. (2010)
pDONR221-PpCOP1a	Gateway entry clone containing the PpCOP1a CDS	Kan	Dickopf (2015)
pDONR221-PpHY5b	Gateway entry clone containing the PpHY5b CDS	Kan	this study
pDONR221-PpSPAb	Gateway entry clone containing the PpSPAb CDS	Kan	Dickopf (2015)
pENSG-CFP	Gateway destination vector for 35S-driven expression of CFP-fusion proteins	Amp	Laubinger (2006)
pENSG-CFP-PpCOP1a	Gateway expression clone for 35S-driven expression of CFP-PpCOP1a	Amp	Dickopf (2015)

Table 10: (continued)

Plasmid	Description	Res.[1]	Reference
pENSG-CFP-PpHY5b	Gateway expression clone for 35S-driven expression of CFP-PpHY5b	Amp	this study
pENSG-CFP-PpSPAb	Gateway expression clone for 35S-driven expression of CFP-PpSPAb	Amp	Dickopf (2015)
pENSG-YFP	Gateway destination vector for 35S-driven expression of YFP-fusion proteins	Amp	Laubinger (2006)
pENSG-YFP-PpCOP1a	Gateway expression clone for 35S-driven expression of YFP-PpCOP1a	Amp	Dickopf (2015)
pENSG-YFP-PpHY5b	Gateway expression clone for 35S-driven expression of YFP-PpHY5b	Amp	this study
pENSG-YFP-PpSPAb	Gateway expression clone for 35S-driven expression of YFP-PpSPAb	Amp	Dickopf (2015)
pJET-sgRNA 132	PpU6-driven sgRNA 132	Amp	this study
pJET-sgRNA 234	PpU6-driven sgRNA 234	Amp	this study
pJET-sgRNA 237	PpU6-driven sgRNA 237	Amp	this study
pJET-sgRNA 749	PpU6-driven sgRNA 749	Amp	this study
pJP118	pB42AD with an introduced gateway cassette, contains LexA-AD for yeast-two-hybrid assays, confers tryptophan protrophy	Amp	Jathish Ponnu, unpublished
pJP118-AtCRY2	Gateway expression clone for LexA AD-AtCRY2 expression	Amp	this study
pJP118-PpCOP1a	Gateway expression clone for LexA AD-PpCOP1a expression	Amp	this study

Table 10: (continued)

Plasmid	Description	Res.[1]	Reference
pJP118-PpHY5b	Gateway expression clone for LexA AD-PpHY5b expression	Amp	this study
pJP118-PpSPAb	Gateway expression clone for LexA AD-PpSPAb expression	Amp	this study
pJP119	PEG202 with an introduced gateway cassette, contains LexA-BD for yeast-two-hybrid assays, confers histidine protrophy	Amp	Jathish Ponnu, unpublished
pJP119-AtCOP1	Gateway expression clone for LexA BD-AtCOP1 expression	Amp	this study
pJP119-PpCOP1a	Gateway expression clone for LexA BD-PpCOP1a expression	Amp	this study
pJP119-PpHY5b	Gateway expression clone for LexA BD-PpHY5b expression	Amp	this study
pJP119-PpSPAb	Gateway expression clone for LexA BD-PpSPAb expression	Amp	this study
PpHY5b-3HA knock-in	For knocking-in a 3HA-tag at the 3' end of the PpHY5b CDS via homologous recombination	Amp	this study

[1] Antibiotic resistance conferred to transformed bacteria

5.1.11 Bacterial and yeast strains

The *E. coli* strain DH5α was used for standard cloning. The ccdB-resistant *E. coli* strain DB3.1 was used for propagating empty Gateway® vectors (Life Technologies, Karlsruhe, Germany). The yeast strain EGY48 was used for yeast-two-hybrid assays.

5.1.12 Plant material

Physcomitrella mutant lines used in this study are listed in Table 11. The Gransden strain (Rensing et al., 2008) was used as a wild type. HR: homologous recombination, CC9: CRISPR/Cas9

Table 11: Physcomitrella mutant lines used in this study

Name	**Line ID**	**Background**	**Method**[1]	**Reference**
PpHY5b-3HA	27	wild type	HR	this study
PpHY5b-3HA	42	wild type	HR	this study
PpHY5b-3HA	2_18	*PpHY5b-3HA 27*	CC9	this study
PpspaA	23/29_3	wild type	HR	Dickopf (2015)
PpspaA	7-2-A1	wild type	HR	Dickopf (2015)
PpspaA	2_2R	wild type	HR	Dickopf (2015)
PpspaB	3_47	wild type	HR	Dickopf (2015)
PpspaB	4/4_1	wild type	HR	Dickopf (2015)
PpspaB	4/4_2	wild type	HR	Dickopf (2015)
PpspaB	7-3-A1	wild type	HR	Dickopf (2015)
PpspaB	3/3_7	wild type	HR	Dickopf (2015)
PpspaAB	2/7_9	*PpspaB* 7-3-A1	HR	Dickopf (2015)
PpspaAB	7/42_9	*PpspaB* 7-3-A1	HR	Dickopf (2015)
PpspaAB	26/42_13	*PpspaB* 7-3-A1	HR	Dickopf (2015)
PpspaAB	35/42_7	*PpspaB* 7-3-A1	HR	Dickopf (2015)
PpspaAB	1_39	wild type	CC9	this study
PpspaAB	1_42	wild type	CC9	this study
PpspaAB	1_47	wild type	CC9	this study

[1] Employed method of gene-targeting

5.1.13 Physcomitrella genes

Physcomitrella gene sequence information was retrieved from Phytozome providing the version 3.3 annotation of the version 3.0 assembly as described in Lang et al. (2018) (https://phytozome.jgi.doe.gov/). Gene identifiers are listed in Table 12.

Table 12: Physcomitrella genes mentioned in this study

name	**alias (V3)**	**alias (V6)**
PpCOP1a	Pp3c2_24290.v3	Pp1s135_17V6
PpCOP1b	Pp3c1_13190.v3	Pp1s86_153V6
PpCOP1c	Pp3c11_15840.v3	Pp1s11_401V6
PpCOP1d	Pp3c7_14320.v3	Pp1s264_64V6
PpCOP1e	Pp3c3_16700.v3.1	Pp1s25_325V6.1
PpCOP1f	Pp3c13_21340.v3.1	Pp1s37_28V6.1
PpCOP1g	Pp3c16_19410.v3.1	Pp1s81_234V6.1
PpCOP1h	Pp3c5_26150.v3.1	Pp1s154_52V6.1
PpCOP1i	Pp3c6_5030.v3.1	Pp1s180_148V6.1
PpFEDa	Pp3c4_8159V3.1	no information
PpFNR	Pp3c9_25700V3.1	Pp1s131_154V6
PpHY5a	Pp3c7_11360.v3.1	Pp1s87_156V6.1
PpHY5b	Pp3c11_17710.v3.1	Pp1s80_72V6
PpPOR	Pp3c12_20650V3.1	Pp1s108_171V6.2
PpSPAa	Pp3c1_24850.v3.1	Pp1s59_66V6.1
PpSPAb	Pp3c2_15860.v3.1	Pp1s30_295V6.1

5.2 Methods

5.3 General cultivation of Physcomitrella

Physcomitrella was cultivated axenically on solid KNOP medium. Plants were grown in walk-in growth chambers (Johnson Controls, Milwaukee, WI, USA) at 21°C and 60% humidity under long day conditions (16 h light, 8 h darkness). Light intensity varied between 50 and 100 μmol m^{-2}s^{-1} and was generated by Lumilux L58W/840 cool white fluorescent tubes (Osram, Munich, Germany). Plates were sealed with Parafilm (Roth, Karlsruhe) to prevent excess water loss. Stock cultures were maintained by inoculating two KNOP plates and one KNOP plate supplemented with 0.5% glucose for every genotype with three gametophores every three month. The KNOP plate supplemented with 0.5% glucose served as a contamination control and was discarded after the next subcultivation. Liquid cultures were cultivated in Erlenmeyer flasks sealed with a silicon plug (Hirschmann, VWR, Darmstadt) and incubated shaking (140 rpm) under long day conditions at 21°C and 60% humidity. For subcultivation, fresh KNOP medium was inoculated from an older liquid culture or tissue harvested from a plate and dispersed using an Ultra-Turrax® (T18 basic, IKA, Staufen, Germany) at 19.000 rpm for 30-60 s. To test for contaminations the disperser-tool was pressed on a Petri dish filled with LB or KNOP medium supplemented with 0.5% glucose immediately after use. Plates were kept at room temperature and checked before every further subcultivation of the respective culture.

5.3.1 Phenotypic analysis of gametophores in light

Single gametophores were inoculated on KNOP medium overlaid with cellophane (Hans Schuett, Halstenbek, Germany). Depending on the experiment, plants were incubated in long day conditions and 80 μmol m^{-2}s^{-1} W light in a walk-in chamber or continuous R light at 46 μmol m^{-2}s^{-1} in a light cabinet until new gametophores had formed, usually three to four weeks. New gametophores were then dissected from the main plant with a forceps. Leaflets were counted using binoculars (Nikon SMZ-U, Düsseldorf, Germany or

Zeiss AXIO Zoom.V16, Oberkochen, Germany). Subsequently, gametophores were stored in 150 μl fixing solution at 4°C until further use. Gametophore length and cell area were determined on the same day. Hence, 1 μl of a 0.1 mg/ml propidium iodide solution was added to the stored gametophores and incubated for 10 min. Gametophores were transferred to a microscope slide. For length measurements pictures were taken at a binocular. For cell area measurement pictures were taken at a Leica SP8 confocal laser scanning microscope (Leica Microsystems, Wetzlar, Germany) using the standard Leica/dsRed settings. Quantification was performed using the ImageJ 1.52h Fiji distribution (Wayne Rasband, NIH, Bethesda, USA).

5.3.2 Phenotypic analysis of gametophores in darkness

Single gametophores were inoculated on KNOP medium overlaid with cellophane (Hans Schuett, Halstenbek, Germany). Plants were incubated in long day conditions and 80 μmol $m^{-2}s^{-1}$ W light in a walk-in chamber for 7 d. Afterwards, the cellophane including all plants was transferred to solid KNOP medium supplemented with 0.5% glucose. Plates were oriented upright and incubated in darkness for another 2 weeks. Counting of leaflets and measurement of gametophore length was performed in the same way as for gametophores grown in light, however only gametophore tissue that had developed in darkness was considered for measurements.

5.3.3 Phenotypic analysis of colony growth

Tissue from liquid culture was harvested using cell strainers (mesh size: 70 μm, Greiner bio-one) and spotted on KNOP medium. Plants were incubated in long day conditions and 80 μmol $m^{-2}s^{-1}$ W light in a walk-in chamber for 21 days. Pictures were taken without opening the Petri dishes at the indicated time points using binoculars (Zeiss AXIO Zoom.V16, Oberkochen, Germany). Quantification was performed using the ImageJ 1.52h Fiji distribution (Wayne Rasband, NIH, Bethesda, USA).

5.3.4 Phenotypic analysis of gravitropic response

Tissue from liquid culture was harvested using cell strainers (mesh size: 70 μm, Greiner bio-one) and spotted on KNOP medium overlaid with cellophane (Hans Schuett, Halstenbek, Germany). Plants were incubated in long day conditions and 80 μmol $m^{-2}s^{-1}$ W light in a walk-in chamber for 7 d. Afterwards, the cellophane including all plants was transferred to solid KNOP medium supplemented with 0.5% glucose. Plates were oriented upright and incubated in darkness for another 2 weeks. Pictures of whole colonies and single filaments were taken with a binocular.

5.4 Molecular biology methods

5.4.1 Agarose gel electrophoresis

Nucleic acids were separated by agarose gel electrophoresis in 0.5% TBE using standard protocols (Sambrook and Russell, 2001). For visualization of nucleic acid 0.25 μg/ml ethidium bromide was added to the gels. Signals were detected using a GEL Stick "Touch" imager (INTAS Science Imaging Instruments, Göttingen, Germany).

5.4.2 Polymerase chain reaction (PCR)

A standard PCR was performed using 1 μl home-made *Taq* DNA polymerase in 1 x PCR reaction buffer, 500 nM forward primer, 500 nM reverse primer, 250 nM dNTPs and 1 μl template DNA. The reaction volume was adjusted to a total of 20 μl using autoclaved double-distilled water. The standard PCR program comprised an initial denaturation step at 95°C for 3 min and 40 cycles of denaturation at 95°C for 30 s, annealing at 55°C for 30 s and elongation at 72°C for 30 s. A final elongation step was performed at 72°C for 10 min. Samples were stored at 15°C until further processing.

5.4.3 DNA sequencing and sequence analysis

Sanger sequencing of DNA was performed by GATC Biotech (Konstanz, Germany; now part of Eurofins, Ebersberg, Germany). Obtained sequences were analyzed using Geneious® software package (version 7.1.7) (Biomatters Ltd, Auckland, New Zealand).

5.4.4 Cloning

Conventional cloning was performed according to standard protocols (Sambrook and Russell, 2001). Gateway® cloning was performed according to the manufacturer's instructions with the following modifications: BP and LR reactions were scaled down to 10 μl and 0.5 μl BP or LR clonase were used per reaction. PCR products or digested DNA fragments were either purified from agarose gels or directly form PCR reaction mixtures using the NucleoSpin® Gel and PCR Clean-up kit (Macherey Nagel, Düren, Germany). For plasmid isolation from *E. coli* cells the NucleoSpin® Plasmid kit (Macherey Nagel, Düren, Germany) was used. If high amounts of plasmid DNA were needed, plasmids were extracted using the Plasmid Plus Midi kit (Qiagen, Hilden, Germany).

5.4.5 Cloning strategy for *PpHY5b-3HA*knock-in construct

Cloning of the *PpHY5b-3HA* knock-in construct was entirely done by Stephen Dickopf. FlankA was amplified from wild-type genomic DNA using the primers SacI-NheI-FlankA fwd and PstI-FlankA rev. The amplicon was ligated into pBluescript SK (+) (Stratagene, discontinued) using the SacI and PstI restriction sites resulting in the pBS FlankA vector. The 3HA tag and NOS Terminator (NosT) were amplified from the vector pAUL1 using the primers EcoRI-3HA fwd2 and NosT rev2 (Lyska et al., 2013). The selection cassette consisting of a 35S-driven *nptII* gene was amplified from the pBS PpSPAa KO vector (Rensing, unpublished) using the primers nptII fwd and nptII rev2. The nptII rev2 primer introduced a fragment complement to the 3HA NosT fragment. Hence, both fragments were combined via overhang extension PCR. This fragment was amplified using the primers EcoRI-3HA fwd2 and EcoRI AscI nptII rev and ligated into the EcoRI restriction site of the pBS FlankA vector resulting in the pBS FlankA 3HA NosT nptII vector.

Flank B was amplified from wild-type genomic DNA using the primers AscI-FlankB fwd and HindIII-NheI-FlankB rev and ligated into pBS FlankA 3HA NosT nptII via AscI and HindIII. The final plasmid is referred to as PpHY5b-3HA knock-in construct (Figure 15). For stable integration into the genome it is highly recommended to linearize the plasmid by NheI digestion.

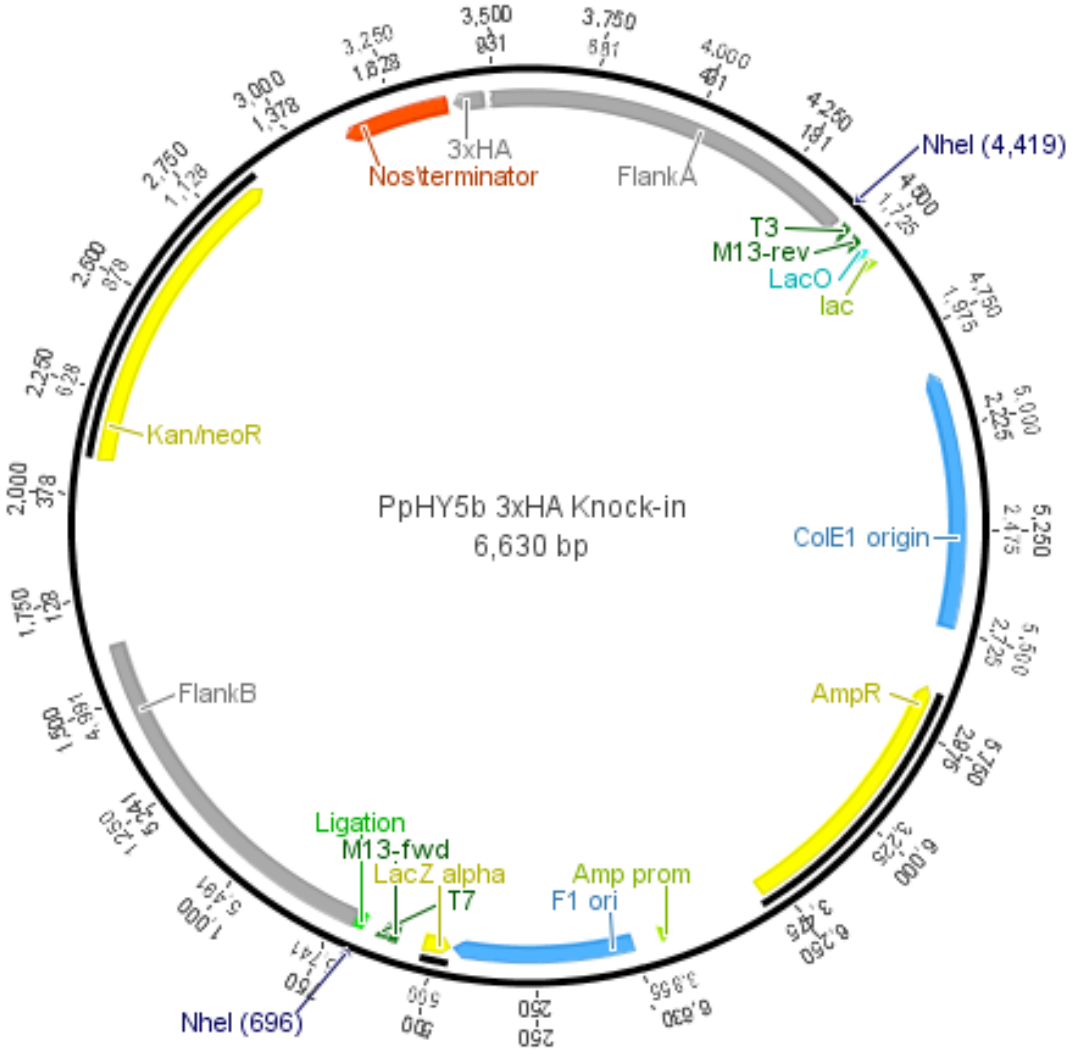

Figure 15: **Plasmid map of the PpHY5b-3HA knock-in construct**

5.4.6 Cloning strategy for the *PpHY5b* CDS

The PpHY5b CDS was cloned via an overhang extension PCR. The first fragment of the CDS was amplified from cDNA using the primers HY5b_CDS_1_F and HY5b_CDS_465_R. The second part was amplified using the primers HY5b_CDS_339_F and HY5b_CDS_834_R. Both fragments had an overlap of 148 bp. In a third PCR both fragments were used as a template to amplify the entire PpHY5b CDS including attB-sites for Gateway® cloning. The stop codon is still present in the CDS.

5.4.7 Preparation and transformation of chemically competent *E. coli*

To prepare highly chemically competent *E. coli* cells for heat shock transformation an LB plate was inoculated with cells from a glycerol stock and incubated at 37°C over night. A single colony was used to inoculate a 20 ml liquid LB preculture, which was incubated at 37°C over night. 2 ml of the preculture were used to inoculate a 250 ml liquid LB main culture, which was incubated at 18°C over night to an OD_{600} of 0.6. Cells were harvested by centrifugation at 2500 g and 4°C for 10 min. The pellet was resuspended in 80 ml ice-cold TB buffer and incubated on ice for 10 min. Cells were pelleted again by centrifugation and resuspended in 20 ml ice-cold TB buffer. DMSO was added to a final concentration of 7% under constant shaking and incubated on ice for 10 min. 100 μl aliquots were prepared and shock frozen in liquid nitrogen immediately. Cells were stored at -80°C. Competence of cells was tested using pBluescript. Only if transformation efficiency was above 10^7 colonies/μg DNA, cells were used for other transformations.

Standard heat shock transformation was carried out by adding 50-100 ng plasmid DNA to a frozen aliquot of competent cells. The aliquot was thawed on ice and flicked regularly to mix cells with DNA. Heat shock was performed at 42°C for 45 s. Afterwards 800 μl ice-cold LB was added and cells were regenerated at 37°C for 20-60 min prior to plating on selective LB plates.

5.4.8 Transformation of Physcomitrella - knock-in

PEG-mediated transformation of Physcomitrella was intially described in Schaefer et al. (1991). To increase transformation efficiency several alteration to the original protocol were made. To isolate protoplasts 200 ml KNOP pH 4.5 medium was inoculated with protonemal tissue. After 4 d plants are transferred to 200 ml fresh KNOP pH 4.5 medium. Protoplast isolation and transformation was carried out 7 dai. To this end the entire plant material was harvested using a 100 μm filter mesh and equilibrated with 12 ml 0.5 M mannitol in a Petri dish for at least 30 min under constant shaking (70 rpm). During the equilibration 0.2 g Driselase® (Cat.: D8037-5G) was dissolved in 5 ml 0.5 M mannitol for at 4°C for at least 30 min in darkness. Afterwards the Driselase® solution was centrifuged at 3500 rpm for 10 min and the supernatant was filter-sterilized. 4 ml of this solution was then added to the equilibrated moss tissue. The plate was covered with aluminium foil and incubated under constant shaking (100 rpm) for 1.5-2 h. Since protoplasts are very sensitive to shearing forces all following steps, especially pipetting, were performed very slowly. Protoplasts were filtered using a 100 μm sieve and a 10 ml pipette into a glass jar. The Petri dish was rinsed with 3 ml 0.5 M mannitol to recover as many protoplasts as possible. The filtrate was filtered again using a 45 μm sieve into a new glass jar. The first jar was rinsed with 3 ml 0.5 M mannitol. The protoplast suspension was equally distributed into two glass vials (approximately 10.5 ml each) and centrifuged at 500 rpm for 10 min with acceleration and break set to 3. After removal of the supernatant both protoplast aliquots were carefully resuspended in 5 ml 0.5 M mannitol by rolling the vials. Protoplasts were centrifuged again at 500 rpm for 10 min with acceleration and break set to 3. Both protoplast aliquots were carefully resuspended in 5 ml 0.5 M mannitol by rolling the vials and both aliquots were combined in one vial. Protoplast yield was determined using a Thoma counting chamber. After another centrifugation at 500 rpm for 10 min with both acceleration and break set to 3 protoplasts were adjusted to 1.2×10^6 with 3M medium. New glass vials were prepared with 50 μg linearized DNA in 0.1 M $Ca(NO_3)_2$), 250 μl protoplast suspension and 350 μl 40% PEG 3M solution. The transformation mix was incubated for

30 min, every 5 min the vials were rolled. Afterwards every 5 min 1, 2, 3, and 4 ml of 3M medium were successively added. Protoplasts were harvested by centrifugation at 500 rpm for 10 min with acceleration and break set to 3 and resuspended in 3 ml regeneration medium. Glass vials were incubated in darkness for 24 h and 5 d in weak light long day conditions. Regenerated protoplasts were then plated on KNOP pH 5.8 plates overlaid with cellophane and incubated in standard cultivation conditions for approximately 10 d until protonemal filaments protruded from the initial protoplast. The cellophane including regenerating plants were moved on selective KNOP pH 5.8 plates and incubated for approximately 10 d until the wild-type control was severely compromised. Plants were transferred to non-selective KNOP pH 5.8 plates and incubated for 10 d. A second round of selection was performed by picking regenerated plants and putting 3 of them together on selective KNOP pH 5.8 plates. Resistant lines were used for genotyping.

5.4.9 Transformation of Physcomitrella - CRISPR/Cas9

The basic principle of CRISPR/Cas9 in Physcomitrella is described in Collonnier et al. (2017) and Lopez-Obando et al. (2016): To induce mutations via CRISPR/Cas9 at least three different plasmids were transformed. The first plasmid, called pACT-Cas9 encoded the Cas9 nuclease (Mali et al., 2013) driven by the *actin* promoter of rice. The second plasmid, called pBNRF, conferred resistance to the antibiotic G418 (Schaefer et al., 2010). For the third plasmid, the sgRNA driven by the U6 RNA polymerase II promoter from Physcomitrella was synthesized (Integrated DNA Technologies, Leuven, Belgium) and cloned into pJET1.2/blunt using the CloneJET PCR Cloning Kit (Thermo Fisher Scientific, Schwerte, Germany) according to the manufacturer's instructions. Two targeting constructs were created for each locus. The 20 nucleotide targeting sequence was chosen using the CRISPOR program (Haeussler et al., 2016) (Supplemental Table S1). Amplification using the U6 promoter works best, if the targeting sequence starts with a guanine nucleotide. Since no stable integration of the transformed plasmid DNA is desired, it is not recommended to open the plasmids via restriction digestion. 5 μg pACT-Cas9, 5 μg pBNRF and a total of 15 μg of an equimolar mix of the different sgRNA-encoding

plasmids was transformed. After transformation only one round of antibiotic selection was performed. Resistant plants were subsequently genotyped by Sanger sequencing the *PpSPAb* locus. Plants that harbored a frameshift mutation leading to a premature stop codon in *PpSPAb* were then Sanger sequenced at the *PpSPAa* loci.

5.4.10 Isolation of genomic DNA from Physcomitrella

Approximately 10 gametophores or the equivalent amount of protonemal tissue was harvested and immediately frozen in liquid nitrogen. Only green and healthy tissue was chosen. Material was ground using a plastic pestle. 200 μl EB buffer were added and the sample was vortexed vigorously. After centrifugation at 13000 rpm for 3 min 150 μl of the supernatant were transferred to a new reaction tube. 150 μl isopropanol was added and the sample was incubated at room temperature for 2 min. After another centrifugation at 13000 rpm for 10 min the supernatant was removed and samples were dried on tissue paper for at least 15 min. Alternatively, samples were dried in a vacuum-concentrator (BA-VC-300H, Helmut Saur, Reutlingen) for 3 min. DNA was resuspended in 100 μl H_2O.

For Southern blot analysis high amounts of gDNA were needed. Here, a CTAB-based extraction method was used: Tissue from a fresh liquid culture was harvested, frozen in liquid nitrogen and ground with pestle and mortar. Tissue was incubated with 8 ml preheated CTAB buffer for 1 h at 65°C. Samples were cooled down on ice for 2 min. 8 ml of a 24:1 chloroform:isoamyl alcohol mix was added and mixed by inverting. Samples were centrifuged at 2500 g and 4°C for 10 min. The upper aqueous phase was transferred into a new plastic tube. If chloroform:isoamyl alcohol washing was repeated until the aqueous phase was yellow or clear. RNaseA was added to a concentration of 100 μg/ml and incubated at 37°C for at least 45 min. DNA was precipitated adding 1/10 of the volume of 3 M sodium acetate and 1 volume cold isopropanol and incubating the mixture at -20^{c}ircC over night. DNA was pelleted in a centrifuge at 2500 g and 4°C for 30 min. The pellet was washed with 10 ml washing buffer for 20 min. After centrifugation at 2500 g for 5 min, the pellet was washed with 10 ml 70% ethanol for 5 min. The sample

was centrifuged at 2500 g for 5 min and the supernatant was completely removed. The pellet was dried as described above and resuspended in 100-500 μl H_2O. Resuspension was performed at 4°C over night. The solution was incubated at 65°C for 10 min and transferred to a 1.5 ml reaction tube.

5.4.11 Genotyping

Successful integration of the 3HA-tag at the 3' end of the PpHY5b CDS was confirmed using the two primer pairs PpHY5b 1,833 F/PpHY5b 4,063 R and PpHY5b 3,812 F/PpHY5b 4,951 R on cDNA and Sanger sequencing of the fragments after gel extraction.

To genotype putative *PpspaAB* mutant plants after successful transformation genomic DNA was prepared as described above. For amplification DreamTaq™Hot Start DNA polymerase (Thermo Fisher Scientific, Schwerte, Germany) or GoTaq® G2 Hot Start Green Master Mix (Promega, Mannheim, Germany) were used. After gel extraction one of the primers used for amplification (Table 13) was also used for Sanger sequencing.

Table 13: Primer combinations used for genotyping of putative *PpspaAB* mutant lines

Locus	Forward primer	Reverse primer	Amplicon size
132 target	SPAa_132_1,954 F	SPAa_132_2,508 R	555 bp
749 target	guideRna749forwLeft	guideRna749forwRight	668 bp
234 target	guideRna237forwLeft	guideRna237forwRight	700 bp
237 target	guideRna237forwLeft	guideRna237forwRight	700 bp
132 off-target 1	SPAa_132_1F	SPAa_132_1R	541 bp
132 off-target 2	SPAa_132_2 F	SPAa_132_2R	667 bp
132 off-target 3	SPAa_132_3F	SPAa_132_3R	684 bp
132 off-target 4	SPAa_132_4F	SPAa_132_4R	653 bp
132 off-target 5	SPAa_132_5F	SPAa_132_5R	564 bp
749 off-target 1	SPAa_749_1F	SPAa_749_1R	516 bp

Table 13: (continued)

Locus	Forward primer	Reverse primer	Amplicon size
749 off-target 2	SPAa_749_2F	SPAa_749_2R	695 bp
749 off-target 3	SPAa_749_3_2F	SPAa_749_3_2R	881 bp
234 off-target 1	SPAb_234_1_2F	SPAb_234_1_2R	934 bp
234 off-target 2	SPAb_234_OFF_2_524 F	SPAb_234_OFF_2_1049 R	526 bp
234 off-target 3	SPAb_234_3F	SPAb_234_3R	591 bp
234 off-target 4	SPAb_234_4F	SPAb_234_4R	542 bp
237 off-target 1	SPAb_237_1F	SPAb_237_1R	591 bp
237 off-target 2	SPAb_237_2F	SPAb_237_2R	643 bp
237 off-target 3	SPAb_237_OFF3_621F	SPAb_237_OFF3_1,160R	540 bp
237 off-target 4	SPAb_237_4F	SPAb_237_4R	617 bp

5.4.12 Isolation of total RNA from Physcomitrella

Total RNA was isolated from 100 ng snap-frozen plant material, mostly protonemal filaments using the RNeasy® Plant Mini Kit (Qiagen, Hilden, Germany) according to the manufacturer's instructions. RNA yield was determined using a Nanodrop ND-1000 spectrophotometer (Thermo Fisher Scientific, Schwerte, Germany). RNA integrity was assessed on a 1% agarose gel. RNA samples were stored at -80°C.

5.4.13 DNase treatment of RNA

To remove DNA contaminations, 1 μg RNA was treated with 1 μl TURBO™DNase (Life Technologies, Karlsruhe, Germany) in a 20 μl reaction containing 1 x TURBO™DNase buffer at 37°C for 1 h. The DNase was inhibited by adding 2 μl 50 mM EDTA and an incubation at 75°C for 10 min.

5.4.14 Reverse transcription of RNA to cDNA

1 μg DNase-treated RNA was incubated with 2 μl 10μM oligo-$(dT)_{18}$ primers in a 20 μl reaction volume at 65°C for 5 min and cooled down to 4°C for 2 min. Afterwards 4 μl 10 mM dNTPs, 8 μl 5 x RevertAid^{TM}buffer and 1 μl RevertAid^{TM}H Minus M-MuLV Reverse Transcriptase (Thermo Fisher Scientific, Schwerte, Germany) were added to the reaction tube. Samples were incubated at 37°C for 5 min, at 42°C for 60 min and at 70°C for 5 min. cDNA was stored at -20°C.

5.4.15 Quantitative real-time PCR

1 μl cDNA was used as a template in a 10 μl reaction mix containing 1 x KAPA^{TM}SYBR® FAST qPCR Mastermix (PEQLAB Biotechnolgie, Erlangen, Germany) and 125 nM forward and reverse primers. Thermocycling and measurements were performed by an Applied Biosystems® 7300 Real-time PCR system (Life Technologies, Karlsruhe, Germany). After an initial denaturation step at 95°C for 2 min, 40 cycles of 95°C for 2 s and 60°C for 30 s were run. Amplicon dissociation was tested by two cycles of 60°C for 15 s and 95°C for 15 s at the end of the respective run. Relative transcript levels were determined by the $2^{-\Delta\Delta C_T}$ method (Livak and Schmittgen, 2001). Real time PCR was performed on at least two biological and three technical replicates on a QuantStudio 5 Real-Time PCR System (Thermo Fisher Scientific, Schwerte, Germany).

5.4.16 Southern blotting

The probe for Southern blotting was designed to hybridize to a sequence flanking the knock-out cassette of the *PpspaB* knock-out construct (Dickopf, 2015). The DIG-dUTP marked probe was amplified from wildtype gDNA using the DreamTaq^{TM}Hot Start DNA polymerase (Thermo Fisher Scientific, Germany) DNA polymerase and the PCR DIG Labeling Mix^{plus} (Roche Diagnostics, Mannheim, Germany, Cat. 1 835 289) using the primers Probe PpSPAb flanka fwd and Probe PpSPAb flanka rev. The PCR product was run on an agarose gel, purified and stored at -20°C until further use. 3 μg gDNA samples were digested with HindIII over night at 37°C and run on a 0.8% agarose gel for 6 h at

50 V and 1 h at 100 V. The gel was incubated in denaturing solution and neutralizing solution for 1 h each. DNA was blotted on a nylon membrane (Roche, Mannheim, Germany, Cat. 11 209 272 001) using 1 l 10 x SSC buffer over night. Between the following steps, the membrane was stored in 2 x SSC buffer. The DNA was crosslinked to the membrane using the auto-crosslink setting of a UV-Stratalinker ® 1800 (Stratagene, acquired by Agilent, Waldbronn, Germany) twice. Prehybridization was performed in 30 ml hybridization buffer at 65°C for 5 h. Buffer was frozen at -20°C and reused on the following day. Hybridization was performed at 65°C over night in 30 ml hybridization buffer containing 200 ng of the probe. Before usage the probe was denatured at 95°C for 5 min and then added to the preheated hybridization buffer. The following washing steps were all performed at 65°C. The membrane was washed in hybridization buffer used for prehybridization on the previous day for 30 min. Afterwards it was washed in 30 ml 2 x SSC supplemented with 0.1% SDS for 30 min. In the last step the membrane was incubated in 50 ml 0.1 x SSC supplemented with 0.1% SDS for 30 min twice. Blocking was performed at room temperature and comprised the following steps: Incubation in 100 ml washing buffer for 5 min, in B2 for 30 min and in antibody solution (Anti-DIG-AP, Roche, Mannheim, Germany, Cat. 1 093 274) for 30 min to 3 h. The membrane was washed again in 50 ml washing buffer for 5 min and twice in 50 ml washing buffer for 30 min. The membrane was incubated in 20 ml B3 for 5 min and incubated with CSPD (Roche Diagnostics, Mannheim, Germany, Cat. 1 655 884) solution in a small plastic bag at room temperature for 5 min and at 37°C for 20 min. Light emission was detected with an ImageQuant™LAS 4000 mini imaging system (GE Healthcare, Piscataway, USA) in 30 min increment steps over night.

5.5 Biochemical methods

5.5.1 Isolation of total protein from Physcomitrella

For isolation of total protein from Physcomitrella under non-denaturing conditions, tissue was snap-frozen in liquid nitrogen and ground to a fine powder using mortar and pestle. 0.2 g of powder was transferred to a 2 ml reaction tube and 300 μl ice-cold YODA buffer

were added. The samples were mixed vigorously until the mixture was completely thawed. Samples were centrifuged at 20000 g and 4°C for 20 min. Approximately 240 μl of the supernatant were transferred to a new reaction tube.

5.5.2 Bradford assay

Protein concentrations of the total extracts were determined using the Bradford assay (Bio-Rad Laboratories, Munich, Germany). Extracts were diluted 1:10 and 10 μl of the dilutions were mixed with 190 μl of a 1:5 dilution of the Bradford reagent (Bio-Rad Laboratories, Munich, Germany). OD_{595} was measured in an Infinite® M200 plate reader (Tecan, Männedorf, Germany). A standard curve based on the OD_{595} of known concentrations of bovine serum albumin (BSA) was used to calculate protein concentrations in total extracts.

5.5.3 Immunoprecipitation

PpHY5b-3HA protein was concentrated by immunoprecipitation using Pierce™Anti-HA magnetic beads (Thermo Fisher Scientific, Schwerte, Germany, Cat. 88836). Before use beads were washed on a magnetic rack (Promega, Mannheim, Germany) three times in ice-cold YODA buffer. Depending on the total protein concentration 15-130 μg total protein were incubated with 15 μl beads at 4°C on a rotator for 1-3 h. Afterwards samples were incubated on a magnetic rack for 1 min and the supernatant was removed. Elution was performed by adding 20 μl 1 x Lämmli buffer to the samples and incubating them at 95°C under constant shaking for 5 min. If samples were not immediately used for Western blot analysis they were stored at -20°C.

5.5.4 SDS polyacrylamide gel electrophoresis (SDS-PAGE)

SDS-PAGE was performed on a discontinuous gel as described by Laemmli (1970). All experiments were performed using the Mini PROTEAN® Tetra cell electrophoresis system (Bio-Rad Laboratories, Munich, Germany). Stacking gels contained 5% acrylamide and separating gels contained 15% acrylamide. SDS-PAGE gels ran at 50 V for 30 min and

at 150 V for approximately 1 h until the blue running front leaked from the gels into the buffer tank.

5.5.5 Western blotting

After SDS-PAGE proteins were transferred from the gel to a polyvinyledene difluoride (PVDF) membrane that was activated in 100 % methanol. Wet blotting was performed in freshly prepared carbonate blotting buffer at 45 V for 90-120 min using the Mini PROTEAN® Tetra cell wet blot system (Bio-Rad Laboratories, Munich, Germany). After transfer, membranes were incubated in 1 x Roti-Block (Roche Diagnostics, Mannheim, Germany) at room temperature for 1 h or at 4°C over night.

5.5.6 Immunodetection

Membranes were incubated with a primary antibody in a sealed plastic bag rotating at room temperature for 1 h or at 4°C over night. Afterwards membranes were washed three times in approximately 40 ml TBS-T for 5 min and incubated with a secondary HRP-coupled antibody at room temperature for 1 h. Membranes were washed again three times and HRP activity was detected using the SuperSignal® West Femto Maximum Sensitivity kit (Thermo Fisher Scientific, Schwerte, Germany) according to the manufacturer's instructions and the ImageQuant™LAS 4000 mini imaging system (GE Healthcare, Piscataway, USA).

5.6 Protein-protein interaction assays

5.6.1 Colocalization studies in leek epidermal cells

For colocalization studies in leek epidermal cells, gold particles were coated with plasmid DNA. Coated gold particles were then shot into leek cells by particle bombardment. Gold particle solution was prepared by adding 1 ml 70% ethanol to 30 mg particles with a diameter of 1μm. After vortexing the mixture was incubated at room temperature for 15 min. Particles were pulse-centrifuged and washed with 1 ml sterile water twice. Finally,

particles were resuspended in 1 ml sterile water and mixed vigorously. 50 μl aliquots were prepared under constant vortexing. For each transformation 5 μl gold particles were mixed with 600 ng of each respective plasmid, 10 μl 2.5 M $CaCl_2$ and 4 μl 0.1 M spermidine. Samples were pulse-centrifuged, vortexed and incubated for 15 min at room temperature. During the incubation samples were regularly vortexed. Gold particles were pelleted by pulse centrifugation and the supernatant was discarded. The pellet was washed with 100 μl 70% ethanol and 50 μl 100% ethanol. Afterwards gold particles were resuspended in 12 μl 100% ethanol and spotted in the middle of a macrocarrier (Bio-Rad Laboratories, Munich, Germany). Particle bombardment was performed using a helium Helios gun (Bio-Rad Laboratories, Munich, Germany) according to the manufacturer's instructions. The second, third or fourth layer of the bottom white part from a fresh leek stalk was used for transformation. Gold particles were accelerated by 900 psi helium pressure. After transformation, samples were incubated at room temperature for 12-24 h prior to microscopic analysis. Fluorescent proteins were detected using a confocal laser scanning microscope (SP8, Leica Microsystems, Wetzlar, Germany). YFP was excited by an argon laser at 561 nm and detected between 525-600 nm by a HyD (Leica Microsystems, Wetzlar, Germany). CFP was excited by an argon laser at 458 nm and detected between 465-505 nm by a HyD.

5.6.2 FRET-FLIM studies in leek epidermal cells

Leek epidermal cells were transformed as described above. Fluorescent proteins were detected using a confocal laser scanning microscope (SP8, Leica Microsystems, Wetzlar, Germany). YFP was exited by a pulsed picosecond laser at 470 nm with a frequency of 5 to 40 MHz. The detection window was set to 525-559 nm. mCherry was excited with a laser at 561 nm. The detection window was set to 668-740 nm. FRET was inferred by comparing the fluorescence lifetime of the YFP donor in presence or absence of the mCherry acceptor. Lifetimes were measured by time-correlated single photon counting (TCSPC) using the PicoHarp300 unit (PicoQuant, Berlin, Germany). Entire nuclei or nuclear speckles were used as regions of interest to generate TCSPC histograms. Values

were fitted to a mono- or biexponential decay model using the SymPhoTime 32 software (PicoQuant, Berlin, Germany).

5.6.3 Yeast-Two-Hybrid

For yeast transformation the strain EGY48 was used. Chemically competent cells were prepared by inoculating 3 colonies from a fresh SD -uracil plate into 5 ml SD -uracil preculture, which is incubated at 30°C over night. The OD_{600} of a 200 ml SD -uracil main culture was adjusted to 0.3 with cells from the preculture. The main culture was incubated at 30°C for 2-3 h until OD_{600} reached 0.6. Cells were harvested by centrifugation at 2500 rpm for 5 min. The pellet was washed first with 80 ml sterile water and second with 10 ml 1 x TE/LiAc. Cells were resuspended in 6 ml 1 x TE/LiAc/15% glycerol. Aliquots of 100 μl were prepared. If aliquots were not used for transformation immediately, they were put into a styrofoam box at -80°C to allow for a slow freezing process.

Yeast cells were mixed with 1 μg bait- and prey-encoding plasmids and 300 μl PEG/LiAc solution. Samples were incubated shaking at 28°C for 30 min. 35 μl DMSO were added to each samples, mixed by inversion and incubated at 42°C for 15 min. Cells were harvested by centrifugation at 5000 rpm for 1 min, resuspended in 200 μl 1 x TE and incubated on SD -tryptophane -histidine -uracil + glucose plates at 30°C for 4 d. 10 colonies of each combination were combined and OD_{600} was adjusted to 1, 0.1 and 0.01. 10 μl were dropped on a SD -leucine -tryptophane -histidine + galactose + raffinose plates and incubated at 30°C for 4 d.

6 References

References

Abbas, N., Maurya, J. P., Senapati, D., Gangappa, S. N., and Chattopadhyay, S. (2014). Arabidopsis CAM7 and HY5 Physically Interact and Directly Bind to the HY5 Promoter to Regulate Its Expression and Thereby Promote Photomorphogenesis. *The Plant Cell*, 26(3):1036–1052.

Ahmad, M. and Cashmore, A. (1993). HY4 gene of A. thaliana encodes a protein with characteristics of a blue-light photoreceptor. *Nature*, 366(6451):162–166.

Al-Sady, B., Ni, W., Kircher, S., Schäfer, E., and Quail, P. H. (2006). Photoactivated Phytochrome Induces Rapid PIF3 Phosphorylation Prior to Proteasome-Mediated Degradation. *Molecular Cell*, 23(3):439–446.

Ang, L. H., Chattopadhyay, S., Wei, N., Oyama, T., Okada, K., Batschauer, A., and Deng, X. W. (1998). Molecular interaction between COP1 and HY5 defines a regulatory switch for light control of Arabidopsis development. *Molecular Cell*, 1(2):213–222.

Artz, O. (2014). *Analysis of missense mutations in the Arabidopsis thaliana SPA1 N-terminal domain*. Master thesis, Universität zu Köln.

Bae, S., Kweon, J., Kim, H. S., and Kim, J. S. (2014). Microhomology-based choice of Cas9 nuclease target sites. *Nature Methods*, 11(7):705–706.

Balcerowicz, M., Fittinghoff, K., Wirthmueller, L., Maier, A., Fackendahl, P., Fiene, G., Koncz, C., and Hoecker, U. (2011). Light exposure of Arabidopsis seedlings causes rapid de-stabilization as well as selective post-translational inactivation of the repressor of photomorphogenesis SPA2. *The Plant Journal For Cell And Molecular Biology*, 65(5):712–723.

Banerjee, R. and Batschauer, A. (2005). Plant blue-light receptors. *Planta*, 220(3):498–502.

Bateman, R. M., Crane, P. R., DiMichele, W. A., Kenrick, P. R., Rowe, N. P., Speck, T., and Stein, W. E. (1998). EARLY EVOLUTION OF LAND PLANTS: Phylogeny, Physiology, and Ecology of the Primary Terrestrial Radiation. *Annual Review of Ecology and Systematics*, 29(1):263–292.

Becker, B. and Marin, B. (2009). Streptophyte algae and the origin of embryophytes. *Annals of Botany*, 103(7):999–1004.

Biedermann, S. and Hellmann, H. (2011). WD40 and CUL4-based E3 ligases: lubricating all aspects of life. *Trends in Plant Science*, 16(1):38–46.

Binkert, M., Kozma-Bognar, L., Terecskei, K., De Veylder, L., Nagy, F., and Ulm, R. (2014). UV-B-Responsive Association of the Arabidopsis bZIP Transcription Factor ELONGATED HYPOCOTYL5 with Target Genes, Including Its Own Promoter. *The Plant Cell*, 26(10):4200–4213.

Boll, V. (2017). *Evolutionäre Konservierung des COP1/SPA-Komplexes in Physcomitrella patens*. Bachelor thesis, University of Cologne.

Brown, B. A., Cloix, C., Jiang, G. H., Kaiserli, E., Herzyk, P., Kliebenstein, D. J., and Jenkins, G. I. (2005). A UV-B-specific signaling component orchestrates plant UV protection. *Proceedings of the National Academy of Sciences*, 102(50):18225–18230.

Casal, J. J., Sánchez, R. A., and Botto, J. F. (1998). Modes of action of phytochromes. *Journal of Experimental Botany*, 49(319):127–138.

Chaves, I., Pokorny, R., Byrdin, M., Hoang, N., Ritz, T., Brettel, K., Essen, L.-O., van der Horst, G. T. J., Batschauer, A., and Ahmad, M. (2011). The cryptochromes: blue light photoreceptors in plants and animals. *Annual Review of Plant Biology*, 62:335–364.

Chen, H., Huang, X. X., Gusmaroli, G., Terzaghi, W., Lau, O. S., Yanagawa, Y., Zhang, Y. Y., Li, J., Lee, J.-H. J.-H., Zhu, D., and Deng, X. W. (2010). Arabidopsis CULLIN4-damaged DNA binding protein 1 interacts with CONSTITUTIVELY PHOTOMORPHOGENIC1-SUPPRESSOR OF PHYA complexes to regulate photomorphogenesis and flowering time. *The Plant Cell*, 22(1):108–23.

Chen, M., Tao, Y., Lim, J., Shaw, A., and Chory, J. (2005). Regulation of phytochrome B nuclear localization through light-dependent unmasking of nuclear-localization signals. *Current Biology*, 15(7):637–642.

Chen, S., Lory, N., Stauber, J., and Hoecker, U. (2015). Photoreceptor Specificity in the Light-Induced and COP1-Mediated Rapid Degradation of the Repressor of Photomorphogenesis SPA2 in Arabidopsis. *PLOS Genetics*, 11(9):e1005516.

Chen, S., Wirthmueller, L., Stauber, J., Lory, N., Holtkotte, X., Leson, L., Schenkel, C., Ahmad, M., and Hoecker, U. (2016). The functional divergence between SPA1 and SPA2 in Arabidopsis photomorphogenesis maps primarily to the respective N-terminal kinase-like domain. *BMC Plant Biology*, 16(1):165.

Chen, Y.-R., Su, Y.-s., and Tu, S.-L. (2012). Distinct phytochrome actions in nonvascular plants revealed by targeted inactivation of phytobilin biosynthesis. *Proceedings of the National Academy of Sciences of the United States of America*, 109(21):8310–8315.

Christie, J., Arvai, A., Baxter, K., Heilmann, M., Pratt, A., Hara, A., Kelly, S., Hothorn, M., Smith, B., Hitomi, K., Jenkins, G., and Getzoff, E. (2012). Disruption of Cross-Dimer Salt Bridges. *Science*, 335(March):1492–1496.

Christie, J. M. (2007). Phototropin blue-light receptors. *Annual Review of Plant Biology*, 58:21–45.

Collonnier, C., Epert, A., Mara, K., Maclot, F., Guyon-Debast, A., Charlot, F., White, C., Schaefer, D. G., and Nogué, F. (2017). CRISPR-Cas9-mediated efficient directed mutagenesis and RAD51-dependent and RAD51-independent gene targeting in the moss Physcomitrella patens. *Plant Biotechnology Journal*, 15(1):122–131.

Cove, D. J., Schild, A., Ashton, N. W., and Hartmann, E. (1978). Genetic and physiological studies of the effect of light on the development of the moss, Physcomitrella patens. *Photochemistry and Photobiology*, 27(2):249–254.

Delwiche, C. F. and Cooper, E. D. (2015). The evolutionary origin of a terrestrial flora. *Current Biology*, 25(19):R899–R910.

Deng, X. W., Caspar, T., and Quail, P. H. (1991). cop1: a regulatory locus involved in light-controlled development and gene expression in Arabidopsis. *Genes & Development*, 5(7):1172–1182.

Deng, X.-W., Matsui, M., Wei, N., Wagner, D., Chu, A. M., Feldmann, K. A., and Quail, P. H. (1992). COP1, an arabidopsis regulatory gene, encodes a protein with both a zinc-binding motif and a Gβ homologous domain. *Cell*, 71:791–801.

Dickopf, S. (2015). *The role of COP1 and SPA genes in the moss Physcomitrella patens.* PhD thesis, Universität zu Köln.

Dieterle, S. (2013). *Functional analysis of SPA1 N-terminal domain.* Ph.d. thesis, Universität zu Köln.

Dittami, S. M., Heesch, S., Olsen, J. L., and Collén, J. (2017). Transitions between marine and freshwater environments provide new clues about the origins of multicellular plants and algae. *Journal of Phycology*, 53(4):731–745.

Engel, P. P. (1968). The Induction of Biochemical and Morphological Mutants in the Moss Physcomitrella patens. 55(4):438–446.

Favory, J.-J., Stec, A., Gruber, H., Rizzini, L., Oravecz, A., Funk, M., Albert, A., Cloix, C., Jenkins, G. I., Oakeley, E. J., Seidlitz, H. K., Nagy, F., and Ulm, R. (2009). Interaction of COP1 and UVR8 regulates UV-B-induced photomorphogenesis and stress acclimation in Arabidopsis. *The EMBO Journal*, 28(5):591–601.

Fittinghoff, K., Laubinger, S., Nixdorf, M., Fackendahl, P., Baumgardt, R.-L., Batschauer, A., and Hoecker, U. (2006). Functional and expression analysis of Arabidopsis SPA genes during seedling photomorphogenesis and adult growth. *The Plant Journal*, 1(4):577–590.

Frank, W., Decker, E. L., and Reski, R. (2005). Molecular tools to study Physcomitrella patens. *Plant biology (Stuttgart, Germany)*, 7(3):220–227.

Franklin, K. A. and Quail, P. H. (2010). Phytochrome functions in Arabidopsis development. *Journal of Experimental Botany*, 61(1):11–24.

Freemont, P. S. (2000). RING for destruction? *Current biology : CB*, 10(2):R84–7.

Galvão, V. C. and Fankhauser, C. (2015). Sensing the light environment in plants: Photoreceptors and early signaling steps. *Current Opinion in Neurobiology*, 34(Figure 1):46–53.

Gangappa, S. and Botto, J. (2016). The Multifaceted Roles of HY5 in Plant Growth and Development. *Molecular Plant*, 9(10):1353–1365.

Genoud, T., Schweizer, F., Tscheuschler, A., Debrieux, D., Casal, J. J., Schäfer, E., Hiltbrunner, A., and Fankhauser, C. (2008). FHY1 mediates nuclear import of the light-activated phytochrome A photoreceptor. *PLoS Genetics*, 4(8).

Guo, H., Duong, H., Ma, N., and Lin, C. (1999). The Arabidopsis blue light receptor cryptochrome 2 is a nuclear protein regulated by a blue light-dependent post-transcriptional mechanism. *Plant Journal*, 19(3):279–287.

Haeussler, M., Schönig, K., Eckert, H., Eschstruth, A., Mianné, J., Renaud, J. B., Schneider-Maunoury, S., Shkumatava, A., Teboul, L., Kent, J., Joly, J. S., and Concordet, J. P. (2016). Evaluation of off-target and on-target scoring algorithms and integration into the guide RNA selection tool CRISPOR. *Genome Biology*, 17(1):1–12.

Hardtke, C. S., Gohda, K., Osterlund, M. T., Oyama, T., Okada, K., and Deng, X. W. (2000). HY5 stability and activity in arabidopsis is regulated by phosphorylation in its COP1 binding domain. *The EMBO journal*, 19(18):4997–5006.

Hiltbrunner, A., Tscheuschler, A., Viczián, A., Kunkel, T., Kircher, S., and Schäfer, E. (2006). FHY1 and FHL act together to mediate nuclear accumulation of the phytochrome A photoreceptor. *Plant and Cell Physiology*, 47(8):1023–1034.

Hoecker, U. (2017). The activities of the E3 ubiquitin ligase COP1/SPA, a key repressor in light signaling. *Current Opinion in Plant Biology*, 37:63–69.

Hoecker, U. and Quail, P. H. (2001). The phytochrome A-specific signaling intermediate SPA1 interacts directly with COP1, a constitutive repressor of light signaling in Arabidopsis. *The Journal of Biological Chemistry*, 276(41):38173–38178.

Hoecker, U., Tepperman, J. M., and Quail, P. H. (1999). SPA1, a WD-repeat protein specific to phytochrome A signal transduction. *Science*, 284(5413):496–499.

Hoecker, U., Xu, Y., and Quail, P. H. (1998). SPA1: a new genetic locus involved in phytochrome A-specific signal transduction. *The Plant Cell*, 10(1):19–33.

Holm, M., Hardtke, C. S., Gaudet, R., and Deng, X. W. (2001). Identification of a structural motif that confers specific interaction with the WD40 repeat domain of Arabidopsis COP1. *EMBO Journal*, 20(1-2):118–127.

Holtkotte, X., Dieterle, S., Kokkelink, L., Artz, O., Leson, L., Fittinghoff, K., Hayama, R., Ahmad, M., and Hoecker, U. (2016). Mutations in the N-terminal kinase-like domain of the repressor of photomorphogenesis SPA1 severely impair SPA1 function but not light responsiveness in Arabidopsis. *Plant Journal*, 88(2):205–218.

Hori, K., Maruyama, F., Fujisawa, T., Togashi, T., Yamamoto, N., Seo, M., Sato, S., Yamada, T., Mori, H., Tajima, N., Moriyama, T., Ikeuchi, M., Watanabe, M., Wada, H., Kobayashi, K., Saito, M., Masuda, T., Sasaki-Sekimoto, Y., Mashiguchi, K., Awai, K., Shimojima, M., Masuda, S., Iwai, M., Nobusawa, T., Narise, T., Kondo, S., Saito, H., Sato, R., Murakawa, M., Ihara, Y., Oshima-Yamada, Y., Ohtaka, K., Satoh, M., Sonobe, K., Ishii, M., Ohtani, R., Kanamori-Sato, M., Honoki, R., Miyazaki, D., Mochizuki, H., Umetsu, J., Higashi, K., Shibata, D., Kamiya, Y., Sato, N., Nakamura, Y., Tabata, S., Ida, S., Kurokawa, K., and Ohta, H. (2014). Klebsormidium flaccidum genome reveals primary factors for plant terrestrial adaptation. *Nature Communications*, 5(May):1–9.

Huang, X., Ouyang, X., and Deng, X. W. (2014). Beyond repression of photomorphogenesis: role switching of COP/DET/FUS in light signaling. *Current Opinion in Plant Biology*, 21:96–103.

Imaizumi, T., Kadota, A., Hasebe, M., and Wada, M. (2002). Cryptochrome light signals control development to suppress auxin sensitivity in the moss Physcomitrella patens. *The Plant cell*, 14(2):373–386.

Inoue, S.-i., Kinoshita, T., and Shimazaki, K.-i. (2005). Possible Involvement of Phototropins in Leaf Movement of Kidney Bean in Response to Blue Light. *Plant Physiology*, 138(4):1994–2004.

Jaedicke, K., Lichtenthäler, A. L., Meyberg, R., Zeidler, M., and Hughes, J. (2012). A phytochrome-phototropin light signaling complex at the plasma membrane. *Proceedings of the National Academy of Sciences of the United States of America*, 109(30):12231–12236.

Jakoby, M., Weisshaar, B., Dröge-Laser, W., Vicente-Carbajosa, J., Tiedemann, J., Kroj, T., and Parcy, F. (2002). bZIP transcription factors in Arabidopsis. *Trends in Plant Science*, 7(3):106–111.

Jang, I. C., Henriques, R., and Chua, N. H. (2013). Three transcription factors, HFR1, LAF1 and HY5, regulate largely independent signaling pathways downstream of phytochrome a. *Plant and Cell Physiology*, 54(6):907–916.

Jang, I.-C., Henriques, R., Seo, H. S., Nagatani, A., and Chua, N.-H. (2010). Arabidopsis PHYTOCHROME INTERACTING FACTOR Proteins Promote Phytochrome B Polyubiquitination by COP1 E3 Ligase in the Nucleus. *the Plant Cell Online*, 22(7):2370–2383.

Jang, I.-C., Yang, J.-Y., Seo, H. S., and Chua, N.-H. (2005). HFR1 is targeted by COP1 E3 ligase for post-translational proteolysis during phytochrome A signaling. *Genes & Development*, 19(5):593–602.

Jang, S., Marchal, V., Panigrahi, K. C. S., Wenkel, S., Soppe, W., Deng, X. W., Valverde, F., and Coupland, G. (2008). Arabidopsis COP1 shapes the temporal pattern of CO accumulation conferring a photoperiodic flowering response. *EMBO Journal*, 27(8):1277–1288.

Jarillo, J. a., Capel, J., Tang, R.-H., Yang, H.-Q., Alonso, J. M., Ecker, J. R., and Cashmore, A. R. (2001). An Arabidopsis circadian clock component interacts with both CRY1 and phyB. *Nature*, 410(6827):487–490.

Jenkins, G. I., Courtice, G. R. M., and Cove, D. J. (1986). Gravitropic responses of wild-type and mutant strains of the moss Physcomitrella patens. *Plant, Cell and Environment*, 9(8):637–644.

Jiao, Y. (2005). Conservation and Divergence of Light-Regulated Genome Expression Patterns during Seedling Development in Rice and Arabidopsis. *The Plant Cell*, 17(12):3239–3256.

Jiao, Y., Lau, O. S., and Deng, X. W. (2007). Light-regulated transcriptional networks in higher plants. *Nature Reviews Genetics*, 8(3):217–230.

Jing, Y., Zhang, D., Wang, X., Tang, W., Wang, W., Huai, J., Xu, G., Chen, D., Li, Y., and Lin, R. (2013). Arabidopsis Chromatin Remodeling Factor PICKLE Interacts with Transcription Factor HY5 to Regulate Hypocotyl Cell Elongation. *The Plant Cell*, 25(1):242–256.

Kadota, A., Sato, Y., and Wada, M. (2000). Intracellular chloroplast photorelocation in the moss Physcomitrella patens is mediated by phytochrome as well as by a blue-light receptor. *Planta*, 210(6):932–937.

Kaiserli, E. and Jenkins, G. I. (2007). UV-B Promotes Rapid Nuclear Translocation of the Arabidopsis UV-B Specific Signaling Component UVR8 and Activates Its Function in the Nucleus. *the Plant Cell Online*, 19(8):2662–2673.

Kami, C., Lorrain, S., Hornitschek, P., and Fankhauser, C. (2010). Light-Regulated Plant Growth and Development. In *Current Topics in Developmental Biology*, volume 91, pages 29–66.

Kamisugi, Y., Schlink, K., Rensing, S. a., Schween, G., von Stackelberg, M., Cuming, A. C., Reski, R., and Cove, D. J. (2006). The mechanism of gene targeting in Physcomitrella patens: homologous recombination, concatenation and multiple integration. *Nucleic Acids Research*, 34(21):6205–6214.

Kasahara, M. (2004). Phototropins Mediate Blue and Red Light-Induced Chloroplast Movements in Physcomitrella patens. *PLANT PHYSIOLOGY*, 135(3):1388–1397.

Kenrick, P. and Crane, P. R. (1997). The origin and early evolution of plants on land. *Nature*, 389(6646):33–39.

Kianianmomeni, A. and Hallmann, A. (2014). Algal photoreceptors: In vivo functions and potential applications. *Planta*, 239(1):1–26.

Kinoshita, T., Doi, M., and Suetsugu, N. (2001). phot 1 and phot2 mediate blue light regulation of stomatal opening. *Nature*, 414(December):656–660.

Kircher, Kozma-Bognar, Kim, Adam, Harter, Schafer, and Nagy (1999). Light quality-dependent nuclear import of the plant photoreceptors phytochrome A and B. *The Plant cell*, 11(8):1445–1456.

Kircher, S., Gil, P., Kozma-bognár, L., Fejes, E., Speth, V., Husselstein-Muller, T., Bauer, D., Ádám, É., Schäfer, E., and Nagy, F. (2002). Nucleocytoplasmic Partitioning of the Plant Photoreceptors Phytochrome A, B, C, D, and E Is Regulated Differentially by Light and Exhibits a Diurnal Rhythm. *The Plant Cell*, 14(July):1541–1555.

Kiyosue, T. and Wada, M. (2000). LKP1 (LOV kelch protein 1): a factor involved in the regulation of flowering time in arabidopsis. *The Plant Journal For Cell And Molecular Biology*, 23(6):807–815.

Koduri, P. K. H., Gordon, G. S., Barker, E. I., Colpitts, C. C., Ashton, N. W., and Suh, D.-Y. (2010). Genome-wide analysis of the chalcone synthase superfamily genes of Physcomitrella patens. *Plant molecular biology*, 72(3):247–263.

Kong, S. G., Suzuki, T., Tamura, K., Mochizuki, N., Hara-Nishimura, I., and Nagatani, A. (2006). Blue light-induced association of phototropin 2 with the Golgi apparatus. *Plant Journal*, 45(6):994–1005.

Koornneef, M., Rolff, E., and Spruit, C. (1980). Genetic Control of Light-inhibited Hypocotyl Elongation in Arabidopsis thaliana (L.) Heynh. *Zeitschrift für Pflanzenphysiologie*, 100(2):147–160.

Kreiss, M. (2018). *Evolutionäre Konservierung des COP1 / SPA-Komplexes in dem Moos Physcomitrella patens*. Master thesis, Heinrich Heine Universität Düsseldorf.

Laemmli, U. (1970). Cleavage of structural proteins during the assembly of the head of bacteriophage T4. *Nature*, 227(5259):680–685.

Lang, D., Ullrich, K. K., Murat, F., Fuchs, J., Jenkins, J., Haas, F. B., Piednoel, M., Gundlach, H., Van Bel, M., Meyberg, R., Vives, C., Morata, J., Symeonidi, A., Hiss, M., Muchero, W., Kamisugi, Y., Saleh, O., Blanc, G., Decker, E. L., van Gessel, N., Grimwood, J., Hayes, R. D., Graham, S. W., Gunter, L. E., McDaniel, S. F., Hoernstein, S. N., Larsson, A., Li, F.-W. W., Perroud, P.-F. F., Phillips, J., Ranjan, P., Rokshar, D. S., Rothfels, C. J., Schneider, L., Shu, S., Stevenson, D. W., Thümmler, F., Tillich, M., Villarreal Aguilar, J. C., Widiez, T., Wong, G. K.-S. S., Wymore, A., Zhang, Y., Zimmer, A. D., Quatrano, R. S., Mayer, K. F., Goodstein, D., Casacuberta, J. M., Vandepoele, K., Reski, R., Cuming, A. C., Tuskan, G. A., Maumus, F., Salse, J., Schmutz, J., Rensing, S. A., Villarreal A, J. C., Widiez, T., Wong, G. K.-S. S., Wymore, A., Zhang, Y., Zimmer, A. D., Quatrano, R. S., Mayer, K. F., Goodstein, D., Casacuberta, J. M., Vandepoele, K., Reski, R., Cuming, A. C., Tuskan, J., Maumus, F., Salse, J., Schmutz, J., and Rensing, S. A. (2018). The Physcomitrella patens chromosome-scale assembly reveals moss genome structure and evolution. *Plant Journal*, 93(3):515–533.

Lang, D., van Gessel, N., Ullrich, K., and Reski, R. (2016). The Genome of the Model Moss Physcomitrella patens. In *Advances in Botanical Research*, pages 97–140.

Lau, O. S. and Deng, X. W. (2012). The photomorphogenic repressors COP1 and DET1: 20 years later. *Trends in Plant Science*, 17(10):584–593.

Laubinger, S., Fittinghoff, K., and Hoecker, U. (2004). The SPA quartet: a family of WD-repeat proteins with a central role in suppression of photomorphogenesis in Arabidopsis. *The Plant Cell*, 16(September):2293–2306.

Laubinger, S. and Hoecker, U. (2003). The SPA1-like proteins SPA3 and SPA4 repress photomorphogenesis in the light. *The Plant Journal*, 35(3):373–385.

Laubinger, S., Marchal, V., Le Gourrierec, J., Gentilhomme, J., Wenkel, S., Adrian, J., Jang, S., Kulajta, C., Braun, H., Coupland, G., and Hoecker, U. (2006). Arabidopsis SPA proteins regulate photoperiodic flowering and interact with the floral inducer CONSTANS to regulate its stability. *Development*, 133(16):3213–3222.

Le Bail, A., Scholz, S., and Kost, B. (2013). Evaluation of Reference Genes for RT qPCR Analyses of Structure-Specific and Hormone Regulated Gene Expression in Physcomitrella patens Gametophytes. *PLoS ONE*, 8(8):e70998.

Lee, J., He, K., Stolc, V., Lee, H., Figueroa, P., Gao, Y., Tongprasit, W., Zhao, H., Lee, I., and Deng, X. W. (2007). Analysis of Transcription Factor HY5 Genomic Binding Sites Revealed Its Hierarchical Role in Light Regulation of Development. *THE PLANT CELL ONLINE*, 19(3):731–749.

Leivar, P. and Monte, E. (2014). PIFs: systems integrators in plant development. *The Plant Cell*, 26(1):56–78.

Li, F.-W., Melkonian, M., Rothfels, C. J., Villarreal, J. C., Stevenson, D. W., Graham, S. W., Wong, G. K.-S., Pryer, K. M., and Mathews, S. (2015). Phytochrome diversity in green plants and the origin of canonical plant phytochromes. *Nature Communications*, 6(7852):1–12.

Li, J., Li, G., Gao, S., Martinez, C., He, G., Zhou, Z., Huang, X., Lee, J.-H., Zhang, H., Shen, Y., Wang, H., and Deng, X. W. (2010). Arabidopsis Transcription Factor ELONGATED HYPOCOTYL5 Plays a Role in the Feedback Regulation of Phytochrome A Signaling. *the Plant Cell Online*, 22(11):3634–3649.

Li, J., Li, G., Wang, H., and Wang Deng, X. (2011). Phytochrome signaling mechanisms. *The Arabidopsis book / American Society of Plant Biologists*, 9:e0148.

Lian, H.-L. L., He, S.-B. B., Zhang, Y.-C. C., Zhu, D.-M. M., Zhang, J.-Y. Y., Jia, K.-P. P., Sun, S.-X. X., Li, L., and Yang, H.-Q. Q. (2011). Blue-light-dependent interaction of cryptochrome 1 with SPA1 defines a dynamic signaling mechanism. *Genes & Development*, 25(10):1023–1028.

Lin, C., Ahmad, M., and Cashmore, A. (1996). Arabidopsis cryptochrome 1 is a soluble protein mediating blue light-dependent regulation of plant growth and development. *The Plant Journal*, 10(5):893–902.

Lin, C., Yang, H., Guo, H., Mockler, T., Chen, J., and Cashmore, A. R. (1998). Enhancement of blue-light sensitivity of Arabidopsis seedlings by a blue light receptor cryptochrome 2. *Proceedings of the National Academy of Sciences*, 95(5):2686–2690.

Lin, R., Ding, L., Casola, C., Ripoll, D. R., Feschotte, C., and Wang, H. (2007). Transposase-Derived Transcription Factors Regulate Light Signaling in Arabidopsis. *Science*, 318(5854):1302–1305.

Lin, X.-L., Niu, D., Hu, Z.-L., Kim, D. H., Jin, Y. H., Cai, B., Liu, P., Miura, K., Yun, D.-J., Kim, W.-Y., Lin, R., and Jin, J. B. (2016). An Arabidopsis SUMO E3 Ligase, SIZ1, Negatively Regulates Photomorphogenesis by Promoting COP1 Activity. *PLoS genetics*, 12(4):e1006016.

Liu, B., Zuo, Z., Liu, H., Liu, X., and Lin, C. (2011). Arabidopsis cryptochrome 1 interacts with SPA1 to suppress COP1 activity in response to blue light. *Genes & Development*, 25(10):1029–34.

Liu, L.-J., Zhang, Y.-C., Li, Q.-H., Sang, Y., Mao, J., Lian, H.-L., Wang, L., and Yang, H.-Q. (2008). COP1-Mediated Ubiquitination of CONSTANS Is Implicated in Cryptochrome Regulation of Flowering in Arabidopsis. *the Plant Cell Online*, 20(2):292–306.

Livak, K. J. and Schmittgen, T. D. (2001). Analysis of Relative Gene Expression Data Using Real-Time Quantitative PCR and the 2minusdeltadeltaCT Method. *Methods*, 25(4):402–408.

Long, M. (2001). Evolution of novel genes. *Current Opinion in Genetics and Development*, 11(6):673–680.

Lopez-Obando, M., de Villiers, R., Hoffmann, B., Ma, L., de Saint Germain, A., Kossmann, J., Coudert, Y., Harrison, C. J., Rameau, C., Hills, P., and Bonhomme, S. (2018). Physcomitrella patens MAX2 characterization suggests an ancient role for this F-box protein in photomorphogenesis rather than strigolactone signalling. *New Phytologist*, 219(2):743–756.

Lopez-Obando, M., Hoffmann, B., Gery, C., Guyon-Debast, A., Teoule, E., Rameau, C., Bonhomme, S., and Nogue, F. (2016). Simple and Efficient Targeting of Multiple Genes Through CRISPR-Cas9 in Physcomitrella patens. *Genes—Genomes—Genetics*, 6(11):3647–3653.

Lu, X. D., Zhou, C. M., Xu, P. B., Luo, Q., Lian, H. L., and Yang, H. Q. (2015). Red-light-dependent interaction of phyB with SPA1 promotes COP1-SPA1 dissociation and photomorphogenic development in arabidopsis. *Molecular Plant*, 8(3):467–478.

Lyska, D., Engelmann, K., Meierhoff, K., and Westhoff, P. (2013). pAUL: A Gateway-Based Vector System for Adaptive Expression and Flexible Tagging of Proteins in Arabidopsis. *PLoS ONE*, 8(1):1–12.

Maberly, S. C. (2014). The fitness of the environments of air and water for photosynthesis, growth, reproduction and dispersal of photoautotrophs: An evolutionary and biogeochemical perspective. *Aquatic Botany*, 118:4–13.

Maier, A., Schrader, A., Kokkelink, L., Falke, C., Welter, B., Iniesto, E., Rubio, V., Uhrig, J. F., Hülskamp, M., and Hoecker, U. (2013). Light and the E3 ubiquitin ligase COP1/SPA control the protein stability of the MYB transcription factors PAP1 and PAP2 involved in anthocyanin accumulation in Arabidopsis. *The Plant Journal For Cell And Molecular Biology*, 74(4):638–51.

Mali, P., Esvelt, K. M., and Church, G. M. (2013). Cas9 as a versatile tool for engineering biology. *Nature methods*, 10(10):957–63.

Matasci, N., Hung, L. H., Yan, Z., Carpenter, E. J., Wickett, N. J., Mirarab, S., Nguyen, N., Warnow, T., Ayyampalayam, S., Barker, M., Burleigh, J. G., Gitzendanner, M. A., Wafula, E., Der, J. P., DePamphilis, C. W., Roure, B., Philippe, H., Ruhfel, B. R., Miles, N. W., Graham, S. W., Mathews, S., Surek, B., Melkonian, M., Soltis, D. E., Soltis, P. S., Rothfels, C., Pokorny, L., Shaw, J. A., DeGironimo, L., Stevenson, D. W., Villarreal, J. C., Chen, T., Kutchan, T. M., Rolf, M., Baucom, R. S., Deyholos, M. K., Samudrala, R., Tian, Z., Wu, X., Sun, X., Zhang, Y., Wang, J., Leebens-Mack, J., and Wong, G. K. S. (2014). Data access for the 1,000 Plants (1KP) project. *GigaScience*, 3(1):1–10.

Mathews, S. (2006). Phytochrome-mediated development in land plants: red light sensing evolves to meet the challenges of changing light environments. *Molecular ecology*, 15(12):3483–503.

McFadden, G. I. (2001). PRIMARY AND SECONDARY ENDOSYMBIOSIS AND THE ORIGIN OF PLASTIDS. *Journal of Phycology*, 37(6):951–959.

McNellis, T. W., von Arnim, a. G., Araki, T., Komeda, Y., Miséra, S., and Deng, X. W. (1994). Genetic and molecular analysis of an allelic series of cop1 mutants suggests functional roles for the multiple protein domains. *The Plant Cell*, 6(4):487–500.

Menon, C., Sheerin, D. J., and Hiltbrunner, A. (2016). SPA proteins: SPAnning the gap between visible light and gene expression. *Planta*.

Merchant, S. S., Prochnik, S. E., Vallon, O., Harris, E. H., Karpowicz, S. J., Witman, G. B., Terry, A., Salamov, A., Fritz-laylin, L. K., Maréchal-drouard, L., Marshall, W. F., Qu, L.-H., Nelson, D. R., Sanderfoot, A. a., Spalding, M. H., Kapitonov, V. V., Ren, Q., Ferris, P., Lindquist, E., Shapiro, H., Lucas, S. M., Grimwood, J., Schmutz, J., Cardol, P., Cerutti, H., Chanfreau, G., Chen, C.-J. C.-L., Cognat, V., Croft, M. T., Dent, R., Dutcher, S., Fernández, E., Fukuzawa, H., González-ballester, D., González-Halphen, D., Hallmann, A., Hanikenne, M., Hippler, M., Inwood, W., Jabbari, K., Kalanon, M., Kuras, R., Lefebvre, P. a., Lemaire, S. D., Lobanov, A. V., Lohr, M., Manuell, A., Meier, I., Mets, L., Mittag, M., Mittelmeier, T., Moroney, J. V., Moseley, J., Napoli, C., Nedelcu, A. M., Niyogi, K., Novoselov, S. V., Paulsen, I. T., Pazour, G., Purton, S., Ral, J.-P., Riaño-Pachón, D. M., Riekhof, W., Rymarquis, L., Schroda, M., Stern, D., Umen, J., Willows, R., Wilson, N., Zimmer, S. L., Allmer, J., Balk, J., Bisova, K., Chen, C.-J. C.-L., Elias, M., Gendler, K., Hauser, C., Lamb, M. R., Ledford, H., Long, J. C., Minagawa, J., Page, M. D., Pan, J., Pootakham, W., Roje, S., Rose, A., Stahlberg, E., Terauchi, A. M., Yang, P., Ball, S., Bowler, C., Dieckmann, C. L., Gladyshev, V. N., Green, P., Jorgensen, R., Mayfield, S., Mueller-roeber, B., Rajamani, S., Sayre, R. T., Brokstein, P., Dubchak, I., Goodstein, D., Hornick, L., Huang, Y. W., Jhaveri, J., Luo, Y., Martínez, D., Ngau, W. C. A., Otillar, B., Poliakov, A., Porter, A., Szajkowski, L., Werner, G., Zhou, K., Grigoriev, I. V., Rokhsar, D. S., Grossman, A. R., Karpowicz, J., Witman, G. B., Terry, A., Salamov, A., Fritz-laylin, L. K., Maréchal-drouard, L., Marshall, W. F., Qu, L.-H., Nelson, D. R., Sanderfoot, A. a., Spalding, M. H., Kapitonov, V. V., Ren, Q., Cardol, P., Cerutti, H., Chanfreau, G., Ferris, P., Fukuzawa, H., González-ballester, D., Mueller-roeber, B., Rajamani, S., Sayre, R. T., Dubchak, I., Goodstein, D., Hornick, L., Huang, Y. W., Luo, Y., Martínez, D., Chi, W., Ngau, A., Otillar, B., Porter, A., Szajkowski, L., Werner, G., Zhou, K., Igor, V., Rokhsar, D. S., and Grossman, A. R. (2007). The Chlamydomonas Genome Reveals the Evolution of Key Animal and Plant Functions. *Science*, 318(5848):245–250.

Mittmann, F., Brücker, G., Zeidler, M., Repp, A., Abts, T., Hartmann, E., and Hughes, J. (2004). Targeted knockout in Physcomitrella reveals direct actions of phytochrome in the cytoplasm. *Proceedings of the National Academy of Sciences of the United States of America*, 101(38):13939–44.

Mockler, T. C., Guo, H., Yang, H., Duong, H., and Lin, C. (1999). Antagonistic actions of Arabidopsis cryptochromes and phytochrome B in the regulation of floral induction. *Development*, 126(10):2073–2082.

Moon, J., Parry, G., and Estelle, M. (2004). The ubiquitin-proteasome pathway and plant development. *The Plant cell*, 16(12):3181–95.

Nelson, D. C., Lasswell, J., Rogg, L. E., Cohen, M. a., and Bartel, B. (2000). FKF1, a clock-controlled gene that regulates the transition to flowering in Arabidopsis. *Cell*, 101(3):331–40.

Nixdorf, M. and Hoecker, U. (2010). SPA1 and DET1 act together to control photomorphogenesis throughout plant development. *Planta*, 231(4):825–833.

Ohgishi, M., Saji, K., Okada, K., and Sakai, T. (2004). Functional analysis of each blue light receptor, cry1, cry2, phot1, and phot2, by using combinatorial multiple mutants in Arabidopsis. *Proceedings of the National Academy of Sciences*, 101(8):2223–2228.

Ordoñez-Herrera, N., Fackendahl, P., Yu, X., Schaefer, S., Koncz, C., and Hoecker, U. (2015). A cop1 spa mutant deficient in COP1 and SPA proteins reveals partial co-action of COP1 and SPA during Arabidopsis post-embryonic development and photomorphogenesis. *Molecular Plant*, 8(3):479–81.

Ordoñez-Herrera, N., Trimborn, L., Menje, M., Henschel, M., Robers, L., Kaufholdt, D., Hänsch, R., Adrian, J., Ponnu, J., and Hoecker, U. (2017). The transcription factor COL12 is a substrate of the COP1/SPA E3 ligase and regulates flowering time and plant architecture. *Plant Physiology*, 176(February):pp.01207.2017.

Osterlund, M. T., Hardtke, C. S., Wei, N., and Deng, X. W. (2000). Targeted destabilization of HY5 during light-regulated development of Arabidopsis. *Nature*, 405(6785):462–6.

Pacin, M., Legris, M., and Casal, J. J. (2014). Rapid Decline in Nuclear COSTITUTIVE PHOTOMORPHOGENESIS1 Abundance Anticipates the Stabilization of Its Target ELONGATED HYPOCOTYL5 in the Light. *Plant Physiology*, 164(3):1134–1138.

Paz-Ares, J., Valencia, A., Costantino, P., Vittorioso, P., Davies, B., Gilmartin, P., Giraudat, J., Parcy, F., Reindl, A., Sablowski, R., Coupland, G., Martin, C., Angenent, G. C., Baumlein, H., Mock, H. P., Carbonero, P., Colombo, L., Tonelli, C., Engström, P., Droege-Laser, W., Gatz, C., Kavanagh, T., Kushnir, S., Zabeau, M., Laux, T., Hordsworth, M., Ruberti, I., Ratcliff, F., Smeekens, S., Somssich, I., Weisshaar, B., and Traas, J. (2002). REGIA an EU project on functional genomics of transcription factors from Arabidopsis thaliana. *Comparative and Functional Genomics*, 3(2):102–108.

Pfeiffer, A., Kunkel, T., Hiltbrunner, A., Neuhaus, G., Wolf, I., Speth, V., Adam, E., Nagy, F., and Schäfer, E. (2009). A cell-free system for light-dependent nuclear import of phytochrome. *Plant Journal*, 57(4):680–689.

Pfeiffer, A., Nagel, M.-K., Popp, C., Wust, F., Bindics, J., Viczian, A., Hiltbrunner, A., Nagy, F., Kunkel, T., and Schafer, E. (2012). Interaction with plant transcription factors can mediate nuclear import of phytochrome B. *Proceedings of the National Academy of Sciences*, 109(15):5892–5897.

Podolec, R. and Ulm, R. (2018). Photoreceptor-mediated regulation of the COP1/SPA E3 ubiquitin ligase. *Current Opinion in Plant Biology*, 45:18–25.

Possart, A. and Hiltbrunner, A. (2013). An evolutionarily conserved signaling mechanism mediates far-red light responses in land plants. *The Plant cell*, 25(1):102–14.

Possart, A., Xu, T., Paik, I., Hanke, S., Keim, S., Hermann, H.-M., Wolf, L., Hiss, M., Becker, C., Huq, E., Rensing, S. A., Hiltbrunner, A., Hiß, M., Becker, C., Huq, E., Rensing, S. A., and Hiltbrunner, A. (2017). Characterization of Phytochrome Interacting Factors from the Moss Physcomitrella patens Illustrates Conservation of Phytochrome Signaling Modules in Land Plants. *The Plant Cell*, 29(2):tpc.00388.2016.

Possart, A. S. (2013). *P Lant P Hytochrome S Ignaling in an*. PhD thesis.

Prigge, M. J. and Bezanilla, M. (2010). Evolutionary crossroads in developmental biology: Physcomitrella patens. *Development*, 137(21):3535–43.

Ranjan, A. (2010). *The role of COP1 / SPA in light signaling : Growth control , cell-cell communication and functional conservation in plants*. PhD thesis, Universität zu Köln.

Ranjan, A., Dickopf, S., Ullrich, K. K., Rensing, S. A., and Hoecker, U. (2014). Functional analysis of COP1 and SPA orthologs from Physcomitrella and rice during photomorphogenesis of transgenic Arabidopsis reveals distinct evolutionary conservation. *BMC plant biology*, 14(1):178.

Rensing, S. a., Lang, D., Zimmer, A. D., Terry, A., Salamov, A., Shapiro, H., Nishiyama, T., Perroud, P.-F., Lindquist, E. a., Kamisugi, Y., Tanahashi, T., Sakakibara, K., Fujita, T., Oishi, K., Shin-I, T., Kuroki, Y., Toyoda, A., Suzuki, Y., Hashimoto, S.-I., Yamaguchi, K., Sugano, S., Kohara, Y., Fujiyama, A., Anterola, A., Aoki, S., Ashton, N., Barbazuk, W. B., Barker, E., Bennetzen, J. L., Blankenship, R., Cho, S. H., Dutcher, S. K., Estelle, M., Fawcett, J. a., Gundlach, H., Hanada, K., Heyl, A., Hicks, K. a., Hughes, J., Lohr, M., Mayer, K., Melkozernov, A., Murata, T., Nelson, D. R., Pils, B., Prigge, M., Reiss, B., Renner, T., Rombauts, S., Rushton, P. J., Sanderfoot, A., Schween, G., Shiu, S.-H., Stueber, K., Theodoulou, F. L., Tu, H., Van de Peer, Y., Verrier, P. J., Waters, E., Wood, A., Yang, L., Cove, D., Cuming, A. C., Hasebe, M., Lucas, S., Mishler, B. D., Reski, R., Grigoriev, I. V., Quatrano, R. S., and Boore, J. L. (2008). The Physcomitrella genome reveals evolutionary insights into the conquest of land by plants. *Science*, 319(5859):64–9.

Reski, R. (1998). Development , Genetics and Molecular Biology of Mosses. *Bot. Acta*, 111(1915):1–15.

Richardt, S., Lang, D., Reski, R., Frank, W., and Rensing, S. a. (2007). PlanTAPDB, a phylogeny-based resource of plant transcription-associated proteins. *Plant physiology*, 143(4):1452–66.

Rizzini, L., Favory, J. J., Cloix, C., Faggionato, D., O'Hara, A., Kaiserli, E., Baumeister, R., Schäfer, E., Nagy, F., Jenkins, G. I., and Ulm, R. (2011). Perception of UV-B by the arabidopsis UVR8 protein. *Science*, 332(6025):103–106.

Rockwell, N. C., Su, Y.-S., and Lagarias, J. C. (2006). Phytochrome structure and signaling mechanisms. *Annual Review of Plant Biology*, 57:837–58.

Rolauffs, S., Fackendahl, P., Sahm, J., Fiene, G., and Hoecker, U. (2012). Arabidopsis COP1 and SPA genes are essential for plant elongation but not for acceleration of flowering time in response to a low red light to far-red light ratio. *Plant Physiology*, 160(4):2015–27.

Rosler, J., Klein, I., and Zeidler, M. (2007). Arabidopsis fhl/fhy1 double mutant reveals a distinct cytoplasmic action of phytochrome A. *Proceedings of the National Academy of Sciences*, 104(25):10737–10742.

Rozema, J., Blokker, P., Mayoral Fuertes, M. A., and Broekman, R. (2009). UV-B absorbing compounds in present-day and fossil pollen, spores, cuticles, seed coats and wood: Evaluation of a proxy for solar UV radiation. *Photochemical and Photobiological Sciences*, 8(9):1233–1243.

Saijo, Y., Sullivan, J. a., Wang, H., Yang, J., Shen, Y., Rubio, V., Ma, L., Hoecker, U., and Deng, X. W. (2003). The COP1-SPA1 interaction defines a critical step in phytochrome A-mediated regulation of HY5 activity. *Genes & Development*, 17(21):2642–7.

Sakamoto, K. and Briggs, W. R. (2002). Cellular and Subcellular Localization of Phototropin 1. *The Plant Cell*, 14(8):1723–1735.

Sambrook, J. and Russell, D. W. (2001). *Molecular Cloning: A Laboratory Manual*. Cold Spring Harbor Laboratory Press, Cold Spring Harbor, N.Y.

Schaefer, D. and Zrÿd, J. (1997). Efficient gene targeting in the moss Physcomitrella patens. *The Plant Journal*, 11(6):1195–206.

Schaefer, D., Zryd, J.-P., Knight, C., and Cove, D. (1991). Stable transformation of the moss Physcomitrella patens. *MGG Molecular & General Genetics*, 226(3):418–424.

Schaefer, D. G., Delacote, F., Charlot, F., Vrielynck, N., Guyon-Debast, A., Le Guin, S., Neuhaus, J. M., Doutriaux, M. P., and Nogué, F. (2010). RAD51 loss of function abolishes gene targeting and de-represses illegitimate integration in the moss Physcomitrella patens. *DNA Repair*, 9(5):526–533.

Schultz, T. T. F., Kiyosue, T., Yanovsky, M., Wada, M., and Kay, S. A. (2001). A role for LKP2 in the circadian clock of Arabidopsis. *The Plant cell*, 13(December):2659–2670.

Seo, H. S., Watanabe, E., Tokutomi, S., Nagatani, A., and Chua, N.-H. (2004). Photoreceptor ubiquitination by COP1 E3 ligase desensitizes phytochrome A signaling. *Genes & Development*, 18(6):617–22.

Seo, H. S., Yang, J. Y., Ishikawa, M., Bolle, C., Ballesteros, M. L., and Chua, N. H. (2003). LAF1 ubiquitination by COP1 controls photomorphogenesis and is stimulated by SPA1. *Nature*, 423(6943):995–999.

Seol, J. H., Feldman, R. M., Zachariae, W., Shevchenko, A., Correll, C. C., Lyapina, S., Chi, Y., Galova, M., Claypool, J., Sandmeyer, S., Nasmyth, K., Shevchenko, A., and Deshaies, R. J. (1999). Cdc53/cullin and the essential Hrt1 RING-H2 subunit of SCF define a ubiquitin ligase module that activates the E2 enzyme Cdc34. *Genes and Development*, 13(12):1614–1626.

Shalitin, D., Yang, H., Mockler, T. C., Maymon, M., Guo, H., Whitelam, G. C., and Lin, C. (2002). Regulation of Arabidopsis cryptochrome 2 by blue-light-dependent phosphorylation. *Nature*, 417(6890):763–767.

Shalitin, D., Yu, X., Maymon, M., Mockler, T., and Lin, C. (2003). Blue Light-Dependent in Vivo and in Vitro Phosphorylation of Arabidopsis Cryptochrome 1. *The Plant cell*, 15(10):2421–2429.

Sharrock, R. A. and Clack, T. (2002). Patterns of Expression and Normalized Levels of the Five Arabidopsis Phytochromes. *Plant Physiology*, 130(1):442–56.

Sharrock, R. a. and Quail, P. H. (1989). Novel phytochrome sequences in Arabidopsis thaliana: structure, evolution, and differential expression of a plant regulatory photoreceptor family. *Genes & Development*, 3(11):1745–57.

Sheerin, D. J., Menon, C., zur Oven-Krockhaus, S., Enderle, B., Zhu, L., Johnen, P., Schleifenbaum, F., Stierhof, Y.-D., Huq, E., and Hiltbrunner, A. (2015). Light-Activated Phytochrome A and B Interact with Members of the SPA Family to Promote Photomorphogenesis in Arabidopsis by Reorganizing the COP1/SPA Complex. *The Plant Cell Online*, 27(1):189–201.

Shen, H., Moon, J., and Huq, E. (2005). PIF1 is regulated by light-mediated degradation through the ubiquitin-26S proteasome pathway to optimize photomorphogenesis of seedlings in Arabidopsis. *Plant Journal*, 44(6):1023–1035.

Shen, H., Zhu, L., Castillon, A., Majee, M., Downie, B., and Huq, E. (2008). Light-Induced Phosphorylation and Degradation of the Negative Regulator PHYTOCHROME-INTERACTING FACTOR1 from Arabidopsis Depend upon Its Direct Physical Interactions with Photoactivated Phytochromes. *the Plant Cell Online*, 20(6):1586–1602.

Shen, Y., Khanna, R., Carle, C. M., and Quail, P. H. (2007). Phytochrome Induces Rapid PIF5 Phosphorylation and Degradation in Response to Red-Light Activation. *Plant Physiology*, 145(3):1043–1051.

Shimizu, M., Ichikawa, K., and Aoki, S. (2004). Photoperiod-regulated expression of the PpCOL1 gene encoding a homolog of CO/COL proteins in the moss Physcomitrella patens. *Biochemical and biophysical research communications*, 324(4):1296–301.

Simillion, C., Vandepoele, K., Van Montagu, M. C. E., Zabeau, M., and Van de Peer, Y. (2002). The hidden duplication past of Arabidopsis thaliana. *Proceedings of the National Academy of Sciences of the United States of America*, 99(21):13627–32.

Somers, D. E., Schultz, T. F., Milnamow, M., and Kay, S. a. (2000). ZEITLUPE encodes a novel clock-associated PAS protein from Arabidopsis. *Cell*, 101(3):319–29.

Takase, T., Nishiyama, Y., Tanihigashi, H., Ogura, Y., Miyazaki, Y., Yamada, Y., and Kiyosue, T. (2011). LOV KELCH PROTEIN2 and ZEITLUPE repress Arabidopsis photoperiodic flowering under non-inductive conditions, dependent on FLAVIN-BINDING KELCH REPEAT F - BOX1. *Plant Journal*, 67(4):608–621.

Talling, J. F., Wood, R. B., Prosser, M. V., and Baxter, R. M. (1973). The upper limit of photosynthetic productivity by phytoplankton: evidence from Ethiopian soda lakes. *Freshwater Biology*, 3(1):53–76.

Uenaka, H. and Kadota, A. (2007). Functional analyses of the Physcomitrella patens phytochromes in regulating chloroplast avoidance movement. *Plant Journal*, 51(6):1050–1061.

Uenaka, H., Wada, M., and Kadota, A. (2005). Four distinct photoreceptors contribute to light-induced side branch formation in the moss Physcomitrella patens. *Planta*, 222(4):623–31.

Uljon, S., Xu, X., Durzynska, I., Stein, S., Adelmant, G., Marto, J. A., Pear, W. S., and Blacklow, S. C. (2016). Structural Basis for Substrate Selectivity of the E3 Ligase COP1. *Structure*, 24(5):687–696.

Van Buskirk, E. K., Decker, P. V., and Chen, M. (2012). Photobodies in Light Signaling. *PLANT PHYSIOLOGY*, 158(1):52–60.

Vidali, L., van Gisbergen, P. A. C., Guerin, C., Franco, P., Li, M., Burkart, G. M., Augustine, R. C., Blanchoin, L., and Bezanilla, M. (2009). Rapid formin-mediated actin-filament elongation is essential for polarized plant cell growth. *Proceedings of the National Academy of Sciences*, 106(32):13341–13346.

von Arnim, A. and Deng, X.-W. (1994). Light inactivation of Arabidopsis photomorphogenic repressor COP1 involves a cell-specific regulation of its nucleocytoplasmic partitioning. *Cell*, 79(6):1035–1045.

Wada, M., Kagawa, T., and Sato, Y. (2003). Chloroplast Movement. *Annual Review of Plant Biology*, 54(1):455–468.

Wang, H., Ma, L. G., Li, J. M., Zhao, H. Y., and Deng, X. W. (2001). Direct interaction of Arabidopsis cryptochromes with COP1 in light control development. *Science*, 294(5540):154–8.

Wickett, N. J., Mirarab, S., Nguyen, N., Warnow, T., Carpenter, E., Matasci, N., Ayyampalayam, S., Barker, M. S., Burleigh, J. G., Gitzendanner, M. A., Ruhfel, B. R., Wafula, E., Der, J. P., Graham, S. W., Mathews, S., Melkonian, M., Soltis, D. E., Soltis, P. S., Miles, N. W., Rothfels, C. J., Pokorny, L., Shaw, A. J., DeGironimo, L., Stevenson, D. W., Surek, B., Villarreal, J. C., Roure, B., Philippe, H., DePamphilis, C. W., Chen, T., Deyholos, M. K., Baucom, R. S., Kutchan, T. M., Augustin, M. M., Wang, J., Zhang, Y., Tian, Z., Yan, Z., Wu, X., Sun, X., Wong, G. K.-S., and Leebens-Mack, J. (2014). Phylotranscriptomic analysis of the origin and early diversification of land plants. *Proceedings of the National Academy of Sciences*, 111(45):E4859–E4868.

Wolf, L., Rizzini, L., Stracke, R., Ulm, R., and Rensing, S. A. (2010). The molecular and physiological responses of Physcomitrella patens to ultraviolet-B radiation. *Plant physiology*, 153(3):1123–34.

Wu, G. and Spalding, E. P. (2007). Separate functions for nuclear and cytoplasmic cryptochrome 1 during photomorphogenesis of Arabidopsis seedlings. *Proceedings of the National Academy of Sciences*, 104(47):18813–18818.

Wu, H.-P., Su, Y.-S., Chen, H.-C., Chen, Y.-R., Wu, C.-C., Lin, W.-D., and Tu, S.-L. (2014). Genome-wide analysis of light-regulated alternative splicing mediated by photoreceptors in Physcomitrella patens. *Genome biology*, 15(1):R10.

Xu, D., Lin, F., Jiang, Y., Huang, X., Li, J., Ling, J., Hettiarachchi, C., Tellgren-Roth, C., Holm, M., and Deng, X. W. (2014a). The RING-Finger E3 Ubiquitin Ligase COP1 SUPPRESSOR1 Negatively Regulates COP1 Abundance in Maintaining COP1 Homeostasis in Dark-Grown Arabidopsis Seedlings. *The Plant Cell*, 26(5):1981–1991.

Xu, T. and Hiltbrunner, A. (2017). PHYTOCHROME INTERACTING FACTORs from Physcomitrella patens are active in Arabidopsis and complement the pif quadruple mutant PHYTOCHROME INTERACTING FACTORs from Physcomitrella patens are active. 2324.

Xu, X., Paik, I., Zhu, L., Bu, Q., Huang, X., Deng, X. W., and Huq, E. (2014b). PHYTOCHROME INTERACTING FACTOR1 Enhances the E3 Ligase Activity of CONSTITUTIVE PHOTOMORPHOGENIC1 to Synergistically Repress Photomorphogenesis in Arabidopsis. *The Plant Cell*, 26(5):1992–2006.

Yamawaki, S., Yamashino, T., Nakamichi, N., Nakanishi, H., and Mizuno, T. (2011a). Light-responsive double B-box containing transcription factors are conserved in Physcomitrella patens. *Bioscience, biotechnology, and biochemistry*, 75(10):2037–41.

Yamawaki, S., Yamashino, T., Nakanishi, H., and Mizuno, T. (2011b). Functional characterization of HY5 homolog genes involved in early light-signaling in Physcomitrella patens. *Bioscience, biotechnology, and biochemistry*, 75(8):1533–9.

Yang, J., Lin, R., Hoecker, U., Liu, B., Xu, L., and Wang, H. (2005). Repression of light signaling by Arabidopsis SPA1 involves post-translational regulation of HFR1 protein accumulation. *The Plant Journal For Cell And Molecular Biology*, 43(1):131–41.

Yang, J. and Wang, H. (2006). The central coiled-coil domain and carboxyl-terminal WD-repeat domain of Arabidopsis SPA1 are responsible for mediating repression of light signaling. *Plant Journal*, 47(4):564–576.

Yin, R. and Ulm, R. (2017). How plants cope with UV-B: from perception to response. *Current Opinion in Plant Biology*, 37:42–48.

Yu, X., Liu, H., Klejnot, J., and Lin, C. (2010). Tab.0135 (1).Pdf. pages 1–27.

Yu, X., Shalitin, D., Liu, X., Maymon, M., Klejnot, J., Yang, H., Lopez, J., Zhao, X., Bendehakkalu, K. T., and Lin, C. (2007). Derepression of the NC80 motif is critical for the photoactivation of Arabidopsis CRY2. *Proceedings of the National Academy of Sciences of the United States of America*, 104(17):7289–94.

Zhang, H., He, H., Wang, X., Wang, X., Yang, X., Li, L., and Deng, X. W. (2011). Genome-wide mapping of the HY5-mediated genenetworks in Arabidopsis that involve both transcriptional and post-transcriptional regulation. *Plant Journal*, 65(3):346–358.

Zheng, X., Wu, S., Zhai, H., Zhou, P., Song, M., Su, L., Xi, Y., Li, Z., Cai, Y., Meng, F., Yang, L., Wang, H., and Yang, J. (2013). Arabidopsis Phytochrome B Promotes SPA1 Nuclear Accumulation to Repress Photomorphogenesis under Far-Red Light. *The Plant Cell*, 25(1):115–133.

Zhu, D., Maier, A., Lee, J.-H., Laubinger, S., Saijo, Y., Wang, H., Qu, L.-J., Hoecker, U., and Deng, X. W. (2008). Biochemical characterization of Arabidopsis complexes containing CONSTITUTIVELY PHOTOMORPHOGENIC1 and SUPPRESSOR OF PHYA proteins in light control of plant development. *The Plant Cell*, 20(9):2307–23.

Zobell, O., Coupland, G., and Reiss, B. (2005). The family of CONSTANS-like genes in Physcomitrella patens. *Plant biology (Stuttgart, Germany)*, 7(3):266–75.

Zuo, Z., Liu, H., Liu, B., Liu, X., and Lin, C. (2011). Report Blue Light-Dependent Interaction of CRY2 with SPA1 Regulates COP1 activity and Floral Initiation in Arabidopsis. *Current Biology*, 21(10):841–7.

7 Supplement

Table S1: CRISPR/Cas9 sgRNA sequences used to generate *PpSPAab* double knock-out mutants

locus	**name in thesis**	**alternative name**	**sequence**
PpSPAa	1	132	GTAGACTCCGAGGGGAGCGAGGG
PpSPAa	2	749	GGCATGGTATACTAGCCCAGAGG
PpSPAb	3	234	GCAACATAACACCTTGACCGTGG
PpSPAb	4	237	GATTTCGTAGACCTAGCCCACGG

Table S2: Tested off-target sequences in *PpspaAB* double knock-out lines

locus	**sgRNA**	**ID**	**sequence**
PpSPAa	132	1	GGAGACTCCAAGCGGAGAGAAGG
PpSPAa	132	2	GTTGACACCGACGGAAGCGATGG
PpSPAa	132	3	GAAGACGCCGAGGAGGGCGAGGG
PpSPAa	132	4	CCCTCGCCCCCCTCGCATTCTCC
PpSPAa	132	5	ATCGACTGCGAGGGGGGCGAGGG
PpSPAa	749	1	GGCATGGTACACTAGCTCGGAGG
PpSPAa	749	2	GGCAGGGTATAGCAGCCAAGCGG
PpSPAa	749	3	GCCATGGTACACTAGTCCAGAGG
PpSPAb	234	1	GCAACATAACATCTTCACATTGG
PpSPAb	234	2	GCAACATAAGACCTTATCAGAGG
PpSPAb	234	3	CCATGGCCAAGGCGTTATGTTGC
PpSPAb	234	4	CCGAGGTCAAGGCGTTATGTCTC
PpSPAb	237	1	GATTTTGTAGACCTCGCCCATGG
PpSPAb	237	2	CATTTTGTAGACCCAGACCATGG
PpSPAb	237	3	GATTTCATAGACATTGTCCAAGG
PpSPAb	237	4	GATATCGTAGCCCTTGCTCATGG

Table S3: Summary of sequencing results for the *PpSPAb* locus after transformation

ID	**transformed sgRNAs**	**237/234 locus**
1_36	132, 749, 234, 237	12 bp deletion, no frameshift
1_37	132, 749, 234, 237	single basepair exchanges
1_39	132, 749, 234, 237	19 bp deletion, premature stop
1_40	132, 749, 234, 237	2 bp exchange, G to T
1_41	132, 749, 234, 237	12 bp deletion, no frameshift
1_42	132, 749, 234, 237	34 bp deletion, premature stop
1_44	132, 749, 234, 237	12 bp deletion, no frameshift
1_45	132, 749, 234, 237	single basepair exchanges
1_47	132, 749, 234, 237	8 bp deletion, premature stop
1_48	132, 749, 234, 237	9 bp deletion, no frameshift
1_50	132, 749, 234, 237	12 bp deletion, no frameshift
1_54	132, 749, 234, 237	12 bp deletion, no frameshift
1_56	132, 749, 234, 237	12 bp deletion, no frameshift
1_57	132, 749, 234, 237	12 bp deletion, no frameshift
1_59	132, 749, 234, 237	12 bp deletion, no frameshift
1_60	132, 749, 234, 237	12 bp deletion, no frameshift
1_61	132, 749, 234, 237	12 bp deletion, no frameshift
1_63	132, 749, 234, 237	12 bp deletion, no frameshift
1_67	132, 749, 234, 237	12 bp deletion, no frameshift
1_74	132, 749, 234, 237	12 bp deletion, no frameshift
1_75	132, 749, 234, 237	12 bp deletion, no frameshift
1_82	132, 749, 234, 237	12 bp deletion, no frameshift
2_14	749, 237	wild type
2_39	749, 237	6 bp deletion, no frameshift
2_40	749, 237	6 bp deletion, no frameshift
2_41	749, 237	12 bp deletion, no frameshift

Table S3: (continued)

ID	**transformed sgRNAs**	**237/234 locus**
2_42	749, 237	12 bp deletion, no frameshift
2_43	749, 237	single basepair exchanges
2_44	749, 237	6 bp deletion, no frameshift
2_46	749, 237	12 bp deletion, no frameshift
2_48	749, 237	12 bp deletion, no frameshift
2_52	749, 237	12 bp deletion, no frameshift
2_53	749, 237	12 bp deletion, no frameshift
3_13	749, 234, 237	wild type
3_28	749, 234, 237	12 bp deletion, no frameshift
3_30	749, 234, 237	12 bp deletion, no frameshift
3_32	749, 234, 237	12 bp deletion, no frameshift
3_33	749, 234, 237	12 bp deletion, no frameshift
3_37	749, 234, 237	12 bp deletion, no frameshift
3_39	749, 234, 237	12 bp deletion, no frameshift
3_40	749, 234, 237	12 bp deletion, no frameshift
3_48	749, 234, 237	12 bp deletion, no frameshift
3_51	749, 234, 237	12 bp deletion, no frameshift

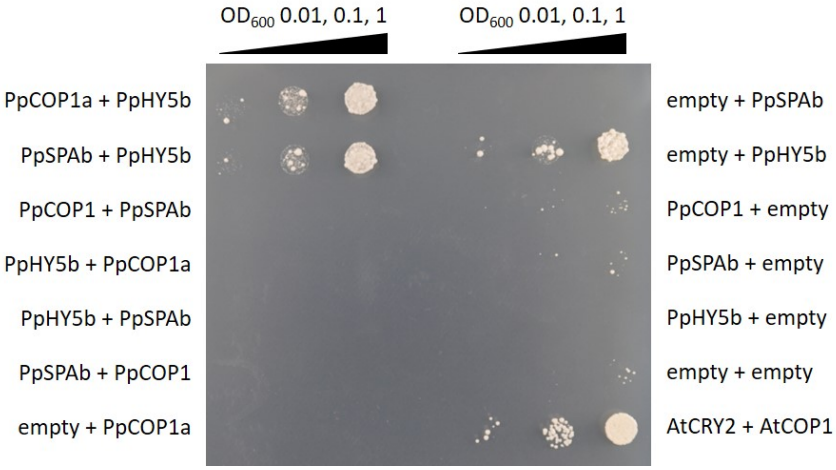

Figure S1: **No interaction of PpCOP1a, PpSPAb and PpHY5b was detected in yeast-two-hybrid assay (LexA system).**
After transformation with the respective bait and prey constructs yeast was grown in liquid culture to an OD_600 of 1. Different dilutions were dropped out on synthetic dropout medium lacking leucine, tryptophan and histidine supplemented with galactose and raffinose. Growth was assessed after incubation at 30°C for 4 d.

8 Acknowledgements

Blood, sweat and tears went into this work to varying degrees and while it was not always fun and easy it was enjoyable and rewarding every step of the way. One thing I learned early in my career as a Ph.D. student was that I knew nothing and desperately needed help to get anything done. Luckily, I met a plethora of people with redundant but distinct functions helping me to grow.

First and foremost I would like to thank Ute Höcker for her unmatched investment in my academic and personal development. Her guidance, expert advice and encouragement to take on new challenges greatly contributed to the success of this project and my personal growth.

I am grateful to Martin Hülskamp and Wolfgang Werr for being part of the examination committee. I would like thank Stefan Rensing and Bernd Reiss for supporting me as part of my Thesis Advisory Committee and Sandrine Bonhomme for introducing me into the Physco-adapted CRISPR/Cas9 technology.

Thanks to my closest allies in my everyday battle against stubborn Physco plants, the past and present members of the Höcker lab: Christian, Eva, Jathish, Krzysztof, Leonie, Lisa, Martin, Martina, Melanie, Moni, Natalia, Pan Pan, Song, Stefan, Stephan, Tobias and Xu as well as all student helpers. I wish Melanie great success with our little Physcos. Additionally, I would like to express my sincere gratitude to the other members of the Botanical Institute and the MPI that I was fortunate enough to meet, interact with and get help from.

I owe a lot to my oldest and also some of my newest friends. Thanks for being at my side Artem, Dominik, Konstantin, Philipp, Steffen, Stephan and Tobias. Thanks also to two beings who rolled with me the longest part of the journey: Jessica and Bär.

Last but not least, it fills me with nameless joy to know that I always had and will have the support of my mom, dad and sister who regularly go beyond all measure to improve my life in all possible domains - Thank you.

9 Declaration

I hereby declare that except where specific reference is made to the work of others, the contents of this dissertation are original and have not been submitted in whole or in part for consideration for any other degree or qualification in this, or any other University. This dissertation is the result of my own work and includes the contribution of students, from the University of Cologne, who were involved with the experiments listed below.

Name	**Contribution**	**Reference**
Elena Abraham	qRT-PCR analysis of light-regulated genes; Determination of *PpHY5b-3HA* mRNA and protein levels	Module report
Vanessa Boll	Yeast-two-hybrid assays (Gal4-system) testing PpCOP1a, PpSPAb and PpHY5b interactions; Genotyping *PpHY5b-3HA PpspaAB* lines; Determination of protein levels in different *PpHY5b-3HA* lines	Bachelor Thesis, Module report

10 Erklärung

Ich versichere, dass ich die von mir vorgelegte Dissertation selbständig angefertigt, die benutzten Quellen und Hilfsmittel vollständig angegeben und die Stellen der Arbeit - einschließlich Tabellen, Karten und Abbildungen -, die anderen Werken im Wortlaut oder dem Sinn nach entnommen sind, in jedem Einzelfall als Entlehnung kenntlich gemacht habe; dass diese Dissertation noch keiner anderen Fakultät oder Universität zur Prüfung vorgelegen hat; dass sie - abgesehen von unten angegebenen Teilpublikationen - noch nicht veröffentlicht worden ist sowie dass ich eine solche Veröffentlichung vor Abschluss des Promotionsverfahrens nicht vornehmen werde.

Die von mir vorgelegte Dissertation ist von Prof. Dr. Ute Höcker betreut worden.

Oliver Artz

11 Lebenslauf

Oliver Artz

Hüttenstraße 8
50823 Köln
Tel. (mobil): 0179 20251717
E-Mail: artz.oliver@gmail.com

Persönliche Daten

◇	Geburtsdatum	16.11.1988
◇	Geburtsort	Goch

Hochschulausbildung

◇	Seit 2014	Promotion am Botanischen Institut der Universität zu Köln Titel: "On The Evolution of Light Signaling: The COP1/SPA complex in *Physcomitrella patens*" unter Betreuung von Prof. Dr. Ute Höcker
◇	2012 - 2014	Masterstudium an der Universität zu Köln Titel der Abschlussarbeit: "Analysis of missense mutations in the *Arabidopsis thaliana* SPA1 N-terminal domain" unter Betreuung von Prof. Dr. Ute Höcker
◇	2009 - 2012	Bachelorstudium an der Universität Heidelberg Titel der Abschlussarbeit: "Misexpression of plasma-membrane localised calcium sensors manipulates growth in *Arabidopsis thaliana*" unter Betreuung von Prof. Dr. Karin Schumacher

Berufserfahrung

◇	Sommer 2013	Gastwissenschaftler an der University of California at Berkeley, USA Aufgabenbereich: Genetische, molekulare und biochemische Analyse der Lichtsignaltransduktion in *Arabidopsis thaliana* unter Betreuung von Prof. Dr. Peter Quail
◇	Sommer 2012	Gastwissenschaftler am Royal Melbourne Institute of Technology, Australien Aufgabenbereich: Genetische, molekulare und biochemische Analyse der Schmutzwasser Bioremediation durch Süsswasseralgen unter Betreuung von Dr. Aidyn Mouradov
◇	2010 - 2011	Studentische Hilfskraft an der Universität Heidelberg

Publikationen

- Holtkotte, X., Dieterle, S., Kokkelink, L., **Artz, O.**, Leson, L., Fittinghoff, K., Hayama, R., Ahmad, M.; Hoecker, U. (2016) Mutations in the N-terminal kinase-like domain of the repressor of photomorphogenesis SPA1 severely impair SPA1 function but not light responsiveness in Arabidopsis. Plant J., 88(2):205-18
- Brenig J., de Boor S., Knyphausen P., Kuhlmann N., Wroblowski S., Baldus L., Scislowski L., **Artz O.**, Trauschies P., Baumann U., Neundorf I., Lammers M. (2015) Structural and Biochemical Basis for the Inhibitory Effect of Liprin-α3 on Mouse Diaphanous 1 (mDia1) Function. J. Biol. Chem., 290(23): 14314-27

Teilnahme an wissenschaftlichen Konferenzen

◇	2018	Young Researchers Symposium on Plant Photobiology, Köln, Deutschland
◇	2018	International Symposium on Plant Photobiology, Matsue, Japan
◇	2018	Molecular Biology of Plants, Dabringhausen, Deutschland
◇	2016	EMBO Workshop: New model systems for early land plant evolution, Wien, Österreich
◇	2015	International Symposium on Plant Photobiology, Austin, TX, USA

Stipendien und Auszeichnungen

◇	seit 2014	International Max Planck Research School Fellowship, Max Planck Institut für Pflanzenzüchtungsforschung
◇	2018	Reisestipendium für Teilnahme an Molecular Biology of Plants 2018, Deutsche Botanische Gesellschaft
◇	2018	Reisestipendium für Teilnahme am International Symposium on Plant Photobiology 2018, IPAK, Universität zu Köln
◇	2015	Reisestipendium für Teilnahme am International Symposium on Plant Photobiology 2015, Organisationskommittee (Enamul Huq)
◇	2012 - 2014	Deutschlandstipendium zur Förderung des Masterstudiengangs, Bundesministerium für Bildung und Forschung
◇	2013	PROMOS Stipendium für Aufenthalt an der University of California at Berkeley, Deutscher Akademischer Austauschdienst
◇	2012	RISE Stipendium für Aufenthalt am Royal Melbourne Institute of Technology, Deutscher Akademischer Austauschdienst

Fremdsprachenkenntnisse

◇	Muttersprache	Deutsch
◇	Fremdsprachen	Englisch (fließend), Französisch, Spanisch (Grundkenntnisse)